Retinal Blood Flow and Vascular Reactivity in Chronic Smokers

by

Kalpana Rose

A thesis
presented to the University of Waterloo
in fulfilment of the
thesis requirement for the degree of
Master of Science
in
Vision Science

Waterloo, Ontario, Canada, 2013

I hereby declare that I am the sole author of this thesis. This is a true copy of the thesis, including any required final revisions, as accepted by my examiners.

I understand that my thesis may be made electronically available to the public.

ABSTRACT

Purpose

To investigate the impact of cigarrete smoking in a group of otherwise healthy young individuals on:

1) Retinal blood flow using Doppler based SD-OCT,

2) Retinal vascular reactivity using a gas sequencer to provoke hypercapnia via constant changes in $P_{ET}CO_2$ (end-tidal partial pressure of CO_2) and in $P_{ET}O_2$ (end-tidal partial pressure of O_2).

Methods

An automated gas flow controller was used to achieve normoxic hypercapnia in ten non-smokers (mean age 28.9 yrs, SD 4.58) and nine smokers (mean age 27.55 yrs, SD 4.77). Retinal blood flow measurements were obtained using Doppler OCT and cannon laser blood flowmeter (CLBF) during baseline, normoxic hypercapnia (15% increase in $P_{ET}CO_2$ relative to homeostatic baseline) and post-hypercapnia in both the groups. Exhaled carbon monoxide level was measured in all subjects.

Results

In non-smokers, retinal arteriolar diameter, blood velocity and flow increased by +4.1% (SD 2.8, $p<0.0001$), +16.7% (SD 14.6, $p=0.0004$) and +29.6% (SD 12.5, $p<0.0001$) respectively, during normoxic hypercapnia; Similarly, the venous area, venous velocity and total retinal blood flow increased by 7% (SD 8.6, $p=0.0418$), 18.1% (SD 20.8,

p=0.0068) and 26% (SD 22.9, p<0.0001) respectively. In smokers, normoxic hypercapnia resulted in a significant increase in velocity by 12.0% (SD 6.2, p=0.0019) and flow by 14.6% (SD 9.5, p=0.0029); though arteriolar diameter increased by 1.7% (SD 1.7, p=0.2616), the result was not statistically significant. Total retinal blood flow increased significantly by 19.3% (SD 18.4, p=0.002) in response to normoxic hypercapnia. However, there was no significant difference in venous area (p=0.3322) and venous velocity measurements (p=0.1185) during hypercapnia compared to baseline and recovery. Comparing smokers and non-smokers, only the percentage change in arteriolar diameter (p=0.0379) and flow (p=0.0101) was significantly different among the groups. Group mean $P_{ET}CO_2$ was increased by 15.9% in the non-smoking group and by 15.7% in the smoking group, with a concomitant increase in $P_{ET}O_2$ by approximately 1.5 to 2% in both groups. There was no significant difference in baseline $P_{ET}CO_2$ level between smokers and non-smokers.

Conclusions

Retinal vascular reactivity in response to normoxic hypercapnia is significantly reduced in young healthy individuals who smoke compared to non-smokers. Further studies are needed to elucidate the exact reason behind the impaired retinal autoregulation to provocative stimuli in smokers.

ACKNOWLEDGEMENTS

I thank god for who gives me the strength and ability to pursue my dreams.

I would like to sincerely thank my supervisors Dr. Christopher Hudson and Dr. John Flanagan for their guidance, support and encouragement throughout my program.

I would like to extend my gratitude to Dr. Richard Hughson and Dr. Trefford Simpson for being in my advisory committee and suggesting valuable ideas to improve this thesis.

My sincere thanks to Dr. Joseph Fisher for suggesting the carbon monoxide monitor used in this study.

I would want to thank the entire team of Hudson lab mates for their help and participation in the study. Special thanks to Rickey Cheng, Alanna Adleman, Firdaus Yusof, Dr. Monica Jong, Dr. Ayda Shahidi and Dr. Sunni Patel for helping me run the study. I also want to thank Dr. Sunita Shankar for her friendly advice and encouragement.

I thank all my friends who helped me in finding subjects for this study. Special thanks to Dr. Raiju Babu and Dr. Krithika Nandakumar for their love and support.

My gratitude extends to graduate officers, graduate co-ordinator, graduate colleagues and staff of the school of optometry and vision science.

Thanks to the Ontario Research Fund – Research Excellence Award (ORF-RE) for the financial support.

Finally, I thank my husband Prem and my 4 year old son Praveen for their patience, motivation and love. Without their understanding I would not have accomplished this much.

TABLE OF CONTENTS

List of Tables

List of Figures

List of Abbreviations

ARMD	Age related macular degeneration
BLDV	Bi-directional laser Doppler velocimetry
BP	Blood pressure
BH4	Tetrahydrobiopterin
CO_2	Carbon dioxide
CRA	Central retinal artery
CRV	Central retinal vein
cGMP	Cyclic guanosine monophosphate
CDI	Colour Doppler imaging
CLBF	Cannon laser blood flowmeter
CO	Carbon monoxide
COHb	Carboxyhaemoglobin
DR	Diabetic retinopathy
DSCP	Double circular scan protocol
DOCTORC	Doppler optical coherence tomography of retinal circulation
DVA	Dynamic retinal vessel analyser
EDRF	Endothelial derived relaxing factor
EDCF	Endothelial derived constricting factor
ET	Endothelins
eNOS	Endothelial nitric oxide synthase
FTQ	Fagerstrom tolerance questionnaire
IOV	Inferior ophthalmic vein
LDF	Laser Doppler flowmetry
LDV	Laser Doppler velocimetry
µl /min	Microliter/minute

mm/sec	Millimeter/second
μm	Micrometer
ms	Millisecond
NADPH	Nicotinamide adenine dinucleotide phosphate
NO	Nitric oxide
O_2	Oxygen
OA	Ophthalmic artery
OPP	Ocular perfusion pressure
ONH	Optic nerve head
$PaCO_2$	Partial pressure of arterial concentration of carbon dioxide
PaO_2	Partial pressure of arterial concentration of oxygen
PCA	Posterior ciliary artery
PGI_2	Prostacyclin
$P_{ET}CO_2$	End-tidal partial pressure of CO_2
$P_{ET}O_2$	End-tidal partial pressure of O_2
PPM	Parts per million
RBCs	Red blood cells
SOV	Superior ophthalmic vein
SD-/- FD OCT	Spectral domain - / - Fourier domain optical coherence tomography
SLO	Scanning laser ophthalmoscopy
TRBF	Total retinal blood flow

1 Introduction

Blood supply to the human retina is derived from two distinct vasculatures namely: the central retinal artery and the choroidal vessels. The central retinal artery supplies the inner two-third of the retina whereas the outer retina including the retinal pigment epithelium and photoreceptors are nourished by the choriocapillaris via short and long posterior ciliary arteries (Kaufman and Alm 2003). In adults, both the vascular beds (i.e. retina and choroid) vary in their embryonic differentiation pattern as well as in their function. Retinal vessels do not exhibit fenestrations similar to those observed in the brain, whereas the choroidal vessels are fenestrated (Saint-Geniez and D'Amore 2004).

Despite varying metabolic demand, blood oxygen and carbon dioxide concentration, and perfusion pressure changes, the retina is capable of regulating blood flow. The magnitude of change in retinal hemodynamic measurements to provocative stimuli, such as that elicited by change in arterial blood partial pressure of carbon dioxide ($PaCO_2$) or oxygen (PaO_2) is known as “vascular reactivity”. Several studies have demonstrated changes in retinal vessel diameter, velocity and flow to various provocative stimuli such as CO_2, O_2 and flicker (Luksch et al. 2002; Gilmore et al. 2005; Garhofer et al. 2011). Changes in retinal vascular reactivity and blood flow have been reported in major retinal diseases (Gilmore et al. 2007; Venkataraman et al. 2010). Ocular blood flow measurement techniques utilising Doppler technology are promising for early detection of hemodynamic disturbances and might improve our understanding of disease mechanisms.

1.1 Retinal blood supply and drainage

Ocular blood supply is primarily derived from the ophthalmic artery (OA), a branch of the internal carotid artery. Three major branches of OA supply the extra ocular muscles, the central retinal artery (CRA), and the posterior and anterior ciliary arteries respectively (Hayreh 1962; Harris et al. 2003). The CRA enters the optic nerve from below, approximately 10-15mm behind the globe, from where it runs within the central portion of the optic nerve, adjacent to the central retinal vein (CRV). The CRA further subdivides into four major arteriolar branches supplying each quadrant of the retina. Venous blood is drained into the superior ophthalmic vein or directly into the cavernous sinus by the CRV, which leaves the eye through the optic nerve (Pournaras 2008).

1.2 Choroidal blood supply and drainage

The choroid is a mesh lying between the sclera and the retina. The choroid is rich in blood vessels and most of this blood is derived from posterior ciliary arteries. A medial and lateral posterior ciliary artery (PCA) branch runs from the ophthalmic artery. Before piercing the sclera, each PCA divides into a long posterior ciliary artery, which supplies the anterior choroid as well as into 10 to 20 short posterior ciliary arteries, which supply the posterior choroid. The deeper outer layers of the retina including photoreceptors and bipolar cells are specifically supplied by the choriocapillaris, a single layer of choroidal capillaries containing fenestrated endothelium without tight junctions (Jakobiec 1982). Venous blood from the choriocapillaris is drained through the vortex veins into the inferior ophthalmic vein (IOV) and the superior ophthalmic vein (SOV). Both the IOV and SOV

further drains into the cavernous sinus (Hart and Adler 1992; Harris et al. 2003; Kaufman and Alm 2003).

1.3 Structure of retinal blood vessels

Retinal blood vessels include arterioles, venules and capillaries. The blood vessel wall consists of three layers namely: 1) innermost endothelial cells 2) middle layer of smooth muscle cells and 3) outermost adventitia (Kaufman and Alm 2003). The endothelial cells are monolayer of cells located between the circulating blood and the smooth muscle layer (Haefliger and Flammer 2001). It plays a significant role in the autoregulation of blood flow as described in the following section. The diameter of vascular lumen is controlled by the contraction and relaxation of smooth muscle cells (Rensen et al. 2007). The outermost adventitial layer protects and anchors the vessel to the surrounding tissue.

Emerging from the nasal side of optic disc, the retinal vessels are arranged in a radial pattern temporally, and an arching pattern nasally. The retinal arteries and veins remain in the nerve fiber layer of the retina, whereas the arterioles and venules extend more deeply as they form major capillary networks: 1). Superficial radial peripapillary capillaries in the ganglion cell and nerve fiber layer and 2) an inner and outer layer of deep capillaries lying in the inner nuclear layer. Towards the periphery of the retina these capillary networks thin into a single layer (Toussaint 1961).

Retinal arterioles are small resistance vessels of 20-150μm in diameter, regulating the amount of blood delivered to the downstream capillaries. Capillaries are about 6-10μm in diameter, facilitating the exchange of nutrients, waste and other substances between the blood and interstitial fluid. The capillaries lack a smooth muscle layer, but are composed of the thin layer of endothelial cells, pericytes and basement membrane. The endothelial cells have tight junctions (zona occludens) which act as a blood retinal barrier preventing the movement of macromolecules from the lumen to interstitial space, similar to that of blood brain barrier. The capillaries drain the blood into venules. These venules gradually become thicker in diameter and form veins. The veins have thinner vessel wall compared to arteries but have a larger cross sectional area to enable the storage of blood (Kaufman and Alm 2003).

1.4 Autoregulation of retina

Autoregulation is defined as the "ability of the vasculature to maintain blood flow at relatively constant levels despite moderate variations in perfusion pressure" (Guyton 1964). Retina is effectively autoregulated over a substantial range of intraocular pressure and systemic blood pressure (Lester et al. 2007; Robinson and Riva 1986; Schulte 1996; Grunwald et al. 1982). The vascular endothelial cells lining the blood vessel wall releases certain mediators which act on the smooth muscle cells, regulating retinal blood flow locally.

1.4.1 Metabolic, Myogenic and Neurogenic autoregulation

1.4.1.1 Metabolic autoregulation

Metabolic autoregulation is the ability of the vasculature to modulate blood flow in order to maintain metabolic components including tissue oxygen and carbon dioxide at relatively constant levels (Guyton 1964). The term ‘metabolic autoregulation’ is often referred as ‘vascular reactivity’. Increased tissue concentration of oxygen and decreased concentration of carbon dioxide results in vasoconstriction. Conversely, increased tissue concentration of carbon dioxide and decreased tissue oxygen concentration results in vasodilation. However, it is interesting to note that these responses occur, independent of perfusion pressure (Johnson 1986).

1.4.1.2 Myogenic autoregulation

Myogenic autoregulation is responsible for maintaining constant blood flow despite increase in arterial pressure by contracting the smooth muscle of the vessel wall, thereby reducing the blood flow. Conversely, at low pressures, the smooth muscle relaxes and allows increased blood flow. The stretching of smooth muscle increases calcium ion entry from the extra cellular fluid into the smooth muscle cell resulting in contraction (Guyton and Hall 2000). Endothelial derived vasoactive agents are thought to play a major role in myogenic contraction (Furchgott and Vanhoutte 1989; Furchgott 1984).

1.4.1.3 Neurogenic autoregulation

Since the sympathetic nerves supply the retinal vasculature only up to lamina cribrosa, the autonomic nervous system does not contribute to the autoregulation of retina (Harris et al. 2003).

1.5 Endothelial derived vasoactive substances

The endothelial cells lining the retinal vessels synthesize certain substances which, when released, can affect the degree of relaxation and contraction of the arterial wall (Guyton and Hall 2000). They are:

1). Endothelial derived relaxing factor (EDRF) and

2). Endothelial derived constricting factor (EDCF).

These substances are primarily responsible for local retinal blood flow regulation. Previous studies reported that altered production of either of these substances result in patho physiological diseases including arterio-sclerosis, hypercholesterolemia, hypertension and diabetes (Hsueh and Anderson 1992; Davignon and Ganz 2004).

1.5.1 Endothelial derived relaxing factors

1.5.1.1 Nitric oxide

Nitric oxide (NO) is a potent endothelium-derived relaxing factor, produced when L-arginine is transformed to L-citrulline by catalysis of nitric oxide synthase (NOS) in the presence of oxygen and cofactors including calmodulin, tetrahydrobiopterin (BH_4), nicotinamide adenine dinucleotide phosphate (NADPH), heme, flavin adenine

dinucleotide, and flavin mononucleotide. NO binds to the iron atom of heme in guanylate cyclase and thereby increases intracellular cyclic guanosine monophosphate levels, in turn leading to a decrease in intracellular calcium levels and hence vasorelaxation (Gornik 2004).

Various studies indicate the role of NO in controlling blood flow by maintaining hypercapnia induced vasodilation (Schmetterer and Polak 2001), although the underlying mechanism is yet to be clearly understood. NO is also previously reported to regulate blood flow by initiating vasodilation of retinal vessels in response to flicker stimuli (Dorner et al. 2003).

1.5.1.2 Other endothelial derived vasodilators

Prostacyclin (PGI_2) is also a vasodilator synthesized by endothelial cells from arachidonic acid. It acts through the activation of adenylate cyclase, leading to increased levels of cyclic adenosine monophosphate. It is the most potent inhibitor of platelet aggregation (Vane and Botting 1995; Kaufman and Alm 2003).

1.5.2 Endothelial derived constricting factors

1.5.2.1 Endothelin

The endothelins (ET) are a group of vasoconstricting agents released by endothelial cells. Endothelins consist of three 21-amino acid peptides: ET-1, ET-2 and ET-3 which act through the endothelin receptor A (ETA) and endothelin receptor B (ETB). The ETA

receptor is found on vascular smooth muscle cells, whereas ETB receptor is found on vascular endothelial cells. ETA receptors mediate vasoconstriction secondary to increased intracellular calcium (Schiffrin 1998; Lüscher 1997). Various animal (Granstam et al. 1992) and human studies (Dallinger et al. 2000) have reported the role of ET-1 in initiating pronounced vasoconstricting response to hyperoxia in retinal vasculature.

1.5.2.2 Other endothelial derived constricting factors

Norepinephrine and epinephrine are other vasoconstrictive hormones released by endothelial cells. Both are neurotransmitters released by adrenal medulla, which activates the sympathetic nervous system, which excites the heart and contracts the vein and arterioles. Norepinephrine is known to be more potent than epinephrine; in some tissues epinephrine was even known to cause mild vasodilation (Goodall and Norman 1958).

Angiotensin II and vasopressin are other vasoconstrictors to be mentioned. Though vasopressin is known to be more powerful than angiotensin II, the later substance powerfully constricts the small arterioles. If this occurs, the blood flow to that area of tissue could be significantly depressed (Goodall and Norman 1958; Guyton and Hall 2000).

1.6 Vascular reactivity

The magnitude of change in retinal hemodynamic measurements to provocative stimuli, such as that elicited by change in arterial blood partial pressure of carbon dioxide ($PaCO_2$)

or oxygen (PaO_2) is known as “vascular reactivity”. Hyperoxia is an increase in arterial partial pressure of oxygen from baseline homeostatic levels; endothelin-1 is known to mediate the vasoconstrictive response to hyperoxia (Dallinger et al. 2000). On the other hand, hypercapnia refers to an increase in arterial partial pressure of carbon dioxide from baseline homeostatic levels; nitric oxide is thought to regulate blood flow by maintaining vasodilation during hypercapnia (Goldstein et al. 1996; Schmetterer et al. 2001).

Retinal vessels react to hyperoxia by local constriction of arterioles, venules and capillaries; thereby reducing the retinal blood flow (Gilmore et al. 2004; Sponsel et al. 1992). Conversely, hypercapnia induces vasodilation of blood vessels which increase the blood flow (Venkataraman et al. 2006; Venkataraman et al. 2005; Venkataraman et al. 2008; Dorner et al. 2002; Luksch et al. 2002). Previous studies have shown that cerebral vessels react to hypercapnia and hyperoxia similar to retinal vessels (Schmetterer et al. 1997). However, inner retinal circulation was shown to be more sensitive to increased partial pressure of oxygen than carbon dioxide than the cerebral vessels. On the other hand, the cerebral vasculature was shown to react greater to carbon dioxide while showing no significant response to oxygen (Kisilevsky et al. 2008).

1.7 Physiological principles of blood flow

‘Blood flow’ refers to the “quantity of blood that passes a given point in the circulation in a given period of time” (Guyton and Hall 2006). Blood flow is normally measured in microliter/minute (μL/min). Blood velocity refers to the speed of the moving red blood

cells and blood vessel diameter refers to the horizontal distance across the lumen of the vessel wall.

When blood flows with a steady rate along the vessel, the flow is 'streamlined', with each layer of blood remaining equidistant from the vessel wall. This manner of flow is known as '*laminar flow*'. If blood flows in this fashion through the vessel wall, a parabolic pattern develops between the layers of the blood, i.e. the velocity of center layer is much faster compared to the adjacent layers towards the vessel wall. The layer touching the vessel wall has poor velocity due to its adherence to the vessel wall. In contrary to laminar flow, if the rate of flow is much greater, i.e. when blood passes through a bifurcation or any obstruction within the vessel wall, then the usual parabolic pattern is disturbed resulting in '*turbulent flow*' (Guyton and Hall 2000) (Figure 1.1).

(a) (b)

Figure 1.1 Types of flow inside a blood vessel (a) Laminar flow; (b) Turbulent flow

Blood flow (Q) inside a vessel wall is directly proportional to *perfusion pressure* (ΔP), which is the difference in pressure between two ends of the vessel; and inversely proportional to *vascular resistance* (R), which occurs due to the intra vascular friction

between moving blood and endothelial cell layer. The relationship between flow rate, perfusion pressure and resistance based on Ohm's law is given by:

$$Q = \frac{\Delta P}{R} \quad \textbf{(1.1)}$$

Resistance to flow (R) is determined by the properties of fluid as well as the vessel in which the fluid is flowing. R is directly proportional to length of the vessel (L) and viscosity of the fluid (η); whereas inversely proportional to fourth power of the radius (r) of the vessel. This relationship is given by:

$$R = \frac{8\eta L}{\pi r^4} \quad \textbf{(1.2)}$$

The *Hagen-Poiseuille law* gives the relationship between all the factors influencing blood flow through the vessel.

$$Q = \frac{\Delta P \pi r^4}{8\eta L} \quad \textbf{(1.3)}$$

in which Q is the flow rate, ΔP is the pressure difference between two ends of the vessel, r is the radius of the vessel, η is viscosity of the blood and L is length of the vessel. From the equation it is obvious that small change in the diameter of the vessel highly impact the flow to a tissue, since flow is directly proportional to the fourth power of radius of the vessel (Sparks and Rooke 1987).

Perfusion pressure is the difference between arterial and venous pressure. Arterial pressure in the eye is approximately two-thirds of the mean arterial pressure, whereas venous

pressure in the eye is nearly equal to the intraocular pressure (Kaufman and Alm 2003). Therefore, ocular perfusion pressure (OPP) is expressed as the difference between arterial blood pressure minus intra ocular pressure (IOP) (Leske 2009).

$$OPP = \frac{2}{3} BP_{mean} - IOP \quad \text{.....(1.4)}$$

Ocular perfusion pressure could be reduced by decreasing the mean arterial blood pressure or by increasing the IOP (Riva et al. 1997).

1.8 Human retinal blood flow

The retina receives 15% of ocular circulation as compared to 85% to choroidal circulation (Harris et al. 2003). The choroid has a high flow rate compared to the inner retina and brain (Linsenmeier et al. 2000), as well as sympathetic nerves control choroidal blood flow, whereas retinal blood flow is efficiently autoregulated to increase or decrease perfusion pressure by contraction and dilation of retinal resistance arterioles respectively (Vaz et al. 2011). Previous studies have reported that retinal blood flow remains constant over a substantial range of intraocular pressure and systemic blood pressure (Robinson and Riva 1986; Riva et al. 1986). With the flow being steady, blood flow rate (Q) can be expressed as a product of velocity and cross sectional area as below:

$$Q = V_{mean} * S \quad \text{.....(1.5)}$$

where V_{mean} is the mean velocity of moving red blood cells, which is given by V_{max} / 2; S is the cross-sectional area of the blood vessel given by $\pi D^2/4$ (Feke et al. 1989).

1.9 Retinal blood flow assessment techniques

Ocular blood flow assessment may in the future play a vital role to diagnose and treat major ocular pathologies like ARMD, DR and Glaucoma. The assessment techniques that are discussed below are a brief overview of those which are used to assess ocular hemodynamics. Many of these techniques measure surrogate markers of retinal blood flow rather than assessing flow *per se*. For more detailed explanation of ocular blood flow measurement techniques please refer to Harris et al. 2003; Schmetterer and Garhofer 2007 Harris et al. 2008.

1.9.1 Fluorescein angiography

Ocular blood flow can be assessed by passing 'dye' intravenously and photographing it as it passes through the retina and choroid. Fluorescein angiography was originally introduced by Novotny and Alvis (Novotny and Alvis 1961). During fluorescein angiography, a rapid sequence of serial photographs is taken after the administration of intravenous fluorescein to visualize and document choroidal and retinal blood flow (Hurley et al. 2009). This technique was later enhanced by employing video-angiography and scanning laser ophthalmoscopy. This modification to the angiographic technique resulted in improved image quality and spatial resolution. Though several attempts have been made to quantify retinal blood flow using angiographic technique, most approaches were based on the measurement of time required for the dye to pass through the retinal circulation. Invasive procedure and injection of dye are some of the limitations of this technique (Harris et al. 1998; Harris et al. 2003).

1.9.2 Blue Field Entoptic technique

This technique allows the viewer to visualize the movement of leukocytes (white blood cells) through their perimacular capillaries while gazing into bright blue illumination. Most probably the underlying phenomenon is that erythrocytes, but not leukocytes absorb short wavelength light; therefore the passage of leukocytes are perceived as flying corpuscles (Nakahashi et al. 1989). By comparing with their own entoptic observation, subjects can adjust the number of leucocytes, the mean flow velocity and the pulsatility of motion, from which the retinal blood flow and the flow pulsatility can be calculated. This method is limited due to subjective fatigue and poor reproducibility when repeated measurements are done in the same subject (Yap and Brown 1994).

1.9.3 Retinal vessel analyser (RVA)

The RVA system consists of a fundus camera, a high-resolution digital video camera and a personal computer with analyzing software. The diameter of arterioles and venules within one disc diameter from the optic disc were measured using this analyser (Garhofer et al. 2012). A fundus image is captured and were digitalized and analysed in real time with a frequency of 50Hz to determine the diameter of retinal vessels. The time to measure a single value is 40ms, allowing upto 25 measurements per second (Blum et al. 1999). Though proven to yield reproducible vessel diameter measurements (Polak et al. 2000), the retinal vessel analyzer does not measure retinal blood velocity and flow.

1.9.4 Laser Doppler techniques

The laser Doppler techniques are widely used in haemodynamic research to measure the moving red blood cell velocity. The Doppler shift principle is utilised in these techniques. (Figure 1.2) The principle of "Doppler shift" relates the frequency of sound or light reflected from an object to its velocity. When a laser light of frequency, is reflected from a moving particle like red blood cells (RBCs) it has a shift in frequency (Δf) that is proportional to the velocity of the moving RBCs. At the same time, light scattered from stationary tissue like vessel wall is not shifted in frequency (f) and so acts as the reference frequency from which a relative change in blood velocity is measured (Feke 2006).

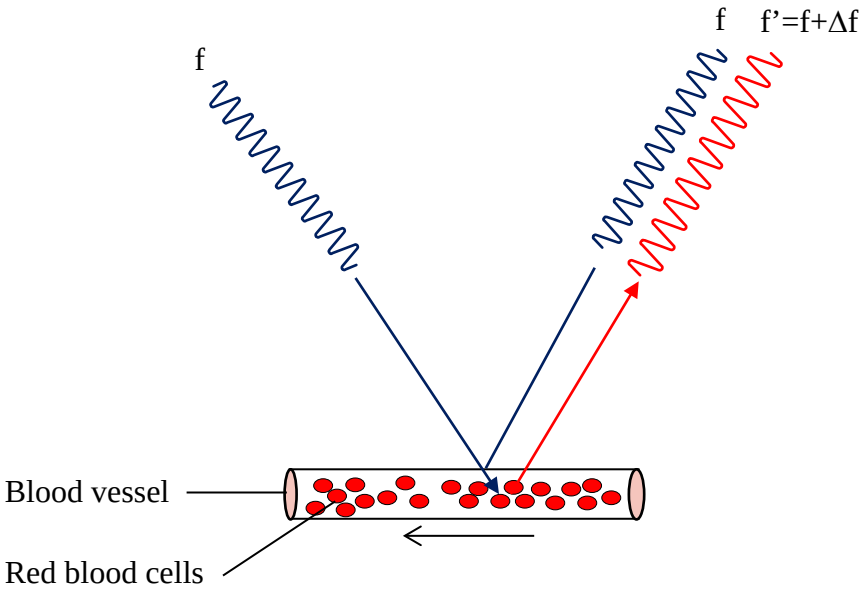

Figure 1.2 The Doppler principle

1.9.4.1 Colour Doppler Imaging (CDI)

The CDI is an ultrasound technique that combines B-scan grey-scale imaging of tissue structure, colour representation of blood flow based on Doppler shifted frequencies and pulsed Doppler measurement of blood flow velocities. CDI measures the frequency of reflected sound waves to determine the blood flow velocity within the long and short posterior ciliary arteries, ophthalmic artery and central retinal artery (Harris et al. 2003). A potential source of error in CDI is the excessive pressure applied to the eyelid. This pressure can result in a significant change in IOP and can lead to changes in perfusion pressure and blood flow (Harris et al. 1998). Also operator experience is critical to acquire repeatable hemodynamic values (Baxter and Williamson 1995), probably due to the fact that the derived velocities are dependent upon the probe angle relative to the moving red blood cells. CDI cannot measure diameter of retinal vessels so quantitating retinal blood flow is impossible.

1.9.4.2 Laser Doppler Flowmeter (LDF)

The LDF is a non-invasive technique that allows the measurement of relative blood velocity, volume and flow within a tissue sampled by the laser beam. LDF measures volumetric flow within the retinal and choroidal capillaries (Harris et al. 2008). The advantage of this technique is the measurement of volumetric flow as compared to other techniques like laser Doppler velocimetry, which are only restricted to blood velocity measurements. The major limitation of LDF is that, the measured Doppler shift frequencies might be from both retinal and choroidal vasculature, therefore interpreting LDF data is difficult (Petrig et al. 1999).

1.9.4.3 Bi-directional Laser Doppler Velocimetry (BLDV)

The BLDV measures the velocity of red blood cells by detecting the frequency shifts in laser light using 'two' photo-detectors (Harris et al. 1998). The absolute quantification of centerline blood velocity is possible by determining the difference in frequency shifts in two directions as represented by wave vectors K_1 and K_2 (Figure 1.3). The two photo-detectors with a known angle of separation record the centerline blood velocity independent of the angle between the moving erythrocytes and reflected beam (Riva et al. 1985). Velocity is determined using the equation:

$$V_{\max} = \frac{\lambda \Delta f}{n \Delta \alpha \cos\beta} \quad \textbf{(1.6)}$$

where,

$$\Delta f = f_2 max - f_1 max = (\alpha_2 - \alpha_1) v/\lambda \quad \textbf{(1.7)}$$

From the above equations, f_1 max and f_2 max are the maximum frequency shifts at K_1 and K_2, respectively. α_1 and α_2 are the angles between the velocity vector V_{max} and K_1 and K_2. $\Delta\alpha$ is the angle between K_1 and K_2; β is the angle between the vector V_{max} and the incident beam.

BLDV is capable of measuring blood velocity from major retinal vessels. If vessel diameter measurements are obtained separately, then volumetric retinal blood flow can be derived from the following equation (Kida et al. 2002; Feke 2006):

$$\text{Flow} = 1/2.\pi.D^2/4.V_{mean}.60 \quad \textbf{(1.8)}$$

where, $V_{mean} = V_{max}/2$; D=diameter of the vessel.

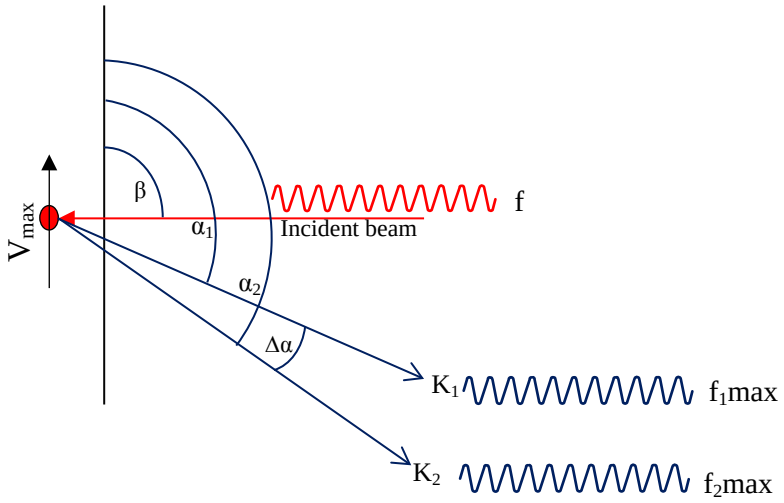

Figure 1.3 Diagram illustrating principle of bidirectional laser Doppler velocimetry

1.9.4.4 Canon Laser Blood Flowmeter (CLBF-100)

In contrast to all the above mentioned instruments which utilize laser Doppler technique, the CLBF achieves simultaneous measurement of blood velocity and vessel diameter, thus volumetric retinal blood flow is derived in absolute units. The CLBF is a fundus-camera type device with two photo-detectors and two lasers. Two sequential velocity measurements are achieved using bi-directional techniques from the maximum frequency shifts at each photomultiplier along two optical paths (path 1 and path 2), to ensure consistency and to obtain single velocity measurement. A red diode laser (675 nm, 80 µm x 50 µm oval) measures velocity every 0.02 seconds across a 2 second measurement window resulting in velocity-time trace. A green diode vessel tracking laser system (543nm, 1500µm x 150µm rectangle) is used to stabilize the laser position at the

measurement site. The vessel tracking system holds the laser in position to compensate for any eye movement while taking measurements (Harris et al. 2008). Diameter measurements are acquired during the first and final 60 *ms* of the 2-s velocity measurement window every 4 *ms*. The CLBF automatically corrects for the magnification effects associated with refractive and axial component of ametropia, to provide absolute measurement of velocity (mm/sec), diameter (μm) and flow (μl/min). The repeatability and consistency of the CLBF has been reported by many researchers (Kida et al. 2002; Guan et al. 2003; Rose and Hudson 2007; Yoshida et al. 2003). The CLBF is limited to measurements on vessels less than 60μm in diameter. A study conducted using in vitro model reports that CLBF requires relatively clear ocular media, if not significant errors might occur in vessel diameter measurements (Azizi et al. 2007).

1.9.4.5 Doppler Spectral- / Fourier- Domain Optical Coherence Tomography (SD-OCT / FD-OCT)

Doppler SD-OCT is a novel technique for non-invasive quantitative measurement of total retinal blood flow in absolute units. Doppler SD-OCT utilizes the principle of 'Doppler effect' to determine the velocity of moving red blood cells. This spectrometer based OCT system contains a superluminescent diode with a center wavelength of 841nm and a bandwidth of 49nm. The axial resolution is 5.6 μm in tissue and transverse resolution is 20 μm as limited by optical diffraction of the eye. The composite signal produced by the interference between the sample and reference arm light in the fibre coupler is detected by a custom spectrometer, consisting of 1024-pixel line-scan camera. Fourier transformation of the resulting interference pattern gives the sample depth profile or A-scan through the

neural layers of the retina, each of which has differing reflectance properties (Figure 1.4). The phase difference between sequential axial scans at each pixel is used to determine the Doppler shift (Wang et al. 2009; Wang et al. 2007; Wang et al. 2008).

To derive total retinal blood flow measurement, Doppler scans are acquired using RTVue FD-OCT (Optovue Inc., Freemont, CA) using a double circular scan protocol (DCSP) (Wang et al. 2009). The DCSP consist of two concentric circles of diameter 3.4 and 3.75mm respectively. These two circles transect all large retinal arterioles and venules located near the optic nerve head in two locations. A total of six dual circular scan frames were obtained and averaged for each ring. From the measured Doppler shift with in the vessel and Doppler angle estimation from the vessel center depth difference between two concentric rings, volumetric flow is automatically achieved using a semi-automated software algorithm named Doppler Optical Coherence of Retinal Circulation (DOCTORC) (Konduru et al. 2012). Total retinal blood flow is calculated by summing up flows from all branch veins at one point in time (Wang et al. 2009).

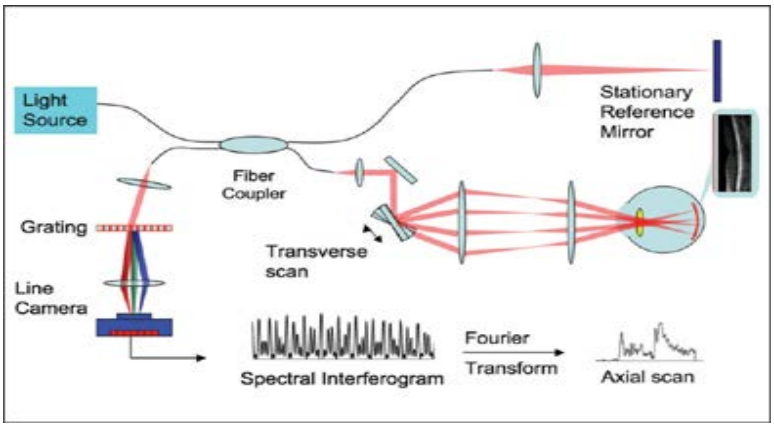

Figure 1.4 Schematics of a spectrometer based Fourier-domain OCT system

(Image reproduced with permission from Ophthalmology management, Springer)

1.10 Extraneous factors influencing retinal blood flow

A plethora of evidence suggest that factors such as smoking (McVeigh et al. 1996; Steigerwalt et al. 2000; Silvestrini et al. 1996; Rogers et al. 1984), hyperglycemia (Gilmore et al. 2007; Chittari et al. 2011), caffeine (Terai et al. 2012; Mathew and Wilson 1985; Lotfi and Grunwald 1991) and high fat diet (West 2001) are well known to alter the vascular reactivity and blood flow in various vascular beds in humans. The effect of cigarette smoking on retinal hemodynamics deserves more attention, since growing evidence from epidemiological studies indicate positive association between smoking and Age Related Macular Degeneration (ARMD) (Thornton et al. 2005; Cheng et al. 2000; Klein et al. 1993; Smith et al. 1996; Vingerling et al. 1996; Cong et al. 2008). ARMD is currently the leading cause of irreversible blindness in developed countries (Friedman et al. 2011; O'Shea 1996). Recent studies emphasize the increased risk of ARMD by two to three- fold in current cigarette smokers compared to non-smokers (Thornton et al. 2005; Seddon et al. 2006). Free radicals from cigarette smoke increases oxidative stress on the retinal pigment epithelium (RPE) - photoreceptor interface where metabolic activity is at its highest (Bertram et al. 2009).

Cardiovascular studies suggest that smoking has detrimental effects on endothelial-derived vasodilation and nitric oxide biosynthetic pathway in humans (Barua et al. 2001; Zeiher et al. 1995). Cerebrovascular research also reports that smoking impairs cerebrovascular regulation (Silvestrini et al. 1996; Terborg et al. 2002).

Several studies have reported the effect of smoking on retinal vascular reactivity; however the results seem to be controversial. Robinson and co-workers (Robinson et al. 1985) reported a 12 % (± 5%) increase in macular leukocyte velocity and presumably retinal blood flow in smokers. Langhans and co-workers (Langhans et al. 1997) reported that smokers showed a reduced reactivity to oxygen compared to non-smokers. Surprisingly, Wimpissinger and co-workers (Wimpissinger et al. 2005) reported that oxygen reactivity of retinal vessel diameter was significantly more pronounced in smokers than non-smokers. Clearly, the retinal vascular reactivity and blood flow changes in cigarette smokers remains ambiguous.

1.11 Summary

In summary, the retinal vascular bed is unique due to the fact that non-invasive direct visualization of microcirculation is possible. Retinal blood flow is efficiently autoregulated. In the absence of direct sympathetic innervation, metabolic and myogenic stimuli play a major role in autoregulation of the retina. Several studies have reported vascular reactivity of retina to various provocative stimuli including flicker (Dorner et al. 2003) and inspired gas challenges (Dorner et al. 2002; Gilmore et al. 2004; Luksch et al. 2002). In healthy individuals, retinal vessels vasoconstrict to hyperoxia due to the release of Endothelin-1 from vascular endothelium, whereas they vasodilate to hypercapnia, due to the release of nitric oxide. However, in healthy young smokers, impaired endothelium dependent vasodilation has been reported in several vascular beds, including the brachial artery (Ozaki et al. 2010; Barua et al. 2001) and coronary artery (Zeiher et al. 1995). Recently, Garhofer and co-workers (Garhofer et al. 2011) reported impaired flicker

induced retinal vasodilation in young healthy smokers. A few other studies also report impaired retinal vascular reactivity to gas provocation stimuli in smokers (Morgado et al. 1994; Wimpissinger et al. 2005; Langhans et al. 1997).

Though various techniques exist to measure retinal blood flow non-invasively, almost all of them have certain limitations. Some of the techniques may not be suitable for routine clinical practise due to high variability in retinal blood flow measurements (Garhofer et al. 2012). At present, only the CLBF and Doppler SD-OCT enables the quantification of retinal blood flow in absolute units. The CLBF is capable of simultaneously measuring blood velocity as well as blood vessel diameter. The reproducibility and repeatability remain well established (Yoshida et al. 2003; Kida et al. 2002; Guan et al. 2003; Rose and Hudson 2007). The recently introduced Doppler SD-OCT measures total retinal blood flow in absolute units for the first time using a “dual scan protocol” (Konduru et al. 2012; Wang et al. 2007; Wang et al. 2008). However, careful validation of new techniques is mandatory prior to application in clinical studies.

2 Rationale, Hypotheses and Aims

2.1 Rationale

Retinal hemodynamic research has grown significantly over past two decades considering the need to understand and diagnose retinal diseases, given the improvement in the ability to quantify ocular blood flow. Retinal blood flow changes might be a pre-cursor for major retinal disease including glaucoma (Grieshaber and Flammer 2005), diabetic retinopathy (Bursell et al. 1996) and age-related macular degeneration (Chung et al. 1999). Various measurement techniques exist to study retinal hemodynamics. Those that utilize laser Doppler technology offer the possibility of measuring the velocity of moving red blood cells, in order to obtain retinal blood flow measurement. Some of the instruments which utilize Doppler technology are laser Doppler velocimetry (LDV) (Garhofer et al. 2012), laser Doppler flowmetry (LDF) (Feke 2006; Kagemann et al. 1998; Michelson et al. 1996) and color Doppler ultrasound imaging (CDI) (Schmetterer and Garhofer 2007).

CDI measures the pulsatile component of the blood, however, retinal vessel diameter cannot be measured and therefore retinal blood flow measurement is impossible (Schmetterer and Garhofer 2007). With LDV only blood velocity of moving erythrocytes can be measured from a single retinal vessel at a time. In order to obtain retinal blood flow, additional retinal vessel diameter measurements need to be made separately. In contrast to LDV, the CLBF is capable of obtaining retinal blood velocity as well as vessel diameter measurements simultaneously to achieve volumetric retinal blood flow in absolute units (μL/min, mm/sec) (Guan et al. 2003). However obtaining total retinal blood flow measurement can be tedious since each retinal vessel needs to be measured individually.

The introduction of laser Doppler spectral domain optical coherence tomography (Doppler SD-OCT) has the potential to greatly enhance the field of haemodynamic research. This high-resolution, cross-sectional retinal blood flow imaging technique offers the opportunity to study the retinal vascular bed more precisely (Wang et al. 2008). In vivo retinal blood flow measurements are achieved by using a double circular scan protocol (DSCP), around the optic disc which transects all branch retinal arterioles and venules simultaneously (Wang et al. 2011; Wang et al. 2008). Studies conducted in young healthy individuals report a coefficient of variability of 10.5% for total retinal blood flow (TRBF) measurements obtained using Doppler SD-OCT. This makes it the only measurement technique so far available, that has the potential to quantitate TRBF in absolute units. The blood flow measures achieved using Doppler SD-OCT was shown to be within the range of values attained using laser Doppler flowmetry (Wang et al. 2008).

In order to obtain TRBF measurement using the Optovue SD-OCT, the Doppler signal information from the OCT data is analyzed using the Doppler OCT of Retinal Circulation (DOCTORC) grading software. Once the software completes the automatic processing of OCT data, a human grader then manually verifies the type of vessel (artery or vein) and refines the blood vessel position and, diameter in subsequent scans in order to achieve total retinal blood flow measurements. This method of calculating TRBF, might be subject to human error with respect to manual estimation of retinal vessel diameter as well as grading of the Doppler signal strength (i.e., assigning confidence score ranging from 0 to 5) in the cross sectional images of retinal vessels. Consequently, it is important to study the learning effect of a human grader, and whether this could influence retinal blood flow

measurements. However, previous studies found that retinal blood flow measures derived from semi-automated Doppler OCT analysis obtained by two trained graders seemed to be similar and reproducible (Konduru et al 2012).

Ongoing studies from our lab show that the TRBF values are repeatable in young healthy individuals. In chapter3, the potential influence of grader's experience on TRBF measurements was determined to report the learning effect in using Doppler OCT semi-automated grading software. In addition, we set out to determine the repeatability (variability of measurements obtained by same grader repeatedly grading the same dataset) and reproducibility (variability of measurements obtained by two different graders grading the same dataset) of the TRBF measurements among trained and novice graders.

Systematic analysis of retinal hemodynamic change to inspired gas challenge has been reported by several research groups (Dorner et al. 2002; Luksch et al. 2002; Sponsel et al. 1992; Roff et al. 1999). However, previous research from our lab (Gilmore et al. 2005; Gilmore et al. 2004), established a novel methodology to comprehensively assess retinal hemodynamic changes in healthy (Venkataraman et al. 2006; Venkataraman et al. 2005; Venkataraman et al. 2008) as well as in diseased cohorts to various hypercapnic and hyperoxic gas provocations (Venkataraman et al. 2010), (Gilmore et al. 2007).

Little is known about the hemodynamic effects of cigarette smoking on retinal autoregulation. Studies on retinal vascular regulation in smokers remain controversial (Morgado et al. 1994; Wimpissinger et al. 2005). Langhans and co-workers (Langhans et

al. 1997) showed reduced retinal capillary reactivity to hyperoxia in smokers, whereas Wimpissinger and co-workers (Wimpissinger et al. 2004) reported that the retinal vascular reactivity in response to carbogen (5% CO_2, 95% O_2) remains unaltered in smokers. This necessitates the need to study whether smoking is paralled by a decreased, increased or unaffected retinal blood flow and vascular regulation using a standardized hypercapnic provocation.

In chapter 4, retinal blood flow and vascular reactivity was investigated in young healthy smokers. Both acute and chronic effect of smoking was studied using Doppler SD-OCT methodology to comprehensively quantify total retinal blood flow, by achieving a more standardized and stable provocation of retinal vascular reactivity via constant changes in end tidal gas concentrations (i.e. $P_{ET}CO_2$ and in $P_{ET}O_2$ level).

2.2 Hypothesis

The study hypothesis for chapter 3 is that there will be a significant difference in total retinal blood flow measurements between trained and novice graders achieved using semi-automated Doppler optical coherence tomography of retinal circulation (DOCTORC) software.

The hypothesis for chapter 4 is that the retinal vascular reactivity to inhaled carbon dioxide will be reduced in otherwise healthy subjects who smoke when compared to non-smoking age-matched controls. The impact of both acute (after smoking) and chronic (before smoking) cigarette smoking on total retinal blood flow measurement has not been simultaneously assessed on young healthy individuals who smoke.

2.3 Aims

The aim of chapter 3 is to investigate

1) The learning effect among novice graders

2) The reproducibility of retinal blood flow measurements between two graders

and

3) The repeatability of retinal blood flow measurements derived using semi-automated DOCTORC analysis software.

The specific aim of chapter 4 is to determine the effect of normoxic hypercapnia on retinal blood flow in individuals who smoke using Doppler SD-OCT, a new non-invasive technique to visualize and quantify total retinal blood flow. The study defines both the acute and chronic effect of cigarette smoking on retinal blood flow and vascular reactivity.

3 Grader learning effect and reproducibility of Doppler spectral domain optical coherence tomography derived retinal blood flow measurements

3.1 Introduction

Though retinal circulation is directly observable, quantitative non-invasive measurement of retinal blood flow was not possible until the evolution of laser Doppler techniques. Laser Doppler techniques enable the non-invasive quantitative absolute measurement of the speed of moving red blood cells (RBCs) in a blood vessel (Feke et al. 1987). This technique is based on the principle of the 'Doppler Effect'. The laser light incident on a stationary target (e.g. vessel wall) as well as moving particles (e.g. RBCs) gets scattered. The scattered light from the stationary target remains unaltered where as those scattered from moving particles is shifted in frequency.

Laser Doppler velocimetry (LDV) measures the velocity of moving red blood cells. In order to determine volumetric flow rate in major retinal vessels, the diameter of retinal vessels is also necessary. Researchers have previously measured blood vessel diameter from a magnified retinal image (Riva and Feke 1981). By summing the blood flow measurements from individual retinal arteries or veins the total retinal arterial or venous blood flow rate was calculated. Though this method of estimating volumetric retinal blood flow is reliable and reproducible (Riva et al. 1985), it should be emphasised that blood vessel diameter measured from an enlarged retinal image might be prone to measurement error induced by magnification.

Unlike the laser Doppler velocimetry, which is restricted to velocity measurements; the CLBF combines the laser Doppler technique (for velocity measures) with simultaneous vessel densitometry (for diameter measures), to quantitate centerline blood velocity (mm/s) as well as vessel diameter (μm) of retinal arterioles and venules. To ensure the consistency of velocity measurements obtained using CLBF, it uses a unique bi-directional technique, i.e. the difference in Doppler shift is recorded via two photo-detectors simultaneously. The calculated difference is used to determine the absolute velocity of moving red blood cells. The CLBF utilizes a vessel tracking mechanism to ensure the fixation stability during the measurements. Reliable and reproducible CLBF measurements were achieved by several research groups (Guan et al. 2003), (Garcia et al. 2002), (Yoshida et al. 2003). However, obtaining total retinal blood flow measurements using this technique seems to be restricted to retinal vessels with a cross-sectional diameter of less than 60 μm, and to specific arteriolar or venular site (Yoshida et al. 2003).

Recently, Garhofer and co-workers (Garhofer et al. 2012) studied total retinal blood flow in a group of young healthy subjects using bi-directional laser Doppler velocimetry (for velocity measurements) and the dynamic retinal vessel analyser (DVA) (for diameter measurements). In their study, only retinal vessels of diameter greater than 60 μm were included for total retinal blood flow calculation. The authors have further mentioned that the LDV technique used in their study, was more time consuming, i.e. requires good fixation stability in order to obtain accurate velocity measurement from all major retinal vessels as well as retinal vessel diameter measurements obtained using DVA needs to be corrected for magnification errors (Garhofer et al. 2012).

Considering the practical difficulties of these measurements techniques in achieving consistent TRBF data, there appears to be a growing need for instruments that are capable of attaining total retinal blood flow measurement with minimum acquisition time as well as optimum consistency. Previous research studies indicate the need for quantification of total retinal blood flow to better understand the pathophysiology of major retinal diseases (Cuypers et al. 2000; Logan et al. 2004).

Doppler Spectral- / Fourier- Domain Optical Coherence Tomography (SD-OCT / FD-OCT) overcome most of the limitations of existing laser Doppler methodologies in terms of retinal blood flow measurements. Doppler SD-OCT offers unparalled image resolution and acquisition time with a wide range of scan protocols and analysis options (Drexler and Fujimoto 2008; Geitzenauer et al. 2011). In addition to revealing precise morphological details of the retina, Doppler SD-OCT also has the potential to give retinal blood flow information in absolute units (µL/min) (Wang et al. 2011; Wang et al. 2008).

Huang and co-workers (Wang et al. 2008) were the first to successfully demonstrate the *in vivo* volumetric retinal blood flow measurement in humans using Doppler SD-OCT. The total retinal blood flow values obtained using Doppler SD-OCT were reported to be reproducible in a group of healthy individuals and these values were also found to be within the range of laser Doppler flowmeter derived retinal blood flow values. However it should be noted that these values are lower than retinal blood flow values that were previously reported using the CLBF (Feke et al. 1989; Garcia et al. 2002).

By combining the principles of laser Doppler velocimetry and optical coherence tomography, Doppler SD-OCT provides both structural and functional information of the retina. In Doppler SD-OCT, the absolute flow velocities of red blood cells and cross sectional area of the blood vessel are determined from the three dimensional structural OCT image of the retina, thus enabling quantification of total retinal blood flow (Wehbe et al. 2007). This way of achieving TRBF is made possible by using a semi-automated software algorithm named Doppler optical coherence tomography of retinal circulation (DOCTORC), in which retinal vessels are identified automatically by computer algorithms as arteries and veins based on their Doppler signal strength. However, a human grader needs to carefully verify the software defined vessel type with a corresponding fundus photograph of the retina. The cross-sectional areas, position of the vessels within the OCT scans need to be refined by a human grader. Konduru and co-workers (Konduru et al. 2012) reported reproducible retinal blood flow measurements among trained graders, which were achieved using DOCTOC software. However, any potential impact of grader's experience on TRBF measurements needs to be established.

The hypothesis for this study is that there will be a significant difference in total retinal blood flow measurements between trained and novice graders achieved using semi-automated Doppler optical coherence tomography of retinal circulation (DOCTORC) software.

3.2 Materials and Methods

3.2.1 Sample

Two experienced operators acquired Doppler SD-OCT scans from 15 eyes of 15 healthy subjects (mean age 28.13 yrs, SD $\pm$ 4). One eye of each subject was randomly chosen for this study. Refraction, best corrected logMAR visual acuity, intra ocular pressure and resting blood pressure were assessed prior to the dilation of study eye with 1% tropicamide (Alcon, Mississauga, Canada). All subjects had a logMAR visual acuity of 0.0, or better. Subjects with refractive error > $\pm$ 6.00 diopters sphere and / or $\pm$ 1.50 diopters cylinder, history of any ocular disease, history of habitual smoking, cardiovascular disease, systemic hypertension and use of medications with known effects on blood flow such as anti-hypertensive, medications with activity at autonomic receptors, smooth muscles, or those affects nitric oxide release are excluded from the study. All participants were asked to abstain from caffeine and red meat for 12 hours prior to the study visit. This study received approval by the University of Waterloo Office of Research Ethics. Informed consent was obtained from each subject after explanation of the nature and possible consequences of the study according to the tenets of the Declaration of Helsinki.

3.2.2 Operators

At the initial examination, SD-OCT image acquisition for all subjects was made by two trained operators. These two operators were trained in using the RTVue SD-OCT (Optovue Inc., Freemont, CA, USA) and were required to have acquired at least 15 SD-OCT images before beginning data collection for this study. Six repeat scans of the optic nerve head (6

superior and 6 inferior pupil scans) were obtained using the circumpapillary double circular scan protocol of the RTVue SD-OCT. The reason to allow only trained operators to acquire SD-OCT images was to avoid any possibility of learning effect in terms of image acquisition.

3.2.3 Graders

One trained and one novice individual graded the 15 Doppler OCT images based on their Doppler signal strength and vessel area estimation using DOCTORC (Centre for Ophthalmic Optic and Lasers, CA, USA) software. The trained grader underwent formal training in using DOCTORC software at the *Doheney Eye Institute*, CA. The trained grader had successfully graded 20 practice cases and several additional subject datasets. The novice grader had no previous grading experience but was trained to understand the DOCTORC grading manual and the basic principles of grading from a trained grader.

3.2.4 Sessions

Each grader graded 15 Doppler OCT images in two sessions separated by a time interval of one week. The novice grader analysed five standard practice datasets established by the *Doheney Eye Institute*, CA in practise session 1 before beginning to grade 15 subject datasets for the study (session 1). After session 1, the novice grader received additional training grading 15 more practice datasets (practice session 2). Following the completion of practice session 2, the novice grader then re-graded the same 15 subject datasets (session 2). A schematic illustration of grading sessions sequence is shown in figure 3.1.

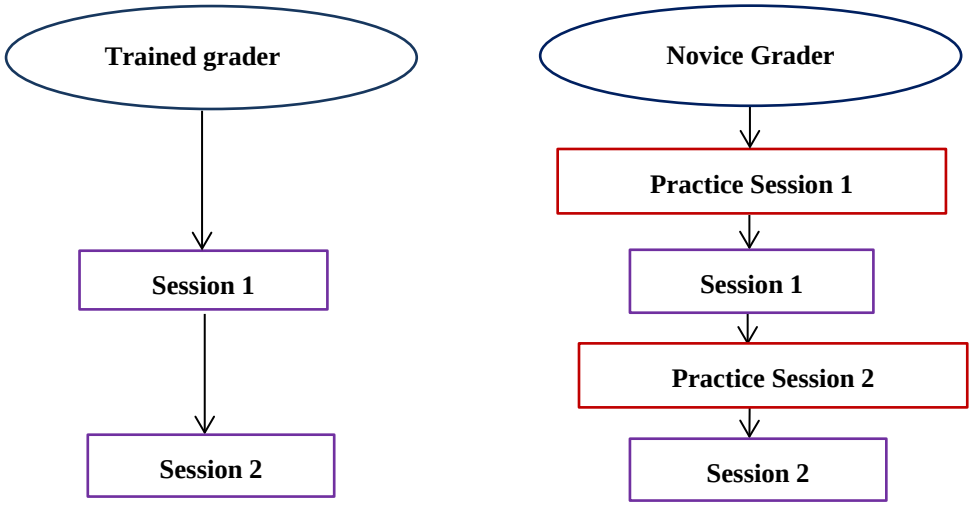

Figure 3.1 Illustration of the grading sessions included in the study.

3.2.5 Doppler SD-OCT

The Doppler spectral-domain OCT is a novel imaging technique capable of providing the *in vivo* non-invasive assessment of retinal hemodynamics. The principle of 'Doppler Effect' has been incorporated into the commercially available Optovue RTVue SD-OCT (Optovue Inc, Freemont, CA). Laser light scattered from a stationary object such as a vessel wall remains unaltered in frequency while light reflected by moving red blood cells inside the vessel incurs a shift in frequency (f_d). The relationship between Doppler frequency shit and velocity of red blood cells is given by

$$f_d = \frac{2nv_a}{\lambda_o} \cos\theta \qquad \textbf{(3.1)}$$

where n is the refractive index of the medium, v_a is the absolute velocity of moving red blood cells, and λ_0 is the central wavelength of the light source and ɵ is the Doppler angle (Wehbe et al. 2007). In order to calculate the absolute velocity from the measured Doppler

shift of moving red blood cells, Doppler angle need to be known. In SD-OCT, Doppler angle is calculated from the acquired three dimensional data, which provides the structural orientation as well as Doppler signal information of retinal vessels within subsequent Doppler scans acquired around the optic disc using the RTVue SD-OCT.

The scan protocol for retinal blood flow measurement consist of double circular Doppler scans in the form of two concentric rings of diameters 3.4 and 3.75mm centered on the optic nerve head, transecting all major branch retinal arteries and veins (Konduru et al. 2012) (Figure 3.2). For image acquisition, the double circular OCT beam passes through the pupil nasally to acquire two sets (i.e. 6 scans in each set) of Doppler scans superiorly and inferiorly. The reason behind acquiring two sets of scan is to ensure good quality as well as to achieve optimum flow measurement from atleast one of the two sets of scans. In the real time display of the scan, the OCT beam position in the retina could be monitored from the sinusoidal variation in the vertical position of the retina (Figure 3.3).

During each scan 30 to 36 frames of Doppler OCT image are registered for each ring. From the acquired SD-OCT images the Doppler angle is estimated by vessel centre depth difference within two consecutive circular OCT scans. The measured Doppler frequency shift along with the Doppler angle estimation, blood vessel diameter measurement from Doppler OCT image is used to compute absolute red blood cell velocity as well as retinal blood flow measurement (Wang et al. 2008).

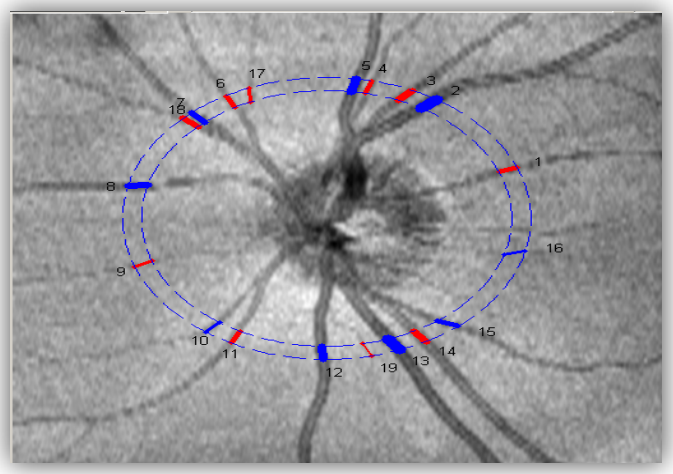

Figure 3.2 En face view of 3D OCT image showing double circular scanning protocol; the retinal vessels are labelled from 1 to 19. The red and blue color represents software identified vessel type as artery and vein respectively based on its Doppler signal.

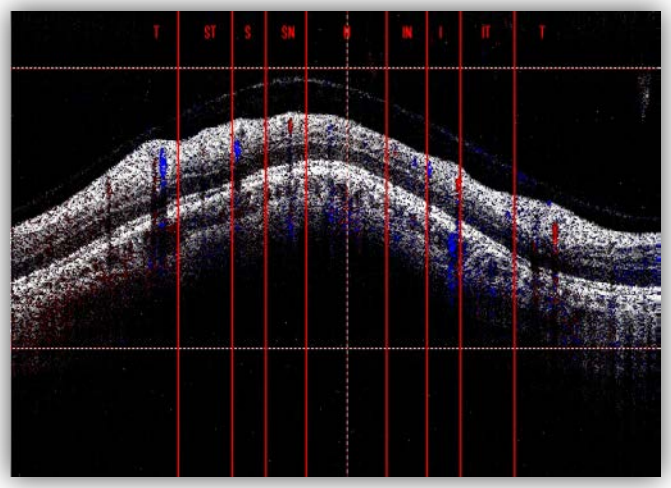

Figure 3.3 Doppler OCT image for OCT beam passing through the superior nasal quadrant of the pupil. The peak of the sinusoidal could be positioned within either superior or inferior quadrant of the pupil i.e. within the respective solid vertical red line as shown in this picture.

3.2.6 Semi-automated Doppler OCT of Retinal Circulation (DOCTORC) software

The acquired Doppler OCT scans along with the three dimensional optic disc SLO (scanning laser ophthalmoscopy) image are exported as raw data using RTVue Doppler transfer output software. The RTVue software converts the exported raw data into DOCTORC grading software (version 2.1.1.4) compatible data for image grading and retinal blood flow calculation (Konduru et al. 2012).

Once the Doppler scan is loaded into DOCTORC, the software does initial automated assessment of the loaded scans, identifies the type of retinal vessel based on Doppler signal (i.e. artery or vein), and registers the Doppler scans with the 3D OCT image and SLO image. This way the grader could correlate the vessels that are identified on the en face image with those seen on the cross-sectional Doppler OCT B-scan image. A color fundus photograph of the optic disc is mandatory for grading to ensure whether the automatic vessel identification performed by the DOCTORC is appropriate. Upon successful completion of manual grading of Doppler OCT images, DOCTORC software then computes the blood flow results and automatically exports them into appropriate subject's folder.

3.2.7 Study Procedure

The Doppler OCT images acquired by two experienced operators on 15 young healthy subjects were included for the study. The Doppler OCT scans were uploaded into the DOCTORC software for image grading and analysis. Both the trained and novice graders graded the images twice separated by a time interval of one week. The grading sessions

conducted in this study are explained in section 3.2.4. Both the graders manually selected every software identified vessel and graded them based on its Doppler signal strength, size and location between inner and outer rings, clarity of the vessel boundary, and then verified the type of vessel. From the cross-sectional B-scan Doppler image, the grader adjusted the blood vessel circumference using a dotted circle and diameter using a horizontal solid line (Figure 3.4). A confidence score ranging from 0 to 5 (*Doheney Eye Institute*, CA) was assigned by the grader to each vessel on every scan based on all the above mentioned parameters.

Once the grading procedure is completed for all the visible retinal vessels in the Doppler OCT image, the software verifies whether or not the flow calculation for each graded vessel is valid, i.e. the veins included for the total retinal venous blood flow calculation should be atleast 50% or more of the total vein area; if not the blood flow result from that eye is considered unreliable. The grader must also carefully check if the flow (µL/min), velocity (mm/sec), and area (mm^2) for all the graded vessels is anatomically acceptable; for example, smaller vessels must have a relatively smaller speed and lower flow compared to larger vessels. In the case where a particular vessel receives a poor confidence score, flow estimation could be made based on its vessel diameter measurement using the mean flow speed of all valid veins.

Following the validity check by DOCTORC software, the total retinal venous blood flow was automatically computed by summing all calculated flow values from all valid veins and the estimated flow from invalid veins (Konduru et al. 2012). Finally an excel file

comprising of retinal blood flow parameters achieved including total retinal venous blood flow (µL/min), superior and inferior hemisphere venous blood flow (µL/min), superior and inferior venous area (mm^2), venous velocity (mm/sec), arterial area (mm^2) and arterial velocity (mm/sec) and were exported into the subject's folder respectively.

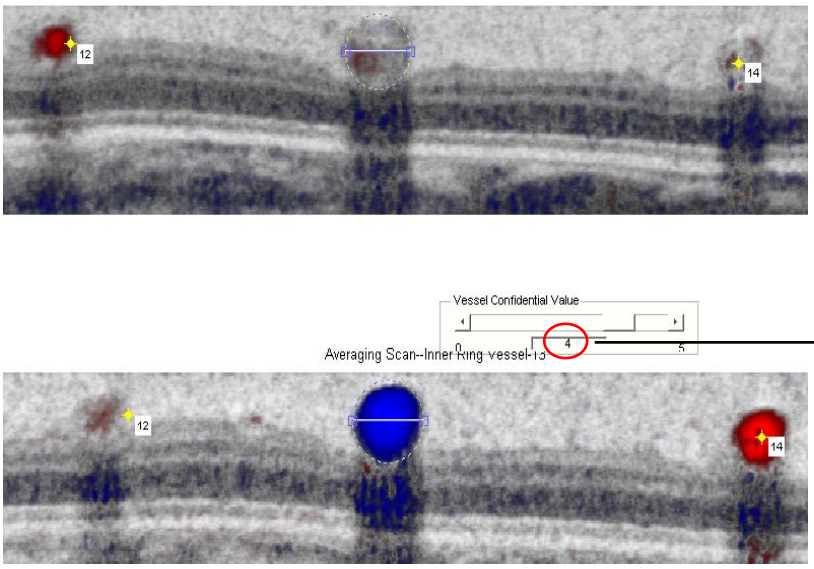

Figure 3.4 Cross-sectional image of blood vessel showing Doppler signal. Grader adjusts the vessel circumference using dotted circle and diameter using horizontal solid line.

3.2.8 Statistical Analysis

The mean total retinal blood flow (TRBF), venous area measurements of the trained grader was used as the standard to analyse any 'learning effect' for the novice grader. The mean values achieved by each grader during each session are plotted against the grading session. The mean and standard deviation for retinal blood flow parameters including TRBF, superior and inferior venous area, superior and inferior hemisphere blood flow, venous velocity, arterial area and arterial velocity measurements for the novice and trained graders for session 1 and session 2 were analyzed using one way analysis of variance (ANOVA).

To quantify the reproducibility of repeated measurements obtained by the same grader, by different graders, and at different sessions, the repeatability and reproducibility were determined. The limits of agreement between graders and sessions were illustrated using Bland-Altman plots. Intra class correlation was also calculated (a value close to 1 indicates good reproducibility). For a trained grader, the co-efficient of variability (SD/mean in %) for TRBF and venous area measurement was assessed for sessions 1 and 2.

The coefficient of repeatability was defined as 1.96 times the standard deviation of the differences between pairs of measurements in the same subject obtained during the same visit by the same observer divided by the average of the measurements of each pair of readings. The coefficient of reproducibility was defined as 1.96 times the standard deviation of the difference between measurements obtained from the repetition of the test under different conditions (change of observer or visit) divided by the average of the

measurements. As the differences follow a normal distribution, 95% of the differences will lie between -1.96 SD and +1.96 SD (Martin Bland and Altman 1986). Statistica software (StatSoft, Inc., Tulsa, OK, USA) version 11.0 and Medcalc software (trial version 11.5.0) was used for analysing the data. A p value of < 0.05 was considered to be significant.

3.3 Results

Doppler scans analysed by both the trained and novice grader acquired from a total of 15 eyes of 15 healthy subjects (mean age 28.13 yrs, SD $\pm$ 4) were included for the data analysis.

3.3.1 Learning effect

Figure 3.5 & 3.6 shows mean TRBF and venous area measurements achieved by both the trained and novice grader in session 1 and session 2 respectively. In session 1, the TRBF achieved by a novice grader was 42.22 $\pm$ 6.74 µL/min and by a trained grader was 46.04 $\pm$ 9.81 µL/min. Of all the other retinal parameters included for the data analysis, the learning trend was statistically significant for venous area measurements (ANOVA, p=0.03), but not significant for TRBF measurements (ANOVA, p=0.22). Both inferior (ANOVA, p=0.00) and superior (ANOVA, p=0.02) venous area measurements by the novice grader were statistically significant from those achieved by a trained grader (Table 3.1). Since a significant learning effect was observed, session 1 results were not considered for analysing reproducibility between two graders.

PARAMETER	Trained Grader Mean ± SD (Range)	Novice Grader Mean ± SD (Range)	p-value (ANOVA)
TRBF (µL/min)	46.04 ± 9.81 (30.78 - 64.21)	42.22 ± 6.74 (32.02 - 54.92)	0.22
Superior flow (µL/min)	25.25 ± 7.06 (17.41 - 39.82)	22.39 ± 5.65 (14.06 - 35.83)	0.23
Inferior flow (µL/min)	20.79 ± 6.66 (10.11 - 34.57)	19.83 ± 4.65 (12.59 - 26.53)	0.65
Venous area (mm^2)	66.58 ± 12.88 (48.30 - 93.74)	56.98 ± 10.13 (43.75 - 75.81)	0.03
Superior venous Area (mm^2)	35.58 ± 6.80 (21.79 - 46.77)	30.02 ± 6.08 (21.14 - 41.31)	0.02
Inferior venous Area (mm^2)	31.00 ± 9.26 (14.68 - 50.99)	26.96 ± 5.82 (18.78 - 37.20)	0.00
Venous velocity (mm/s)	11.68 ± 2.33 (7.53 - 16.97)	12.61 ± 2.70 (9.35 - 18.96)	0.32
Arterial area (mm^2)	42.64 ± 6.80 (32.29 - 58.24)	40.7 ± 8.44 (27.92 - 61.96)	0.30
Arterial velocity (mm/s)	17.94 ± 4.55 (11.04 - 26.07)	17.88 ± 4.51 (12.60 - 29.72)	0.97

Table 3.1 Comparison of mean, SD (standard deviation) of retinal blood flow parameters among graders for session 1. The p-values designate the significance of any change in retinal blood flow parameters between trained and novice grader. Level of significance was set to $p<0.05$

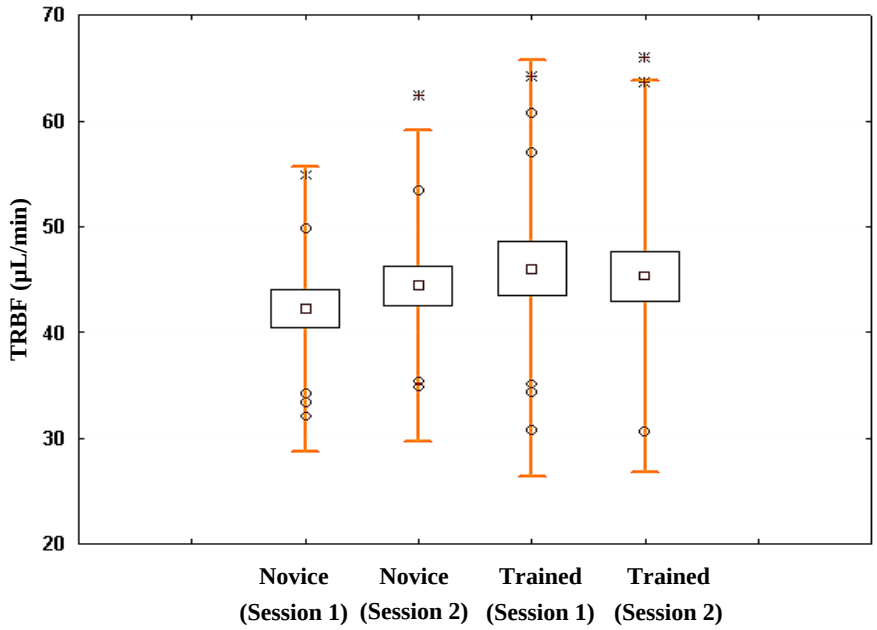

Figure 3.5 Mean total retinal blood flow (µL/min) achieved by novice and trained grader in session 1 and session 2 respectively.

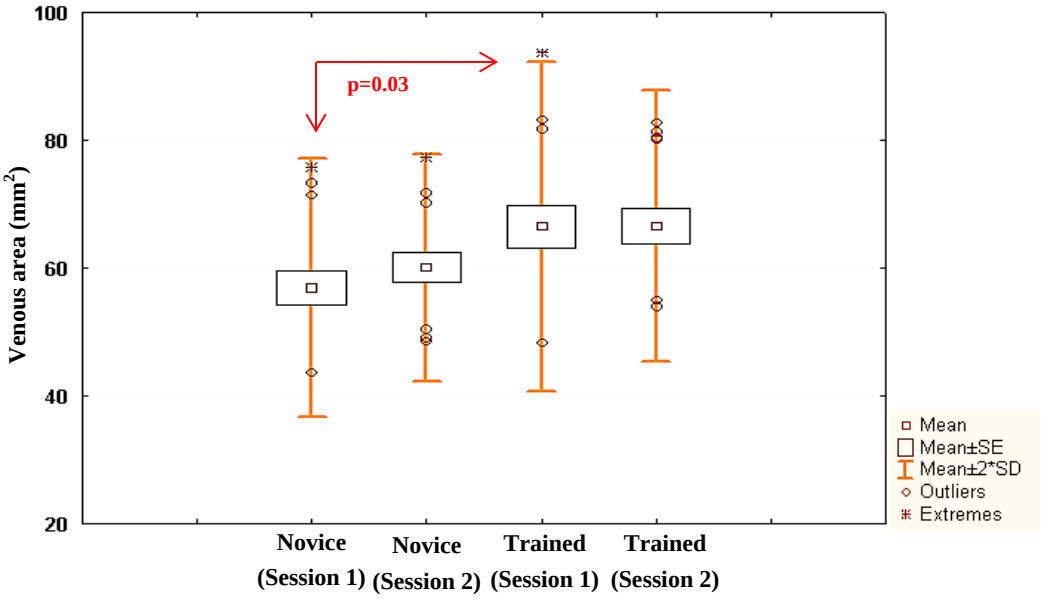

Figure 3.6 Mean venous area (mm^2) achieved by novice and trained grader in session 1 and session 2 respectively. Session 1 results show a significant difference in venous area measurements between trained and novice grader.

3.3.2 Inter grader reproducibility

In session 2, both the trained and novice grader showed no statistically significant difference in TRBF (ANOVA, p=0.77 and ICC of 0.935) and venous area (ANOVA, p=0.07 and ICC of 0.953) measurement (Figure 3.7 & Figure 3.8). The venous velocity (ANOVA, p=0.17), arterial area (ANOVA, p=0.14) and arterial velocity (ANOVA, p=0.48) were also not significantly different among graders. The mean TRBF for session 2 for the trained and novice grader was 45.29 $\pm$ 9.28 µL/min and 44.39 $\pm$ 7.36 µL/min respectively. The COR for retinal blood flow parameters achieved by two graders are shown in Table 3.2. The average confidence score (score of 0.5 to 1 indicates ideal grading score) achieved by both graders for each of 15 eyes graded during session1 and sessions2 are shown in figures 3.9 & 3.10. Following the second practice session, the TRBF and venous area measurements achieved by a novice grader was in good agreement with a trained grader. Figures 3.11 & 3.12 show the Bland – Altman plots with limits of agreement for TRBF and venous area measurements respectively.

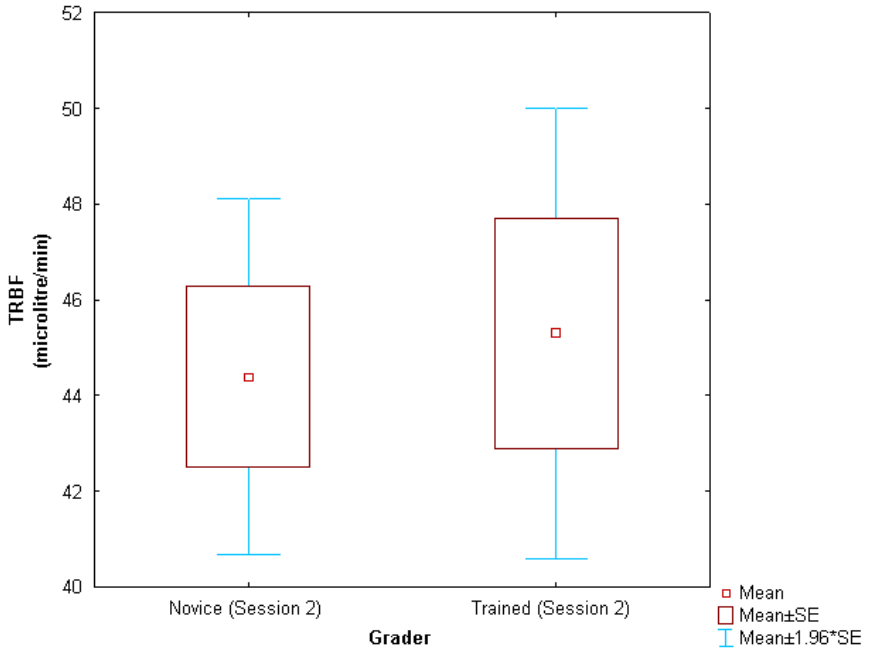

Figure 3.7 Box plots illustrating mean TRBF measurement (µL/min) achieved by trained and novice grader for session 2.

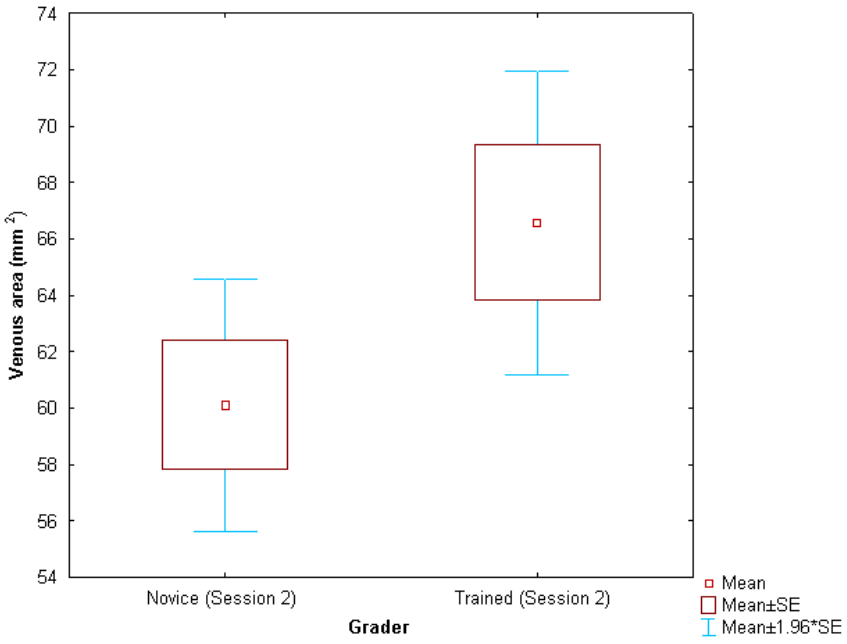

Figure 3.8 Box plots illustrating mean venous area (mm^2) measurement achieved by trained and novice grader for session 2.

PARAMETER	Trained Grader Mean ± SD (Range)	Novice Grader Mean ± SD (Range)	COR	ICC (95% CI)	ANOVA (p value)
TRBF (µL/min)	45.29 ± 9.28 (30.64 - 66.06)	44.39 ± 7.36 (34.81 - 62.41)	8.09	0.935 (0.807 - 0.978)	0.77
Superior flow (µL/min)	24.34 ± 6.43 (14.74 - 36.68)	22.09 ± 4.87 (14.34 - 34.32)	6.89	0.895 (0.687 - 0.964)	0.28
Inferior flow (µL/min)	20.94 ± 5.40 (13.07 - 30.65)	22.30 ± 5.52 (13.38 - 32.31)	4.67	0.950 (0.851 - 0.983)	0.50
Venous area (mm^2)	60.01 ± 8.87 (48.56 - 77.41)	66.72 ± 10.6 (54.04 - 82.86)	8.37	0.953 (0.862 - 0.984)	0.07
Superior venous area (mm^2)	31.21 ± 5.87 (22.4 - 41.16)	35.38 ± 6.77 (24.2 - 46.31)	5.72	0.944 (0.833 - 0.981)	0.08
Inferior venous area (mm^2)	28.89 ± 5.82 (18.36 - 39.21)	31.34 ± 6.46 (21.95 - 42.57)	4.52	0.963 (0.891 - 0.987)	0.28
Venous velocity (mm/s)	11.41 ± 2.07 (7.68 - 15.65)	12.40 ± 1.78 (9.28 - 16.18)	1.92	0.931 (0.796 - 0.977)	0.17
Arterial area (mm^2)	43.88 ± 4.39 (38.09 - 53.16)	41.22 ± 5.32 (33.54 - 54.22)	5.13	0.922 (0.769 - 0.974)	0.14
Arterial velocity (mm/s)	17.17 ± 2.75 (11.57 - 22.12)	17.94 ± 3.21 (13.16 - 23.86)	4.98	0.779 (0.344 - 0.926)	0.48

Table 3.2 Session 2 results showing the comparison of mean ± SD (standard deviation) and range of retinal blood flow parameters achieved by trained and novice grader. Coefficient of reproducibility (COR) and ICC (Intraclass correlation) values between two graders is also presented. $p<0.05$ was considered as statistically significant result between two graders.

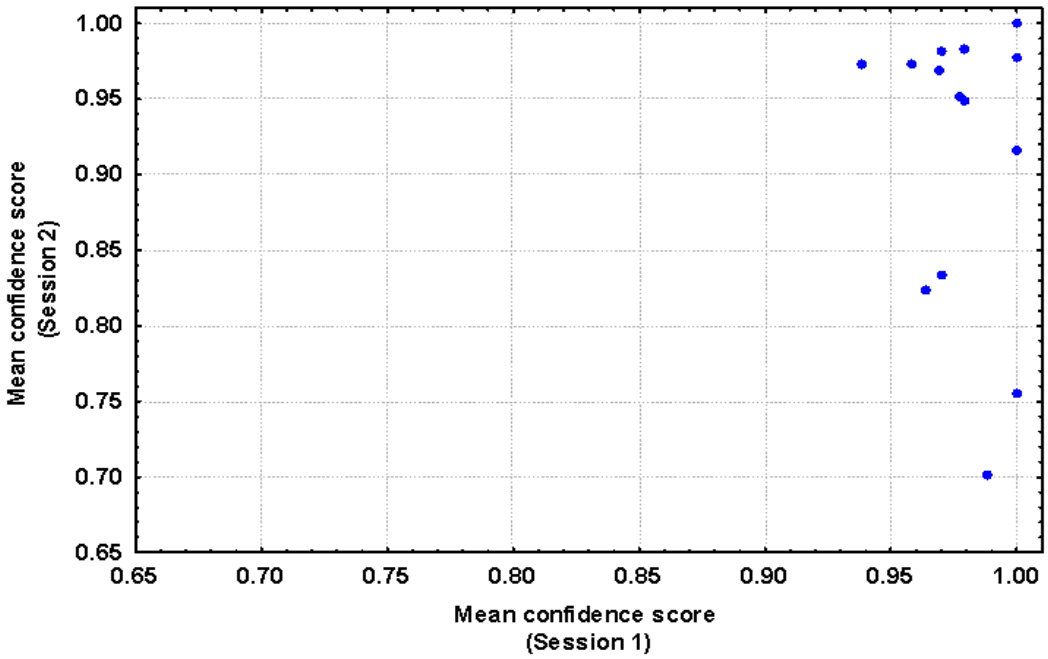

Figure 3.9 Scatterplot illustrating average confidence score for each subject achieved by novice grader in session 1 and session 2 respectively. Blue dots represent datapoints.

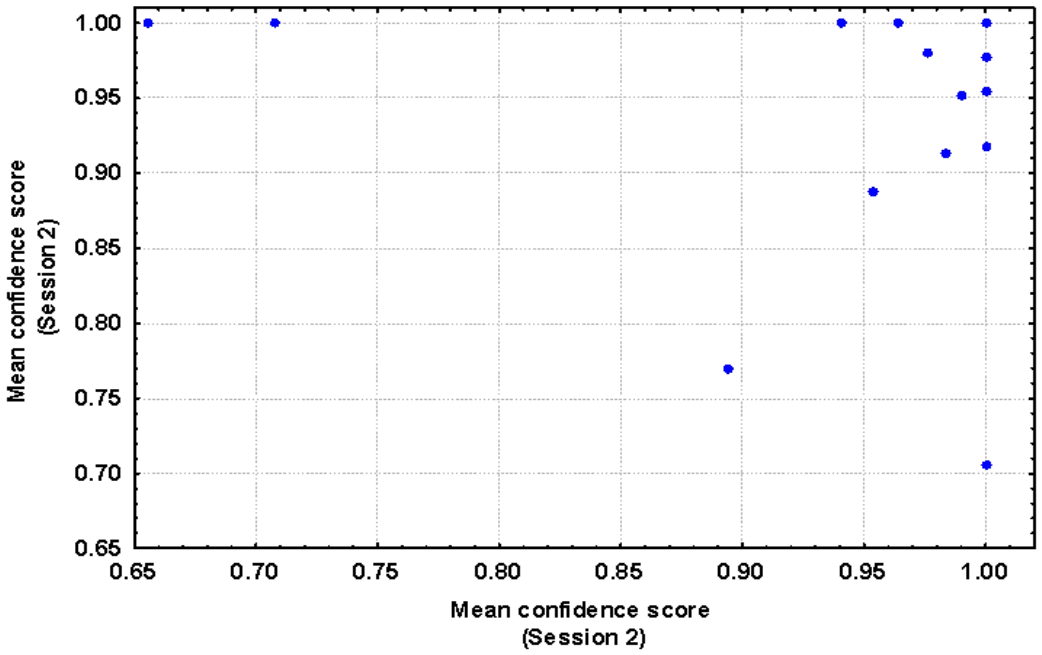

Figure 3.10 Scatterplot illustrating average confidence score for each subject achieved by trained grader in session 1 and session 2 respectively. Blue dots represent datapoints.

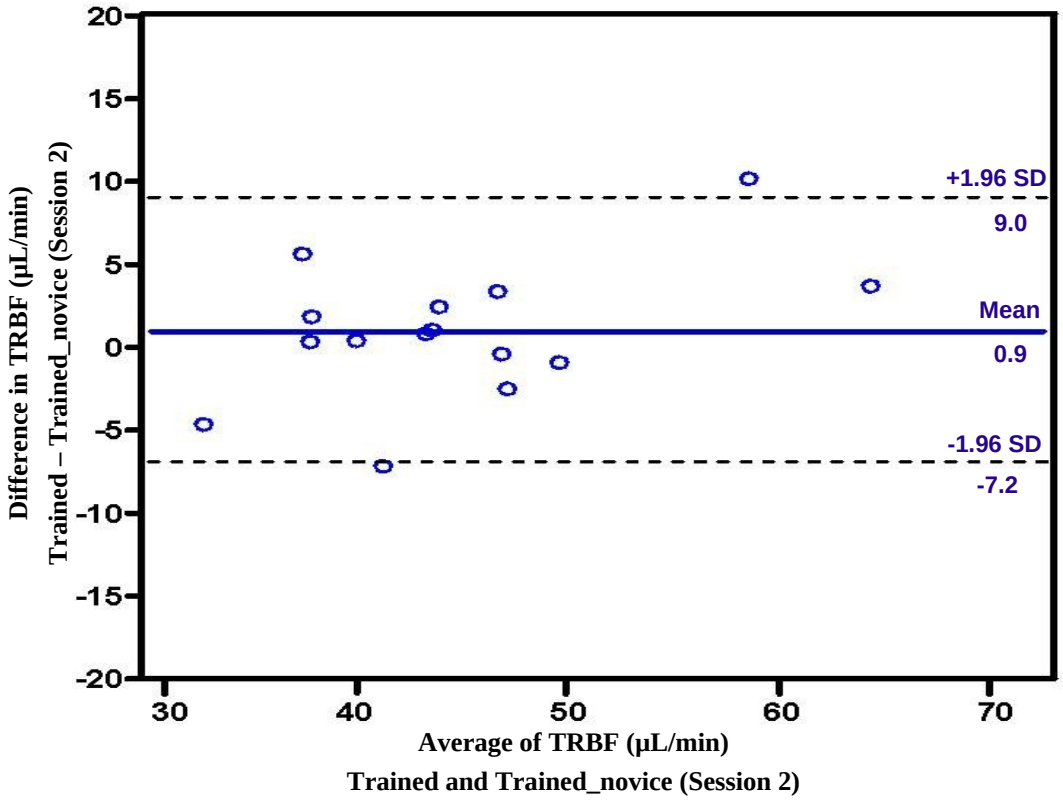

Figure 3.11 Bland-Altman plot of agreement for total retinal blood flow (TRBF) shown as difference in TRBF measurements as a function of average TRBF between trained and novice grader. The solid line in centre indicates mean absolute difference; the dotted line on either side indicates 95% CI limits.

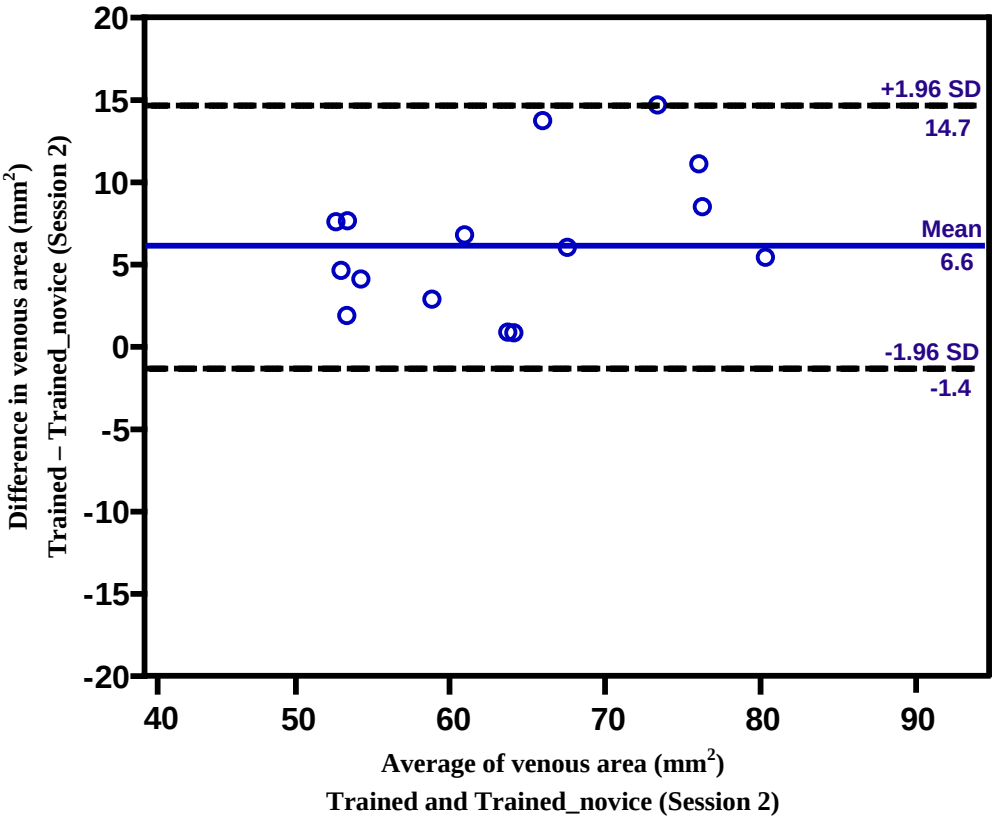

Figure 3.12 Bland-Altman plot of agreement for venous area measurements shown as difference in venous area measurements as a function of average venous area measurements between trained and novice grader. The solid line in centre indicates mean absolute difference; the dotted line on either side indicates 95% CI limits.

3.3.3 Intra grader repeatability

The retinal blood flow parameters achieved by the trained grader in two sessions were used to analyse the repeatability of TRBF measurements achieved using semi-automated DOCTORC software. Figure 3.11 shows a Bland and Altman plot for TRBF measurements achieved by a trained grader in two grading sessions. The overall COV for total retinal blood flow and venous area measurements for a trained grader was 20.90% and 17.64% respectively. The individual CORs (coefficient of repeatability) for TRBF, venous area measurements ranged from 0 – 21.43 µL/min (median 4.06 µL/min) and 0 – 18.75 mm^2 (median 3.69 mm^2). The overall COR for TRBF and venous area measurements was 13.78 µL/min (mean effect 45.67 µL/min) and 12.75 mm^2 (mean effect 66.58 mm^2) respectively (Table 3.3 and 3.4).

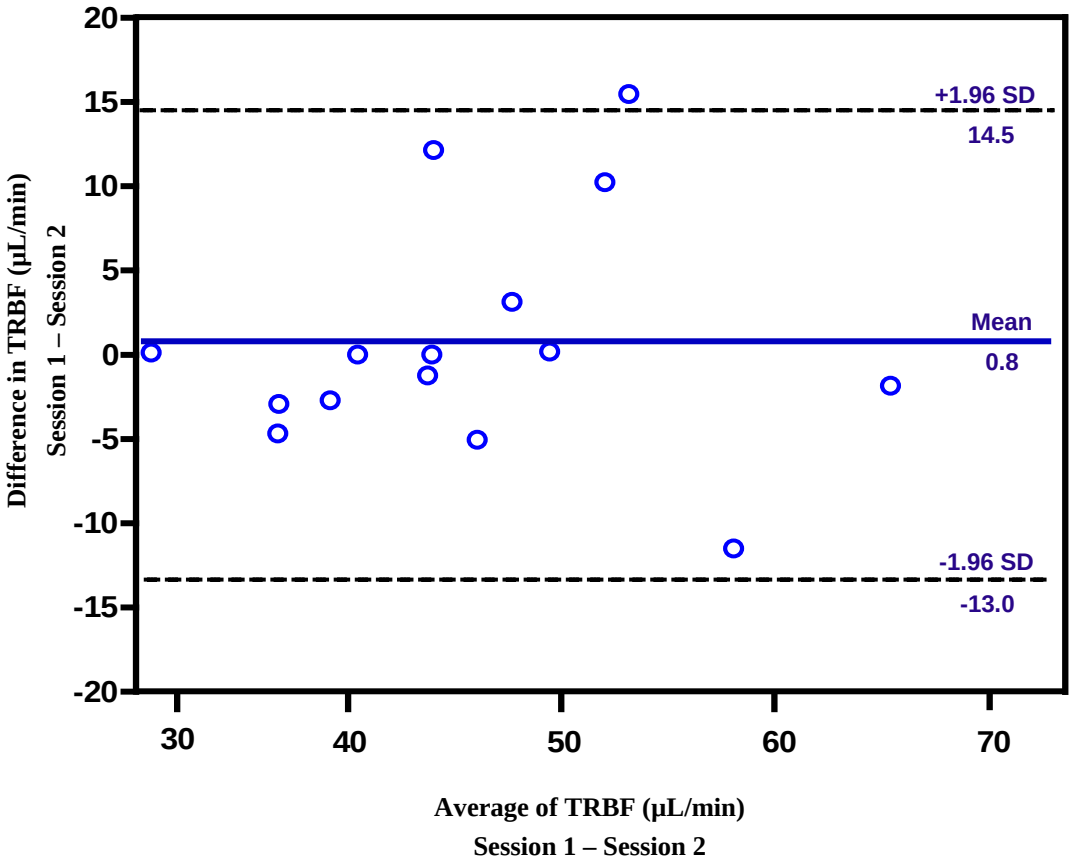

Figure 3.13 Bland-Altman plot of agreement for total retinal blood flow (TRBF) shown as difference in TRBF measurements as a function of average TRBF between sessions of a trained grader. The solid line in centre indicates mean absolute difference; the dotted line on either side indicates 95% CI limits.

PARAMETER	Between sessions	Individual COR		Overall COR	Mean effect
	Difference range	Median	Range		
TRBF (μL/min)	0 – 15.46	4.06	0 – 21.43	13.78	45.67
Venous area (mm^2)	0 – 13.52	3.69	0 – 18.75	12.75	66.58

Table 3.3 Coefficient of repeatability between sessions of a trained grader

PARAMETER	COV (Session 1)	COV (Session 2)	COV (Overall)
TRBF	21.31	20.5	20.90
Venous area	19.34	15.95	17.64

Table 3.2 Coefficient of variability (%) within each session of trained grader and combined

3.4 Discussion

The data from this study suggests that the grader must be thoroughly trained in using DOCTORC software, if not significant error might be introduced in terms of TRBF calculation. A novice individual can gain sufficient experience after 20 practice datasets were analysed, when using DOCTORC software. Konduru and co-workers (Konduru et al. 2012) reported that the DOCTORC software could yield excellent reproducibility of TRBF measurements between trained graders. In the current study, we evaluated the grader learning effect as well as repeatability and reproducibility of the total retinal blood flow measurements derived using semi-automated DOCTORC software.

In this study, the grader learning effect was thoroughly investigated. Session 1 results showed significant differences among trained and novice grader in superior and inferior venous area measurements. Though there was no significant difference observed in TRBF measurements, the difference in venous area estimation among graders might possibly influence TRBF values. Interestingly, upon completing the practice sessions, the venous area measurements achieved by a novice grader showed no significant difference from those achieved by a trained grader. However, one or two more sessions should have been conducted in order to look for the consistency of results achieved by a newly trained grader.

The mean total retinal venous blood flow in the present study as measured in 15 healthy individuals was 45.29 µL/min with a SD of 9.28 µL/min, was comparable with the previously published value of 45.6 (SD 3.8) µL/min using SD-OCT (Wang et al. 2008).

Wang and co-workers (Wang et al. 2008) reported the COV for TRBF measurement to be 10.5% in a sample of ten subjects using Doppler SD-OCT. Recently, Garhofer and co-workers (Garhofer et al. 2012) reported high interindividual variability in total retinal blood flow measurement (44.0 $\pm$13.3 μL/min) using laser Doppler velocimetry. In our study the overall variability of TRBF and venous area measurements between sessions within the same grader was 20.90% and 17.64% respectively.

From a grader's perspective, the reason for the high variability in TRBF and venous area measurements in this study might be due to the fact that the cross-sectional area of retinal vessels, confidence score assigned by a human grader based on the Doppler signal strength, and the positioning of the vessels within the subsequent Doppler scans might not be consistent between two grading sessions. Moreover, the cross sectional area for retinal vessels with poor Doppler signal was estimated based on the intensity shadow of that particular vessel on the B-scan Doppler OCT image. These factors might possibly influence the venous area measurement and the total retinal blood flow calculation.

In the current study, in spite of the fact that the same Doppler OCT scans were graded repeatedly by the same grader (trained), the variability seems to be high for both the TRBF and venous area measurements. This needs to be kept in mind while analyzing Doppler OCT images to derive total retinal blood flow. However, the study limitations are that the learning effect in terms of TRBF measurements has not reached a complete plateau as shown in figure 3.6. Therefore at least two more sessions should have been conducted for both trained and novice graders, in order to completely understand the effect of learning;

only two operators were included in this study, though the operators were well trained, there could be a possibility of inter-operator variability, which was not analyzed; finally, the two graders involved in this study were not independent graders. The trained individual helped the novice grader during the practice sessions so as to improve the grading technique of the novice person. However, both graders performed the grading independently at two separate grading locations.

Recent studies have reported that Doppler SD-OCT measures total retinal blood flow with high speed and optimum reproducibility (Wang et al. 2007; Wang et al. 2009; Wang et al. 2008; Wang et al. 2011). Our data suggests that reproducible and repeatable retinal blood flow measurements could be achieved using DOCTORC software only when a grader is sufficiently trained and completes 20 practice cases before grading the subject data sets. We further emphasis that thorough practice and understanding of semi-automated DOCTORC blood flow analysis is imperative prior to using this novel technique in clinical research.

4 Retinal Blood Flow and Vascular Reactivity in Chronic Smokers

4.1 Introduction

Cigarette smoking is considered to be one of the major risk factors for several ocular diseases. In particular, it is an independent, but avoidable risk factor for Age Related Macular Degeneration (ARMD). Cigarette smoke contains more than 4000 chemicals, 200 poisonous gases and a number of unidentified chemical components (Rodgman and Perfetti 2008). Nicotine and carbon monoxide are identified as two major constituents of cigarette smoke (Smith and Fischer 2001). The cytotoxic effects of free radicals found in cigarette smoke may be the main contributing factor in accelerating smoking-induced disease mechanisms (Burke and Fitzgerald 2003).

Smoking enhances the generation of free radicals and decreases the level of antioxidants in the blood circulation. This places the eye at increased risk to damage due to elevated oxidative stress and the site of this damage is focused on the retinal pigment epithelium (RPE) - photoreceptor interface where metabolic activity is at its highest (Bertram et al. 2009). A causal relationship between smoking and ARMD (Thornton et al. 2005; Cheng et al. 2000) has been clearly elucidated by many studies; especially the Beaver Dam Study (Klein et al. 1993), Rotterdam Study (Vingerling et al. 1996) and Blue Mountains Eye Study (Smith et al. 1996), all of which report a strong association between current smoking and exudative ARMD. Thus, the effect of cigarette smoking on retinal physiology is of highly relevant clinical interest.

Autoregulation in the purest meaning is defined as the ability of the vasculature to maintain blood flow at relatively constant levels despite moderate variations in perfusion pressure (Guyton and Hall 2000). On the other hand, metabolic autoregulation is the ability of the vasculature to modulate blood flow in order to maintain metabolic components including tissue oxygen and carbon dioxide at relatively constant levels. Metabolic autoregulation is otherwise known as "vascular reactivity" (Guyton 1964). The impact of smoking on retinal autoregulation, vascular reactivity and other ocular retinal hemodynamic parameters in otherwise healthy individuals is controversial. Retinal hemodynamic changes in smokers deserve more attention, since these changes might predispose an individual to sight-threatening ARMD, essentially a disease with a clear vascular component in its patho-physiology.

Provocations with various mixtures of inhaled oxygen and carbon dioxide have been undertaken extensively by our research group in the past to assess retinal vascular reactivity in healthy (Gilmore et al. 2005; Gilmore et al. 2004; Venkataraman et al. 2006; Venkataraman et al. 2008) and diseased cohorts (Gilmore et al. 2007; Venkataraman et al. 2010). It has been shown that both retinal and the cerebral vessels react similarly by constricting to oxygen (O_2) and by dilating to carbon dioxide (CO_2) (Dorner et al. 2002; Kisilevsky et al. 2008; Gilmore et al. 2004; Venkataraman et al. 2006).

CO_2 has been suggested to be more potent than O_2 in provoking vascular reactivity in the retina (Sponsel et al. 1992), although Kisilevsky and co-workers (Kisilevsky et al. 2008) showed the inner retinal circulation to be more sensitive to increased partial pressure of

oxygen than carbon dioxide. The cerebral vessels react to carbon dioxide while showing no significant response to oxygen.

Vascular reactivity to CO_2 has long been used to test retinal and cerebrovascular hemodynamics. It has been shown that, increase in $PaCO_2$ above normal resting values, termed “hypercapnia”, results in vasodilation of retinal vessels, thereby increasing retinal arteriolar blood flow. The loss of retinal vascular reactivity to CO_2 provocation may provide in-sight into disease mechanisms and potential treatments (Venkataraman et al. 2010; White and Markus 1997).

In previous studies on smokers, retinal blood flow and autoregulation was assessed by breathing 100% oxygen (hyperoxia) in diabetic patients and controls using laser Doppler velocimetry before and after smoking. In both groups, smoking induced a marked decrease in retinal blood flow and the ability of retinal vessels to autoregulate immediately after smoking (acute effect), which was more pronounced in diabetics than in healthy controls (Morgado et al. 1994). Only a few studies investigated the chronic or long term effects of cigarette smoking in humans. Langhans and co-workers (Langhans et al. 1997) showed reduced reactivity in retinal and optic nerve head capillaries to hyperoxia in smokers, whereas Wimpissinger and co-workers (Wimpissinger et al. 2005) reported abnormal retinal vascular reactivity of the major retinal vessels to hyperoxia in smokers in terms of the diameter response although the change in retinal blood flow was comparable between the two groups. Smoking has been shown to markedly increase the basal cerebral blood flow by about 25% in humans (Wennmalm 1982). Wimpissinger and co-workers

(Wimpissinger et al. 2004) reported that the response to hypercapnia in chronic smokers is altered in the choroid, but not in the optic nerve or retina. Clearly, the vascular reactivity response of the retina to increase in $PaCO_2$ in chronic smokers needs to be clarified.

The hypothesis for this study is that the retinal vascular reactivity to inhaled carbon dioxide will be reduced in otherwise healthy subjects who smoke when compared to non-smoking age-matched controls. The impact of both acute (after smoking) and chronic (before smoking) cigarette smoking on total retinal blood flow measurement has not been simultaneously assessed on young healthy individuals who smoke.

4.2 Materials and Methods

4.2.1 Sample

The sample comprises ten non-smokers (mean age 28.9 yrs, SD 4.58) and nine smokers (mean age 27.55 yrs, SD 4.77). The sample size calculation was determined after estimating the standardized effect size, i.e. Mean effect / SD, for retinal arteriolar blood flow. The two main studies that have investigated the effect of smoking on retinal vascular reactivity (Wimpissinger et al. 2004; Wimpissinger et al. 2005) have found diverse results, ranging from no difference between smokers and non-smokers to 100% difference. As an initial starting point, we will assume that smoking reduces the magnitude of vascular reactivity by 50%. Based on the results of Venkataraman and co-workers (Venkataraman et al. 2008), the effect of hypercapnia on mean retinal arteriolar blood flow in control subjects is an increase of 24.9% (SD 7%). The Standardised Effect Size = Mean Effect Size / Mean

SD = (100-124.9) * 0.5 / 7 = 1.77. Assuming α=0.05 and a β of=0.90, sample size of n=7 was estimated for each group. Conversely, if smoking reduces the magnitude of vascular reactivity by 25% then the required sample size will be 27.

This study was approved by the University of Waterloo Office of Research Ethics, Waterloo, and by the University Health Network Research Ethics Board, Toronto. One eye of each subject was randomly chosen for this study. All subjects had a logMAR visual acuity of 0.0, or better. Smokers with a smoking history of at least 2 years and who regularly smoked 15-25 cigarettes per day were included. All the non-smoking participants had no previous history of smoking. Exclusion criteria included any refractive error > $\pm$ 6.00 Diopters sphere and / or $\pm$ 1.50 Diopters cylinder, intra ocular pressure > 21mm Hg, treatable respiratory disorders (e.g. asthma), systemic hypertension, cardiovascular disease, diabetes, endocrine disorders, medications with known effects on blood flow (e.g.-anti-hypertensive, medications with activity at autonomic receptors, smooth muscles, or those affects nitric oxide release.), family history of glaucoma, or a history of any ocular disease. All the participants were asked to abstain from caffeine, red meat and alcohol for 12 hours and avoid rigorous exercise about 1 hour prior to their study visit. Informed consent was obtained from each subject after a thorough explanation of the nature of the study and its possible consequences, according to the tenets of the Declaration of Helsinki.

4.2.2 Study visit

The study was performed during a single visit for all participants. However, non-smokers had a single session whereas smokers had two sessions. Each session was approximately

1.5 hour in length. The reason for having two session in the smoker group was to measure both the acute (after smoking) and chronic (after non-smoking period of about 6 hours) effect of cigarette smoking.

4.2.3 Instrumentation

4.2.3.1 Doppler Spectral Domain Optical Coherence Tomography (SD-OCT)

The principle of the Doppler Effect has been incorporated into the commercially available Optovue RTVue OCT (Optovue Inc, Freemont, CA). Laser light scattered from a stationary object such as vessel wall remains unaltered in frequency while light reflected by moving red blood cells inside the vessel wall incurs a Doppler frequency shift (f_d). f_d is a function of the Doppler angle, ɵ, between the scanning beam and direction of flow as well as the velocity of the moving red blood cells, such that the Doppler shift is given by;

$$f_d = \frac{2nV_a}{\lambda 0} \cos \theta \qquad \textbf{(4.1)}$$

where n is the refractive index of the medium, *Va* is the absolute flow velocity, and λ_0 is the central wavelength of the light (Wehbe et al. 2007).

4.2.3.1.1 Instrument set up

The Optovue Doppler SD-OCT system uses a super luminescent diode (SLD) with a center wavelength of 841nm and a bandwidth of 49nm. Its axial resolution is 5.6µm in tissue, while transverse resolution is 20µm as limited by optical diffraction of the eye. Light emitted from the SLD traverses through a beam splitter, and passes into the sample arm

(eye) and reference arm (reference mirror). The reflected light that comes back from these arms create an interference pattern which is captured by a CCD (charge-coupled device) line scanning camera located at the spectrometer output. Fourier transformation of the resulting interference pattern gives the sample depth profile or A-scan through the neural layers of the retina, each of which has differing reflectance properties. The phase difference between sequential axial scans at each pixel is used to determine the Doppler shift (Wang et al. 2009).

4.2.3.1.2 Image acquisition and processing

To acquire the retinal blood flow measurements, the SD-OCT beam is scanned on the retina around the optic nerve head (ONH) using a double circular scanning pattern of radii r_1 = 3.4 mm and r_2 = 3.45 mm in order to determine the angle between probe beam and blood flow (Konduru et al. 2012). Four pairs of Doppler SD-OCT images are sampled in each blood flow measurement during a total recording time of approximately 2 seconds (Wang et al. 2008). There are 3000 axial scans sampled in each circle. Each circle transects all branch retinal arterioles and venules.

Total retinal blood flow is measured by summing up flow in the veins. The venules are identified by their centripetal flow direction. The reason for choosing branch veins for the flow calculation rather than arteries is that the latter have higher flow velocities that can cause excessive phase wrapping and Doppler signal fading (Wang et al. 2008). In Doppler SD-OCT, retinal blood flow is calculated in a semi-automatic fashion (Wang et al. 2007) i.e. among the eight sampled Doppler images, the image that contains the maximum

Doppler signal for each vessel is graded manually for vessel diameter calculation using DOCTORC software (*Doheney Eye Institute,* CA) (Konduru et al. 2012). Following this, total retinal blood flow is automatically derived in absolute units (μL / min). Wang and co-workers reported that the double circular scanning method using Doppler SD-OCT is a rapid and reproducible method to measure total retinal blood flow (Wang et al. 2009).

4.2.3.1.3 DOCTORC software analysis for quantification of total retinal blood flow

The acquired Doppler OCT scans along with the three dimensional optic disc SLO (scanning laser ophthalmoscopy) image are exported as raw data using RTVue Doppler transfer output software. This exported data is further converted to DOCTORC grading software (version 2.1.1.4) compatible data using the ReVue software (Optovue Inc.) and finally loaded into the DOCTORC software for image grading and retinal blood flow calculation. Once the Doppler scan is loaded into DOCTORC, the software does initial automated assessment of the loaded scans, identifies the type of retinal vessel based on Doppler signal (i.e. artery or vein), and registers the Doppler scans with the 3D OCT image, SLO image. From the cross-sectional B-scan Doppler image, the grader adjusts the blood vessel circumference using a dotted circle and diameter using a horizontal solid line. A confidence score ranging from 0 to 5 (*Doheney Eye Institute*, CA) is assigned by the grader to each vessel on every scan based on its Doppler signal strength, size and location between inner and outer rings, clarity of the vessel boundary. The total retinal venous blood flow is automatically computed by summing up calculated flow from all valid veins and the estimated flow from invalid veins (Konduru et al. 2012)

4.2.3.2 Canon Laser Blood Flowmeter (CLBF, model 100)

The CLBF measures retinal blood flow (µL/min) in absolute units. The CLBF uses the Doppler shift to identify the fastest moving blood particles in the center of a retinal blood vessel and then calculates the average velocity. The CLBF is a fundus-camera type device with two photo-detectors and two lasers. Two sequential velocity measurements are achieved using bi-directional technique from the maximum frequency shifts at each photomultiplier along two optical paths (path 1 and path 2), to ensure consistency and to obtain single velocity measurement. A red diode laser (675 nm, 80 µm x 50 µm oval) measures velocity every 0.02 seconds across a 2 second measurement window resulting in velocity-time trace. A green diode vessel tracking laser system (543nm, 1500µm x 150µm rectangle) is used to stabilize the laser position at the measurement site. The vessel tracking system holds the laser in position to compensate for any eye movement while taking measurements (Harris et al. 2008). Diameter measurements are acquired during the first and final 60 *ms* of the 2-s velocity measurement window every 4 *ms*. The CLBF automatically corrects for the magnification effects associated with refractive and axial component of ametropia, to provide absolute measurement of velocity (mm/sec), diameter (µm) and flow (µl/min).

Flow is calculated based on the assumption that the vessel wall has a circular profile and the flow is laminar with parabolic velocity profile (i.e. Poiseuille's law) (Feke 2006). Hence flow through the vessel is calculated using the equation:

$$F = V_{mean} \times S \qquad \textbf{(4.2)}$$

where S is the cross-sectional area of the vessel at the site of measurement; V_{mean} is the mean blood velocity derived as:

V mean = V maximum / 2 **(4.3)**

(constant "2" assumes laminar flow obeying Poiseuille's law).

The repeatability and consistency of the CLBF has been reported by many researchers (Kida et al. 2002; Guan et al. 2003; Rose and Hudson 2007; Yoshida et al. 2003).

4.2.3.3 Gas provocation

The inspired and expired gas challenges were manipulated using a sequential rebreathing circuit. The sequential gas delivery breathing circuit (SGD; Hi Ox^{80}, Viasys Healthcare, Yorba Linda CA) comprises a fresh gas reservoir and an expiratory gas reservoir. Each reservoir is connected to a face mask with separate one-way valves. The face mask covers the mouth and nose of the subject. In turn, the two reservoirs are inter-connected using a positive end-expiratory pressure (PEEP) valve which allows subjects to breathe exhaled gas (i.e. rebreathe CO_2-enriched gas) when the fresh gas reservoir is depleted (Gilmore et al. 2004; Slessarev et al. 2006). The subject's minute CO_2 production and O_2 consumption, gas flow and composition entering the SGD breathing circuit will be attained using an automated gas flow controller (Respiract^{TM}, Thornhill Research, Inc., Toronto, Canada) which is connected to a computer. The distinguishing feature of the SGD and automated gas flow controller over other gas delivery systems is the efficacy in 'targeting' end tidal gas concentrations, such that the software enables the user to repeatedly target $P_{ET}CO_2$ and $P_{ET}O_2$, independent of each other and independent of minute ventilation (Slessarev et al. 2007).

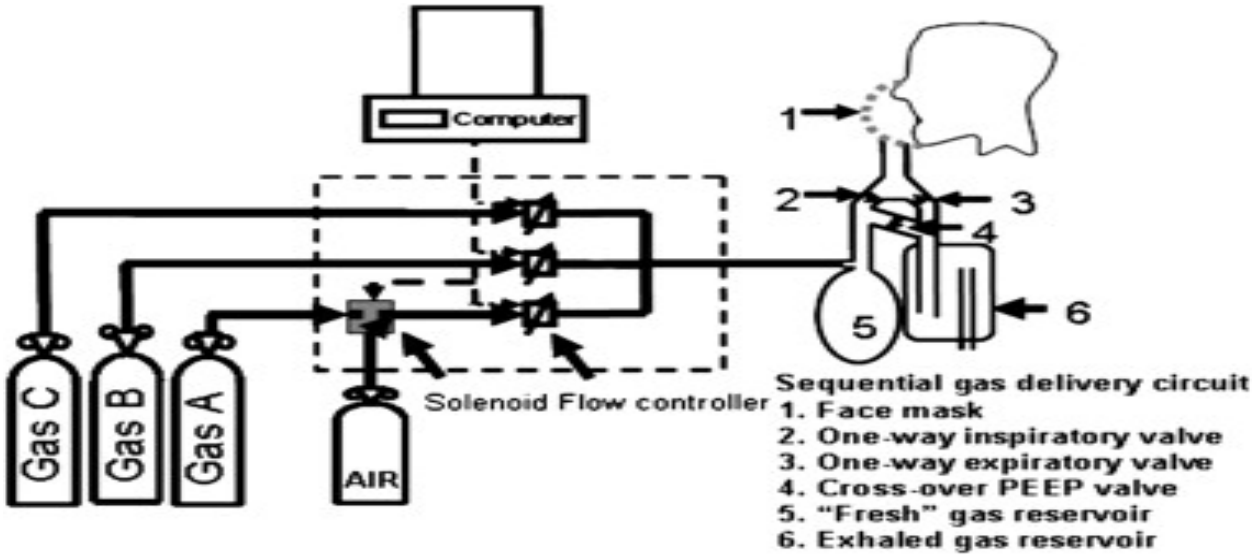

Figure 4.1 Schematic representation of the gas flow controller attached to a sequential gas delivery system (Image reproduced with permission from Elsevier (Exp Eye Res. 2008; 87(6):535-542).

4.2.3.4 Breath carbon monoxide (CO) monitor

CO Sleuth (Breathe E-Z Systems Inc., Leawood, KS) is a simple portable instrument which enables a non-invasive and direct measure of breath carbon monoxide level. The subject breathes out into a disposable mouth piece after holding the breath for 20 seconds. The end-tidal breath sample enters through a non-return valve, and reaches an electrochemical sensor. This novel sensor detects alveolar breath CO concentration, thus enabling the monitor to measure CO level in parts per million (ppm). CO concentration in alveolar breath was found to be highly correlated with blood carboxyhaemoglobin levels (Wald et al. 1981).

4.2.4 Fagerstrom Tolerance Questionnaire (FTQ)

FTQ quantitates the nicotine dependency of a smoker. The daily and frequent pattern of compulsive smoking leads to the categorization of smoker as “dependent” (Fagerstrom and Schneider 1989). The questionnaire has a total of 7 questions regarding the smoking characteristics of an individual (Table 4.1). The FTQ has a scoring range of 0-11 points (Fagerstrom and Schneider 1989). A score of 0 indicates minimum nicotine dependence, whereas a score of 11 indicates maximum nicotine dependence. Under normal smoking condition, sampled CO was studied to be highly correlated with self-reported FTQ scores (Fagerstrom 1982; Tønnesen et al. 1988). The FTQ scoring scale to quantitate nicotine dependence was reported to be valid, reliable and applicable to adolescent smokers (Prokhorov et al. 1996; Prokhorov et al. 1998; Pomerleau et al. 1994).

S.No	Questions	Answers	Score
1.	How many cigarettes a day do you smoke?	> 25	2
		16-25	1
		1-15	0
		<1	0
2.	Do you inhale?	Always	2
		Sometimes	1
		Never	0
3.	Do you smoke more during the first 2 hours of the day than during the rest of the day?	Yes	1
		No	0
4.	How soon after you wake up do you smoke your first cigarette?	<30 min	1
		>30 min but before noon	0
		In the afternoon or evening	0
5.	Which cigarette would you hate to give up?	First one in the morning	1
		Any other before noon	0
		Any other in the afternoon or in the evening	0
6.	Do you find it difficult to refrain from smoking in places where it is forbidden?	Yes	1
		No	0
7.	Do you smoke if you are so ill that you are in bed most of the day?	Yes	1
		No	0

Table 4.1 Fagerstrom Tolerance Questionnaire (obtained permission from Karl Fagerstrom to use the FTQ table for this study (see Appendix))

4.2.5 Procedures

All subjects were made to complete a standard Fagerstrom Tolerance Questionnaire. Log MAR visual acuity (ETDRS log MAR charts) and intra ocular pressures (using the Goldmann Applanation Tonometer) were recorded for both eyes. One eye was randomly selected for the study and dilated with 1.0% Mydriacyl, Tropicamide (Alcon, Mississauga, Canada). Subjects were rested in sitting position for 10 minutes to stabilize baseline cardiovascular and respiratory parameters. Carbon monoxide level in the breath was analysed for all participants using CO Sleuth carbon monoxide monitor (Breathe E-Z Systems, Inc., Leawood, KS). Following that, participants were fitted with a face mask connected distally to the partial rebreathing circuit and the gas sequencer. An automated gas flow monitor connected to the rebreathing circuit was used to sample inspired and expired gases. Retinal blood flow measurements were obtained using Doppler SD-OCT and CLBF, with duration of 45 minutes for each of these methodologies under three following conditions lasting for 15 minutes each:

1). Baseline retinal blood flow (while breathing room air to establish baseline cardiovascular parameters). 2). Retinal blood flow during normoxic hypercapnia (approximately a 15% increase in end-tidal CO_2 relative to the baseline). 3). Retinal blood flow during post-normoxic hypercapnia (while breathing room air to establish recovery from hypercapnia).

Blood pressure, pulse rate and oxygen saturation were monitored continuously during the breathing period using a rapid response critical care gas analyzer (Cardiocap 5, Datex-Ohmeda, Helsinki, Finland). Six CLBF measurements of relatively straight segment of the

superior arteriole, away from bifurcations were acquired during each stage. For total retinal measurement using Doppler SD-OCT, a total of six scans (3 inferior nasal and 3 superior nasal) using 'Double circular scan protocol' were acquired during each breathing condition. The instrument order was randomized between subjects.

For smokers, following completion of session 1 (approx. 1.5 hrs.), a break of 15 minutes was allocated, during which the examiner asked the subject to smoke one full cigarette. After the break, the subject was seated for 10 minutes during which the breath CO level was analysed and subject was fitted again with a face mask and seated comfortably to begin retinal blood flow measurements for session 2. It took almost 30 minutes to start obtaining retinal blood flow measurements after smoking. The order of instruments remained the same as with the previous session. Following completion of the study sessions, a colour fundus photograph of optic disc (Canon non-mydriatic fundus camera, CR-DGI) of the study eye was taken for all participants.

4.2.6 Statistical analysis

A repeated measures analysis of variance (reANOVA) was undertaken to determine any significant change in retinal blood flow and vascular reactivity between smokers and non-smokers in CLBF and Doppler SD-OCT measurements. The dependent variables for CLBF measurements were retinal arteriolar diameter, blood velocity and flow, while the dependent variables for Doppler SD-OCT measurements were total retinal venous blood flow, venous area and venous velocity. In addition separate reANOVA was performed within each group (i.e., smokers and non-smokers) to determine the significance of any change of each dependent variable during baseline, normoxic hypercapnia and recovery. If a significant result was achieved using reANOVA, then post hoc testing was performed using Tukey's HSD (Honestly Significant Difference) test. Significance of change of any systemic and gas parameters including $P_{ET}CO_2$, $P_{ET}O_2$, respiration rate, systolic and diastolic blood pressure, pulse rate and oxygen saturation were also analyzed using reANOVA.

To determine the significance in total retinal blood flow measurements before and after smoking, in a small sample of smokers (n=7), a wilcoxon matched pairs test was performed. Due to small sample size, outliers were also included in the analysis. Carbon monoxide level in non-smokers and smokers (before and after smoking) was compared using one way-ANOVA. Statistica software (StatSoft, Inc., Tulsa, OK, USA) version 11.0 was used for analysing the data. Significance was considered if $p < 0.05$.

4.3 Results

4.3.1 Retinal vascular reactivity and blood flow in non-smokers

A repeated measures ANOVA showed significant increase in retinal arteriolar diameter, blood velocity and flow by +4.1% (SD 2.8, $p<0.0001$), +16.7% (SD 14.6, $p=0.0004$) and +29.6% (SD 12.5, $p<0.0001$) during normoxic hypercapnia (Figure 4.2). Tukey's HSD test revealed significant difference in diameter during hypercapnia relative to baseline ($p=0.0014$) and recovery ($p=0.0002$). Similarly, hypercapnia resulted in a significant difference in velocity measurements relative to baseline ($p=0.0027$) and recovery ($p=0.0006$). Retinal arteriolar flow during hypercapnic provocation was significantly different relative to baseline ($p=0.0001$) and recovery ($p=0.0001$).

Venous area, venous velocity and total retinal blood flow significantly increased during normoxic hypercapnia by 7% (SD 8.6, $p=0.0418$), 18.1% (SD 20.8, $p=0.0068$) and 26% (SD 22.9, $p<0.0001$) respectively, analysed using reANOVA (Figure 4.3). A Tukey's HSD test revealed significant difference in total retinal blood flow during hypercapnia relative to baseline ($p=0.0001$) and recovery ($p=0.0001$). Similarly, hypercapnia resulted in a significant difference in venous velocity measurement relative to baseline ($p=0.0102$) and recovery ($p=0.0204$). Though reANOVA showed a statistically significant difference in venous area measurement during hypercapnia ($p=0.0418$), post hoc testing (Tukey's HSD test) does not show a significant difference in pairwise comparison between baseline and hypercapnia ($p=0.0832$) as well as between hypercapnia and recovery ($p=0.0571$).

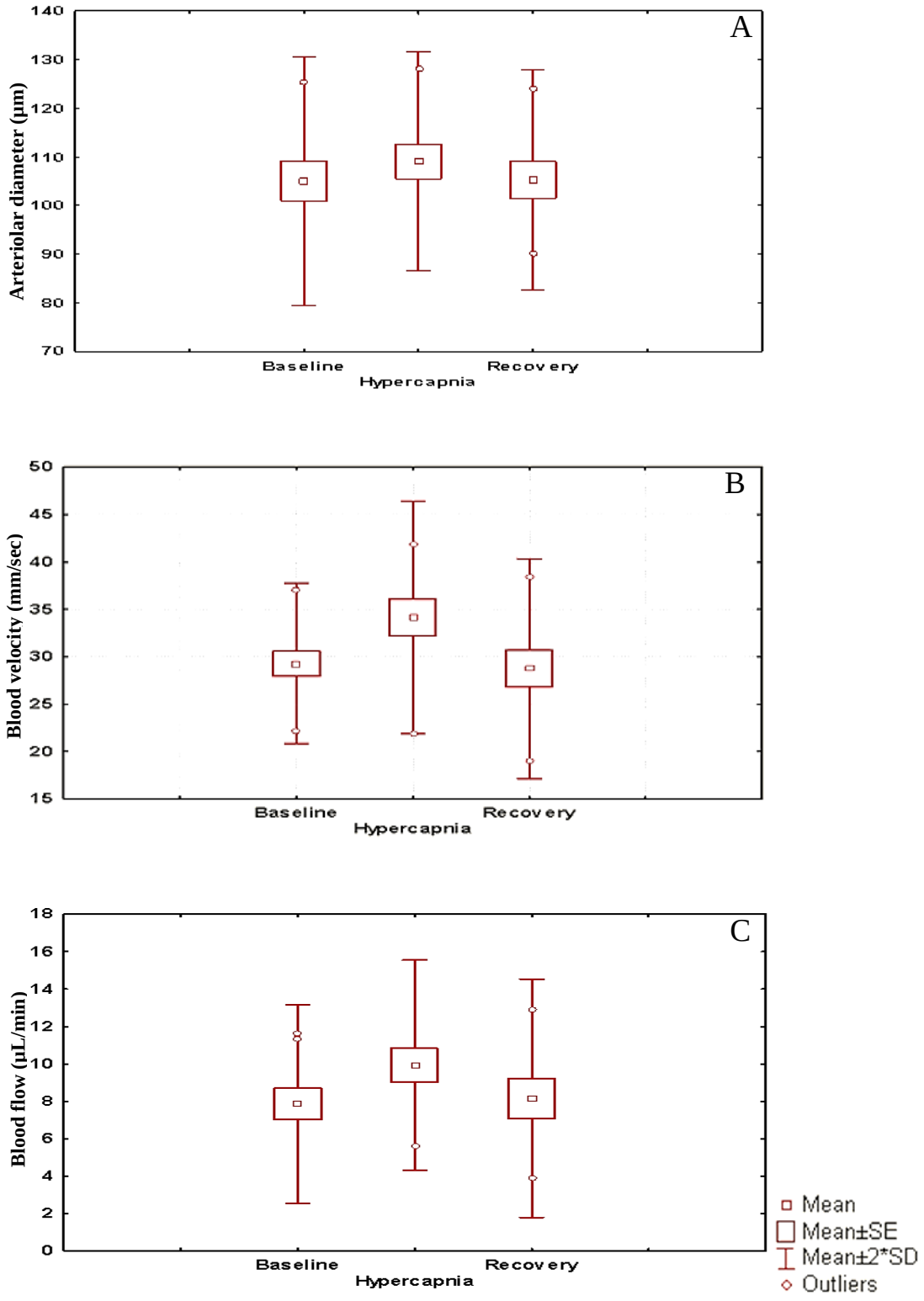

Figure 4.2 Box plots represent A) retinal arteriolar diameter; B) blood velocity; and C) blood flow at baseline, normoxic hypercapnia and recovery in non-smokers.

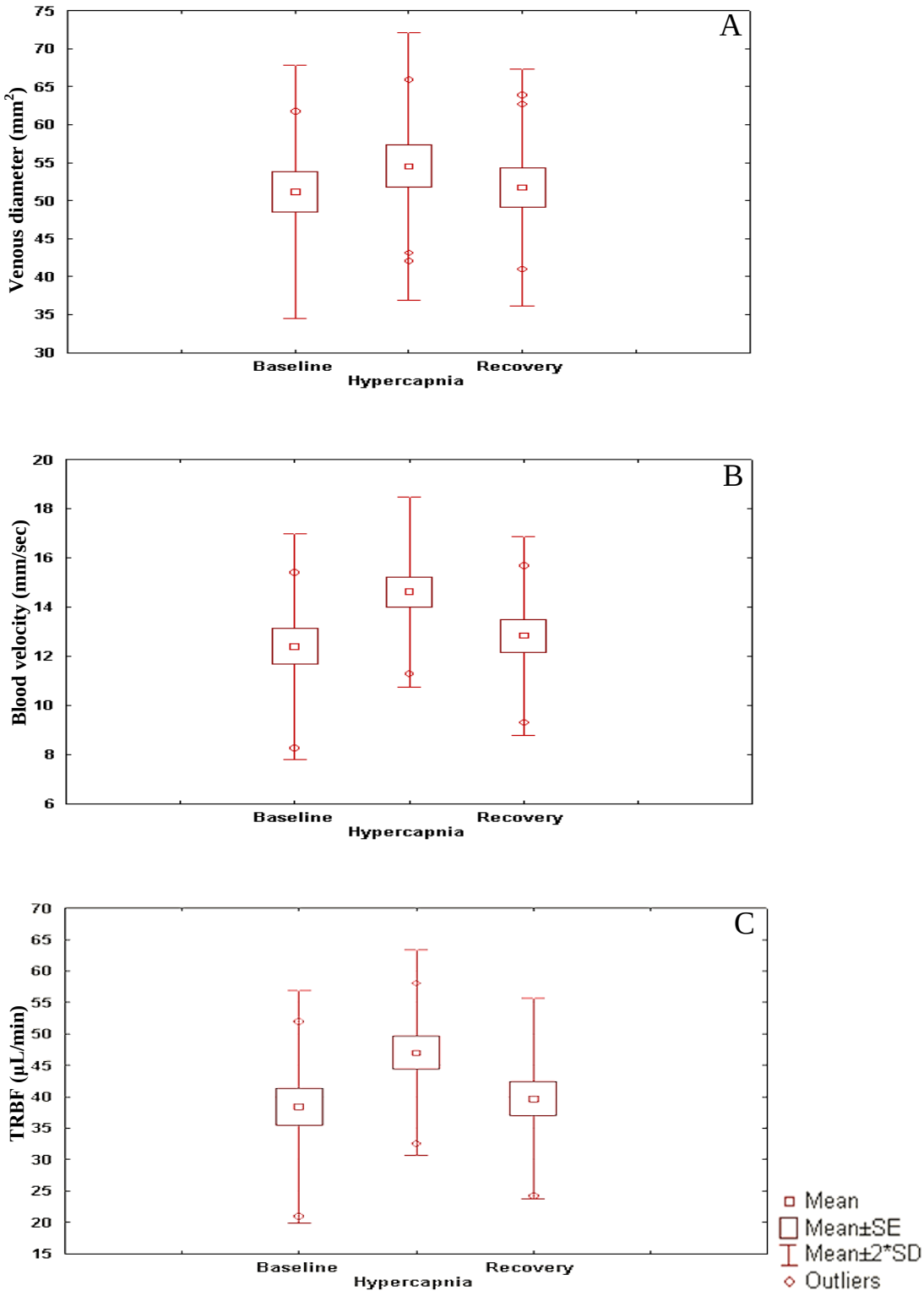

Figure 4.3 Box plots represent A) venous area; B) blood velocity; and C) total retinal blood flow at baseline, normoxic hypercapnia and recovery in non-smokers.

4.3.2 Retinal vascular reactivity and blood flow in smokers

Retinal arteriolar diameter, blood velocity and flow changes during normoxic hypercapnia, were analysed using reANOVA. There was a significant increase in velocity by 12.0% (SD 6.2, p=0.0019) and flow by 14.6% (SD 9.5, p=0.0029), and a non-significant increase in diameter by 1.7% (SD 1.7, p=0.2616) (Figure 4.4). A Tukey's HSD test for pairwise comparison revealed significant difference in blood velocity compared to baseline (p=0.0194) and recovery (p=0.0019). Similarly, there was a significant difference in retinal arteriolar blood flow during normoxic hypercapnia compared to baseline (p=0.0076) and recovery (p=0.0058).

A repeated measures ANOVA showed significant increase in total retinal blood flow (TRBF) by 19.3% (SD 18.4, p=0.002) during normoxic hypercapnia relative to baseline, a Tukey's HSD test showed significant difference in TRBF measurement during hypercapnia compared to baseline (p=0.0035) as well as recovery (p=0.0087). However, there was no significant difference in venous area (p=0.3322) and venous velocity measurements (p=0.1185) during hypercapnia compared to baseline and recovery (Figure 4.5).

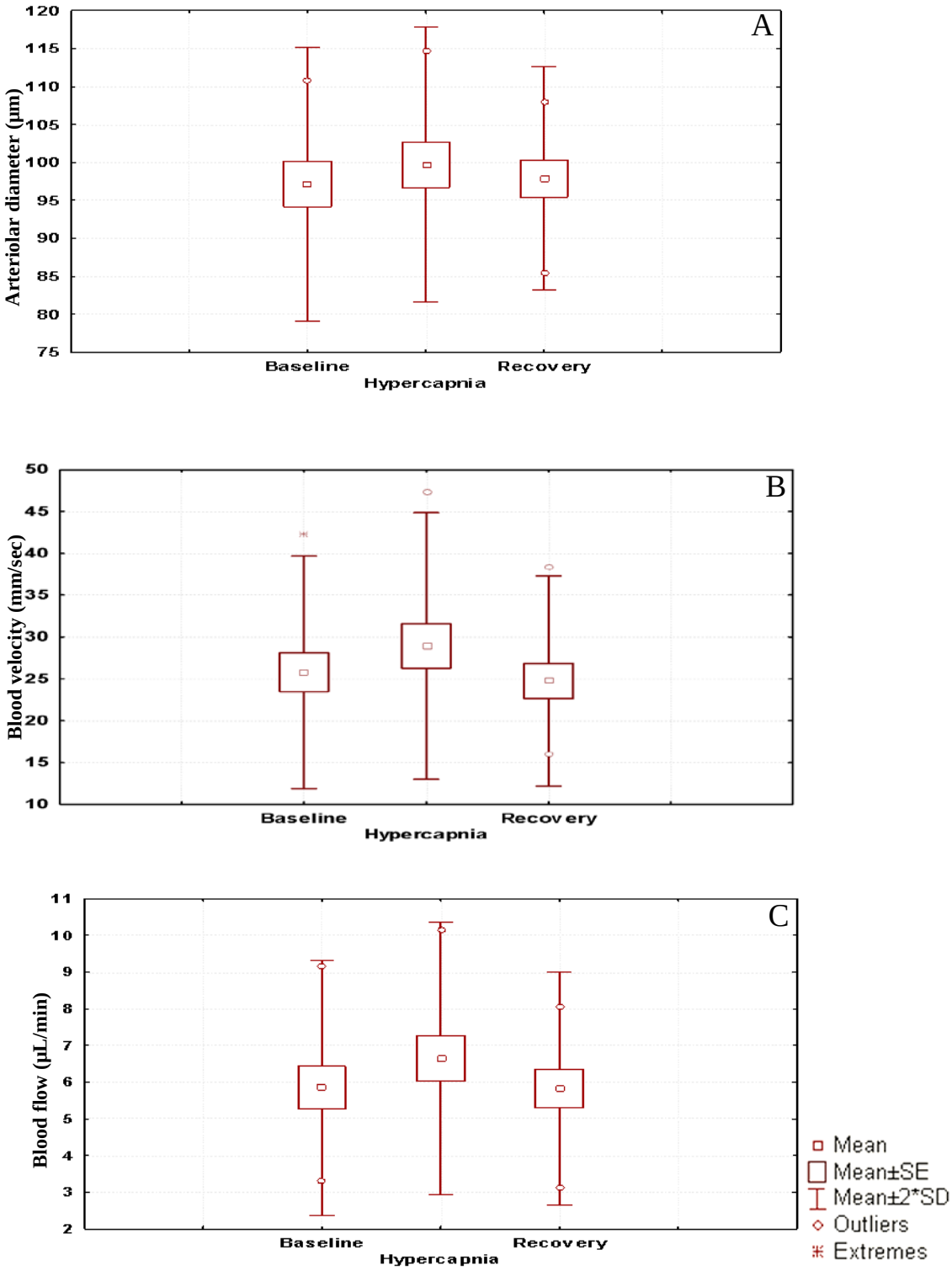

Figure 4.4 Box plots represent A) retinal arteriolar diameter; B) blood velocity; and C) blood flow at baseline, normoxic hypercapnia and recovery in smokers.

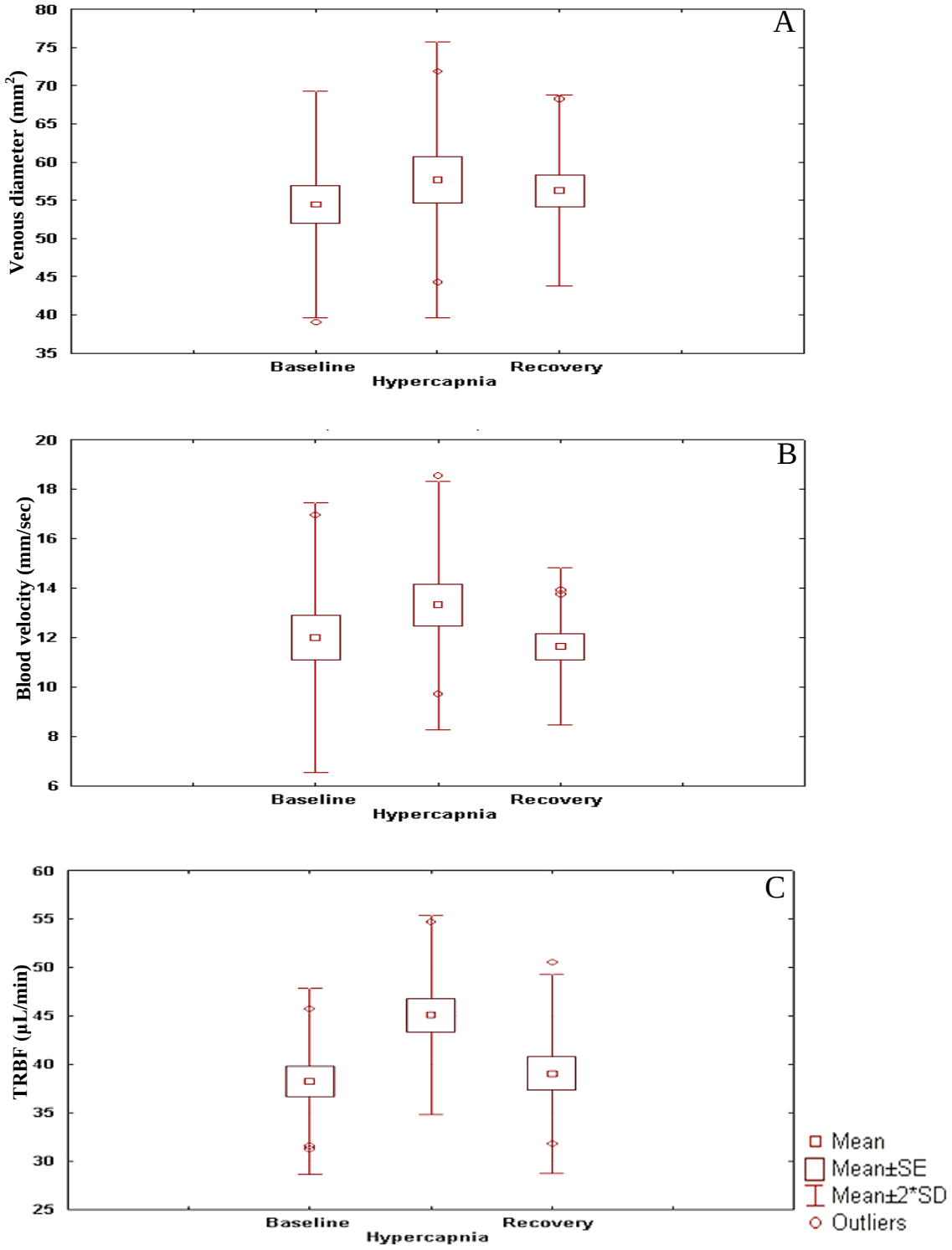

Figure 4.5 Box plots represent A) venous area; B) blood velocity; and C) total retinal blood flow at baseline, normoxic hypercapnia and recovery in smokers.

4.3.3 Comparison of retinal vascular reactivity and blood flow between smokers and non-smokers

A one-way ANOVA showed significant difference in terms of percentage change in retinal arteriolar diameter response to normoxic hypercapnia between smokers and non-smokers ($p=0.0379$). Similarly, percentage change in flow was also significantly different between smokers and non-smokers ($p=0.0101$). However, blood velocity was not significantly different among the groups ($p=0.3851$) (Table 4.2), (Figure 4.6). There was no statistically significant difference in TRBF ($p=0.3624$), venous area ($p=0.5669$) and venous velocity ($p=0.5189$) measurements between smokers and non-smokers (Table 4.3).

Group mean increase (%)	Non-smokers	Smokers	p (ANOVA)
Diameter (µm)	+4.1% (2.9%)	+1.7% (1.8%)	p=0.0379
Velocity (mm/sec)	+16.7% (14.6%)	+12.03% (6.2%)	NS
Flow(µL/min)	+29.6% (12.5%)	+14.6% (9.5%)	p=0.0101

Table 4.2 Group mean (SD) increase in retinal arteriolar diameter, blood velocity and flow in percentage change due to normoxic hypercapnia in non-smokers and smokers. Note: NS denotes not significant; Level of significance was set to $p<0.05$.

Group mean increase (%)	Non-smokers	Smokers	p (reANOVA)
TRBF (µL/min)	+26% (22.9%)	+19.3% (18.4%)	NS
Venous area (mm2)	+7.0% (8.6)	+6.18% (11.1%)	NS
Venous velocity (mm/sec)	+18.1% (20.8%)	+13.7% (22%)	NS

Table 4.3 Group mean (SD) increase in total retinal blood flow (TRBF), venous area, and venous velocity in percentage change due to normoxic hypercapnia in non-smokers and smokers. Note: NS denotes not significant; Level of significance was set to $p<0.05$.

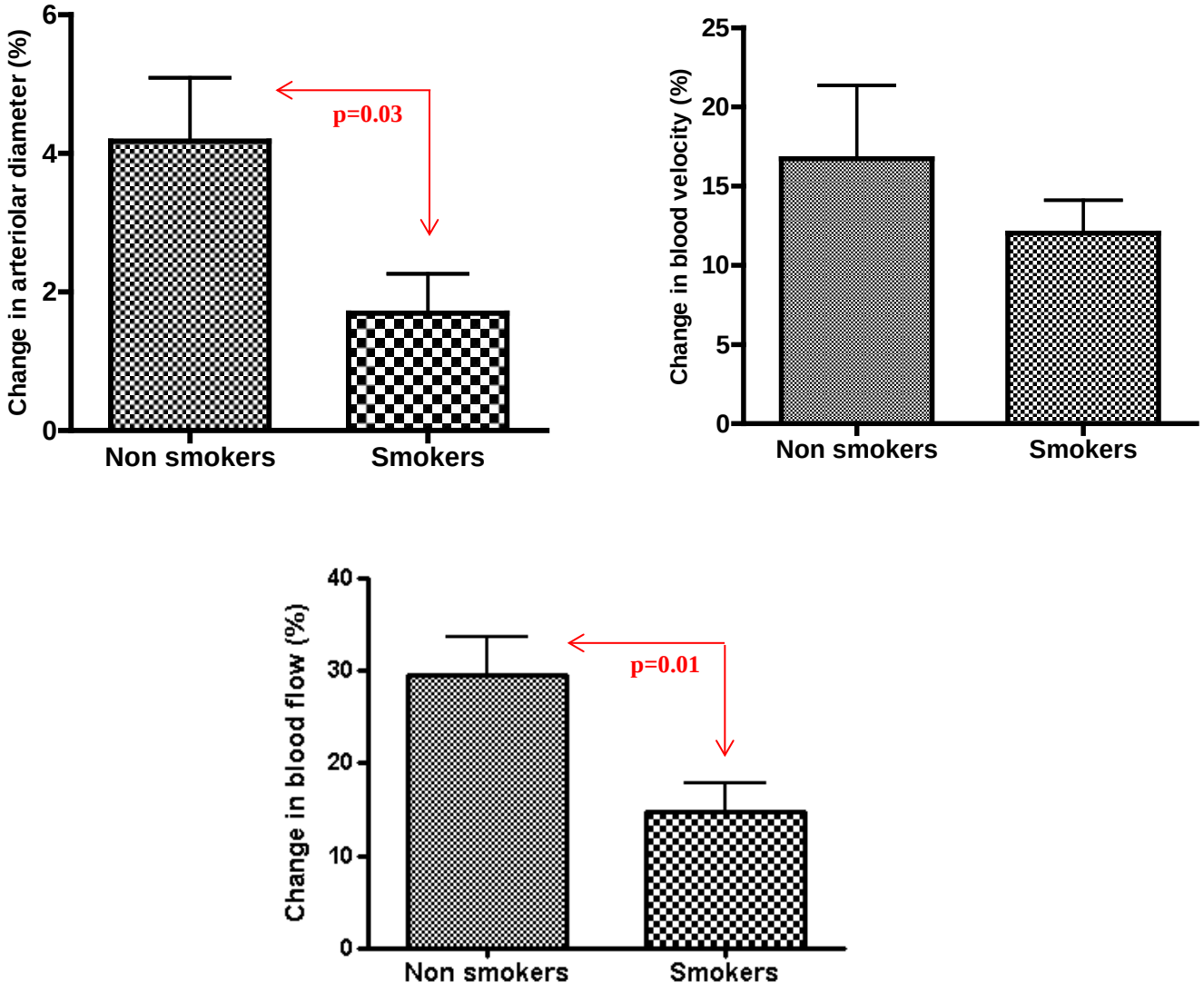

Figure 4.6 Percentage change from baseline in group mean A) arteriolar diameter; B) blood velocity and C) blood flow in response to normoxic hypercapnia in non-smokers and smokers. Level of significance was set to $p<0.05$.

4.3.4 Comparison of retinal vascular reactivity and blood flow before and after smoking

A Wilcoxon matched pairs test was performed to analyse the vascular reactivity to normoxic hypercapnia in terms of percentage change in diameter, velocity and flow before and after smoking. The percentage change in retinal arteriolar diameter, velocity and flow in response to normoxic hypercapnia after smoking was not significantly different when compared to before smoking. In addition, the percentage change in vascular reactivity in response to normoxic hypercapnia was also not significant in terms of total retinal blood flow (Figure 4.7), venous area and venous velocity measurements before and after smoking.

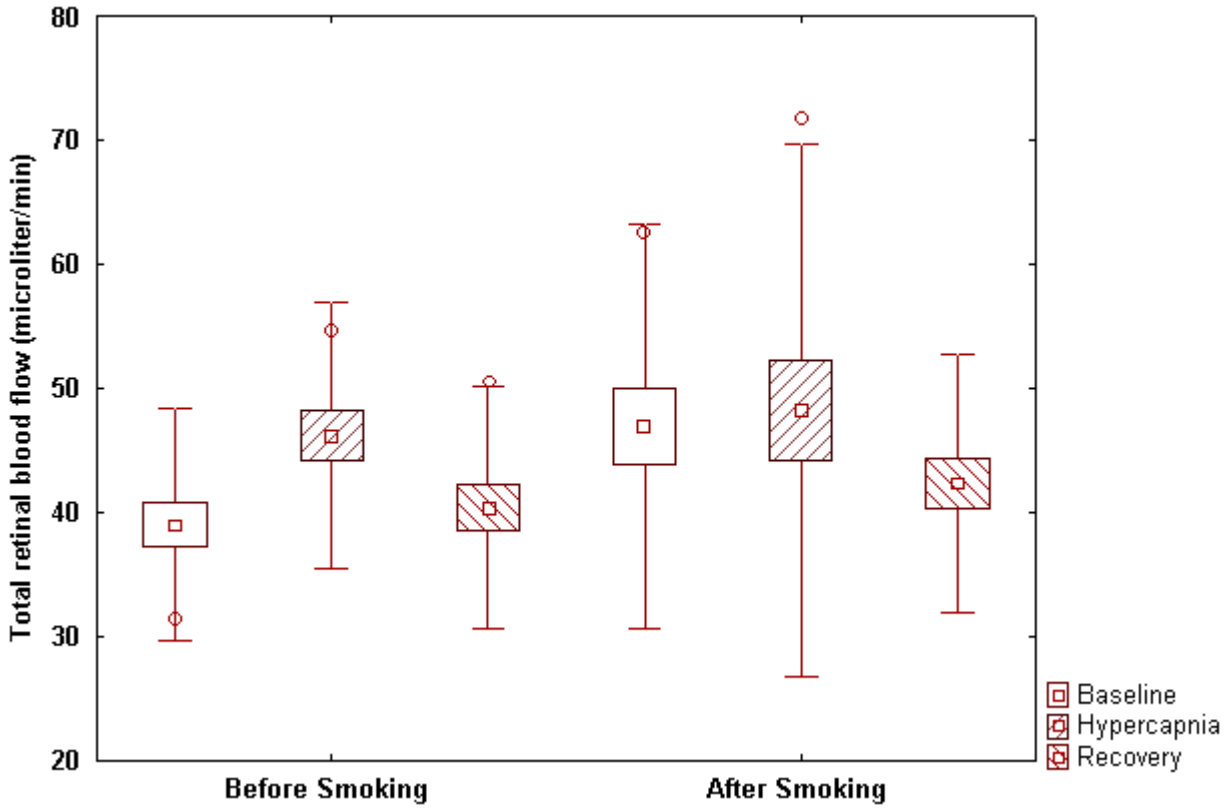

Figure 4.7 Box plots represent total retinal blood flow at baseline, normoxic hypercapnia and recovery as compared to before and after smoking. The center of the box represents group mean, the limits of the box represent mean ± standard error, the whiskers represent ± standard deviation, open circles represent outliers.

4.3.5 Systemic and gas parameters

In non-smoking group, $P_{ET}CO_2$ was increased by 16% (SD 1.7, $p<0.001$) relative to homeostatic baseline with a concomitant non-significant increase in mean $P_{ET}O_2$ by 0.9% (SD 2.1, $p=0.29$) in session 1a. There was a significant increase in mean $P_{ET}CO_2$ by 15.9% (SD 2.9, $p<0.001$) relative to baseline with a concomitant significant increase in mean $P_{ET}O_2$ by 1.8% (SD 0.5, $p=0.005$) in session 1b. There was no significant change in systemic parameters measured during different breathing conditions across both the study sessions (Table 4.4 & 4.5).

In smokers, there was a 15.7% (SD 2.2, $p<0.0001$) increase in $P_{ET}CO_2$ with a concomitant non-significant increase in $P_{ET}O_2$ by 1.7% (SD 1.4, $p=0.3135$) in session 1a. There was a significant increase in $P_{ET}CO_2$ by 15.7% (SD 2.6, $p<0.0001$) with a concomitant non-significant increase in $P_{ET}O_2$ by 1.4% (SD 4.2, $p=0.2168$) relative to baseline in session 1b. There was no significant change in any of the systemic parameters measured across both study sessions (Table 4.6 and 4.7).

Baseline homeostatic $P_{ET}CO_2$ values for non-smokers during session 1a and session 1b was 33.67 $\pm$ 3.15 mmHg and 33.48 $\pm$ 3.66 mmHg respectively. For smokers, baseline homeostatic $P_{ET}CO_2$ values during session 1a and 1b were 35.27 $\pm$ 5.16 mmHg and 35.26 $\pm$ 5.26 mmHg respectively. Repeated measures ANOVA showed no significant difference in $P_{ET}CO_2$ ($p=0.891$) among groups. Similarly no significant difference was found among groups in $P_{ET}O_2$ (reANOVA, $p=0.5526$), systolic (reANOVA, $p=0.5558$) and diastolic

(reANOVA, p=0.3675) blood pressure, pulse rate (reANOVA, p=0.8148), respiration rate (reANOVA, p=0.145) and oxygen saturation (reANOVA, p=0.4309).

In smokers, the homeostatic baseline value of $P_{ET}CO_2$ after smoking was 36.89 $\pm$ 5.43 mmHg and 35.47 $\pm$ 5.31 mmHg in session 2a and 2b respectively. This value is not significantly different form $P_{ET}CO_2$ level before smoking. In session 2a pulse rate was significantly different in baseline (p=0.0279), during hypercapnia (p=0.0179) and recovery (p=0.0464) compared to before smoking, analysed using wilcoxon matched pairs test. Similarly, baseline respiration rate was significantly different (p=0.0267), as compared to before smoking, but showing no significant difference during hypercapnia and recovery. There were no other significant changes in $P_{ET}O_2$, blood pressure (systolic and diastolic) and oxygen saturation. In session 2b, baseline diastolic blood pressure (p=0.0277) was significantly different before and after smoking. However, no significant changes observed in respiration rate during hypercapnia and recovery, before and after smoking. There were no significant changes in $P_{ET}CO_2$, $P_{ET}O_2$, systolic and diastolic blood pressure, pulse rate, respiration rate and oxygen saturation values during baseline, normoxic hypercapnia and recovery when compared before and after smoking in session 2b.

Parameters (n=10)	Baseline	Hypercapnia	Recovery	Re ANOVA
$P_{ET}CO_2$ (mmHg)	33.6 ± 3.1	39.0 ± 3.7	33.3 ± 3.4	p<0.0001
$P_{ET}O_2$ (mmHg)	119.1 ± 5.9	120.2 ± 6.6	119.8 ± 7.1	NS
Respiration rate (breaths/min)	16.9 ± 2.9	18.0 ± 3.1	17.4 ± 2.7	NS
Pulse rate (beats/min)	71.5 ± 8.9	71.6 ± 10.5	73.0 ± 9.8	NS
Systolic blood pressure (mm Hg)	111.2 ± 10	114.4 ± 8.2	111.3 ± 10.7	NS
Diastolic blood pressure (mm Hg)	73.4 ± 5.3	74.1 ± 3.9	72.7 ± 4.7	NS
O_2 saturation (%)	97.3 ± 1.5	97.7 ± 1.3	97.8 ± 1.1	NS

Table 4.4 Group mean (± SD) for gas and systemic parameters across different breathing conditions (i.e., baseline, normoxic hypercapnia and recovery) in non-smokers during session1a. ($P_{ET}CO_2$- partial pressure of end-tidal carbon dioxide, $P_{ET}O_2$-partial pressure of end-tidal oxygen, O_2 saturation – oxygen saturation) Note: NS denotes not significant; Level of significance was set to $p<0.05$.

Parameters (n=10)	Baseline	Hypercapnia	Recovery	Re ANOVA
$P_{ET}CO_2$ (mmHg)	33.4 ± 3.6	38.7 ± 3.7	33.5 ± 3.3	p=0.009
$P_{ET}O_2$ (mmHg)	120.4 ± 7.1	121.8 ± 7.2	120.4 ± 7.1	p=0.005
Respiration rate (breaths/min)	17.6 ± 3.2	18.2 ± 2.9	16.6 ± 1.5	NS
Pulse rate (beats/min)	71.6 ± 8.8	72.2 ± 8.8	70.3 ± 9.3	NS
Systolic blood pressure (mm Hg)	111.7 ± 8.2	113.4 ± 6.8	113.3 ± 6.6	NS
Diastolic blood pressure (mm Hg)	76.5 ± 5.0	77.4 ± 4.4	76.6 ± 4.1	NS
O_2 saturation (%)	97.8 ± 1.0	97.6 ± 1.2	97.6 ± 1.3	NS

Table 4.5 Group mean (± SD) for gas and systemic parameters across different breathing conditions (i.e., baseline, normoxic hypercapnia and recovery) in non-smokers during session1b. ($P_{ET}CO_2$- partial pressure of end-tidal carbon dioxide, $P_{ET}O_2$-partial pressure of end-tidal oxygen, O_2 saturation – oxygen saturation) Note: NS denotes not significant; Level of significance was set to $p<0.05$.

Parameters (n=9)	Baseline	Hypercapnia	Recovery	Re ANOVA
$P_{ET}CO_2$ (mmHg)	35.2 ± 5.1	40.7 ± 5.7	35.1 ± 5.3	p<0.0001
$P_{ET}O_2$ (mmHg)	113.1 ± 10.7	114.7 ± 10.1	112.8 ± 13.0	NS
Respiration rate (breaths/min)	16.3 ± 2.2	16.2 ± 2.5	16.3 ± 2.5	NS
Pulse rate (beats/min)	65.2 ± 9.4	66.4 ± 7.9	67.0 ± 6.3	NS
Systolic blood pressure (mm Hg)	109.0 ± 15.6	110.3 ± 14.3	109.3 ± 14.8	NS
Diastolic blood pressure (mm Hg)	66.8 + 11.0	70.6 ± 11.5	68.6 ± 11.8	NS
O_2 saturation (%)	97.3 + 1.4	98.1 + 0.8	97.7 ± 1.0	NS

Table 4.6 Group mean (± SD) for gas and systemic parameters across different breathing conditions (i.e., baseline, normoxic hypercapnia and recovery) in smokers during session1a. ($P_{ET}CO_2$- partial pressure of end-tidal carbon dioxide, $P_{ET}O_2$-partial pressure of end-tidal oxygen, O_2 saturation – oxygen saturation) Note: NS denotes not significant; Level of significance was set to $p<0.05$.

Parameters (n=9)	Baseline	Hypercapnia	Recovery	Re ANOVA
$P_{ET}CO_2$ (mmHg)	35.0 ± 5.2	40.5 ± 5.6	34.7 ± 5.4	p<0.0001
$P_{ET}O_2$ (mmHg)	112.9 ± 12.9	114.1 ± 11.4	114.7 ± 12.0	NS
Respiration rate (breaths/min)	16.4 ± 2.5	17.0 ± 2.9	16.7 ± 2.8	NS
Pulse rate (beats/min)	66.4 ± 8.3	67.1 ± 7.6	67.4 ± 8.0	NS
Systolic blood pressure (mm Hg)	108.2 ± 15.6	111.6 ± 14.0	110.1 ± 15.4	NS
Diastolic blood pressure (mm Hg)	68.3 ± 11.2	71.3 ± 10.7	71.3 ± 16.9	NS
O_2 saturation (%)	97.5 ± 1.4	98.0 ± 0.9	97.7 + 1.0	NS

Table 4.7 Group mean (± SD) for gas and systemic parameters across different breathing conditions (i.e., baseline, normoxic hypercapnia and recovery) in smokers during session1b. ($P_{ET}CO_2$- partial pressure of end-tidal carbon dioxide, $P_{ET}O_2$-partial pressure of end-tidal oxygen, O_2 saturation – oxygen saturation) Note: NS denotes not significant; Level of significance was set to $p<0.05$.

4.3.6 Breath CO

Breath carbon monoxide (CO) level for non-smokers was 0.3 ppm (SD 0.4), smokers CO level before smoking was 3.33 ppm (SD 2.3), this difference was not statistically significant (p=0.1961) using one-way ANOVA. After smoking the CO level of smokers, was 8.42 ppm (SD 6.6), which was significantly different from CO level before smoking (p=0.0305) as well as from CO level of non-smokers (p=0.0006) (Figure 4.8). The Fagerstrom Tolerance Questionnaire (FTQ) score for non-smokers and smokers were 0±0 and 3.33±2.2 respectively.

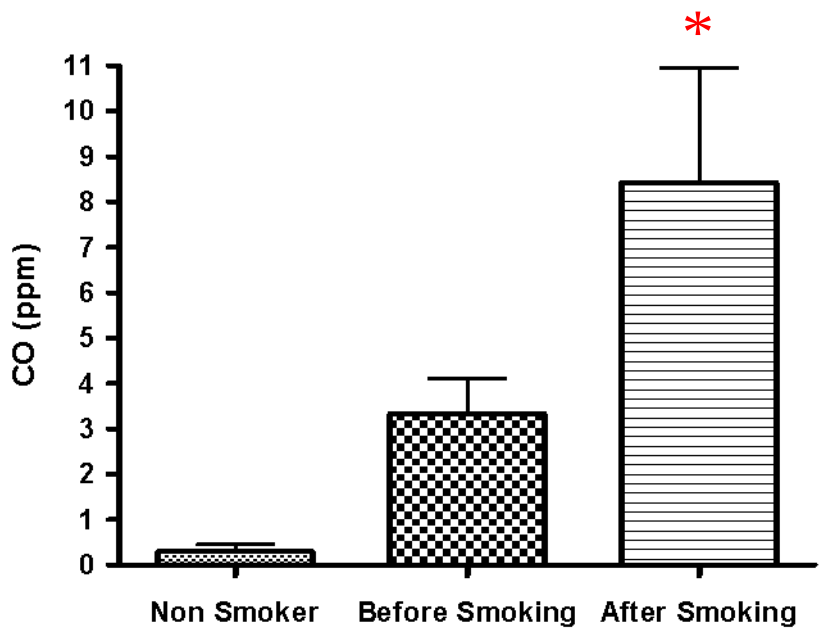

Figure 4.8 Breath carbon monoxide level expressed in parts per million (ppm) in non-smokers and smokers (before and after smoking). * represent significance between the groups at the level of p<0.05.

4.4 Discussion

Retinal vascular reactivity has been widely studied using various gas provocation challenges including hyperoxia, hypercapnia and carbogen (gas mixture of 95% O_2 and 5% CO_2). An increase in arterial carbon dioxide concentration was shown to vasodilate retinal vessels (Venkataraman et al. 2008; Venkataraman et al. 2005). Similarly, an increase in arterial oxygen concentration constricts the retinal vessels (Gilmore et al. 2004; Gilmore et al. 2005; Werkmeister et al. 2012). In the present study, a sustained, stable and standardised hypercapnic stimulus was used for gas provocation in young healthy individuals. Studies from our own lab previously showed that, a 15% increase in $P_{ET}CO_2$ from standardised baseline while simultaneously maintaining isoxia increased the retinal arteriolar vessel diameter, blood velocity and flow by 3.3%, 16.9% and 24.9% respectively.

Various other studies have assessed the retinal vascular reactivity to hypercapnic gas provocation. Dorner and co-workers (Dorner et al. 2002) reported that, to a 21% increase in $P_{ET}CO_2$, retinal arteriolar and venular diameter increased by 4.2% and 3.2% respectively. Sponsel and co-workers (Sponsel et al. 1992) found a 26% increase in perimacular leukocyte velocity using blue field entoptic technique following inhalation of 5% CO_2. For a 10% increase in CO_2 retinal arteriolar and venular diameter increased by +2% and 1% respectively as measured using fundus photograph (Frayser and Hickam 1964). Venkataraman and co-workers (Venkataraman et al. 2006) reported 3%, 26% and 35% increase in retinal arteriolar diameter, blood velocity and flow respectively in response to 12% increase in $P_{ET}CO_2$ using CLBF. Another study from our lab reported

3.3%, 16.9% and 24.9% increase in retinal arteriolar diameter, blood velocity and flow respectively in response to 15% increase in $P_{ET}CO_2$ using CLBF (Venkataraman et al. 2008). In the present study retinal arteriolar diameter, blood velocity and flow increased in response to normoxic hypercapnia by 4.1%, 16.7% and 29.6% respectively using CLBF.

Previous studies from various labs have achieved $P_{ET}CO_2$ by manually adding CO_2 to inspired air (Roff et al. 1999) or by rebreathing subject's own exhaled gases (Harino et al. 1995). Some studies have even failed to consider any concomitant change in PaO_2 during hypercapnia (Roff et al. 1999). This way of achieving vascular reactivity response might be due to the combined effect of both PaO_2 as well as $PaCO_2$. In contrast, the technique of hypercapnic gas provocation used in our lab is unique in the sense that, arterial carbon dioxide concentration is increased whilst maintaining $P_{ET}O_2$ at physiological resting level (Slessarev et al. 2007). So far, studies done by our Research Group confirm that the magnitude of normoxic (i.e. "clamping" of PaO_2) hypercapnia induced using the computer-controlled gas blender is highly repeatable (Venkataraman et al. 2010; Venkataraman et al. 2008; Venkataraman et al. 2006; Venkataraman et al. 2005).

In this study, we used the spectral-domain OCT Doppler technology to measure the total retinal blood flow, venous area and venous velocity changes in response to normoxic hypercapnia along with CLBF measurements. In interpreting the results from these two techniques, one needs to consider that they differ in terms of instrumental set up as well as site of measurement of blood flow. The Doppler OCT scans all branch retinal arterioles and venules using two concentric scans of 3.4 and 3.75mm diameters around the optic

nerve head, whereas CLBF measures the blood velocity and diameter at a single location, in this case along the superior temporal arteriole, after the first bifurcation.

For the first time, this study analysed the retinal vascular reactivity to normoxic hypercapnia using Doppler SD-OCT. Normoxic hypercapnia increased the venous area, venous velocity and total retinal blood flow by 7%, 18.1% and 26% respectively. However, the results of this study could not be directly compared to the previous studies, due to the technological differences in blood flow measurement and differences in magnitude of hypercapnic provocation.

Few studies have assessed the retinal vascular reactivity to a hypercapnic stimulus in smokers. Wimpissinger and co-workers (Wimpissinger et al. 2004) reported that response to carbogen (5%CO_2 and 95%O_2) in chronic smokers is altered in choroid but not in the optic nerve head and retina. However, their results were restricted to only vessel diameter information; retinal blood flow was not assessed. In contrast to their results, results from the present study confirm that retinal arteriolar vascular reactivity (diameter and flow) is significantly reduced in smokers compared to non-smokers in response to normoxic hypercapnia. Though venous area and TRBF measurements showed a reducing trend in terms of magnitude of vascular reactivity, the results were not statistically significant; this may be attributed to the small sample size of the study.

Garhofer and co-workers (Garhofer et al. 2011) reported reduced flicker-induced vasodilation and retinal blood flow as measured in one single vein, in young healthy smokers. It should be noted that retinal diameter measurements and blood velocity measurements were not obtained simultaneously. Heitmar and co-workers (Heitmar et al. 2010) reported no difference in retinal flicker response between smokers and non-smokers using retinal vessel analyser software, but found a significant difference when a different software (sequential and diameter response analysis) was used to analyse the diameter response.

Studies which used 100% oxygen have found that retinal capillary and optic nerve head blood flow was reduced in young healthy smokers using scanning laser Doppler flowmeter (SLDF) (Langhans 1997). In contrast, another study reported that retinal vascular reactivity to 100% oxygen was more pronounced in smokers compared to non-smokers using laser Doppler velocimetry and retinal vessel analyzer (Wimpissinger 2005). Although these two studies used a similar magnitude of gas provocation (100% O_2), the measuring techniques used were different. The results of these studies were attributed to the chronic effect of cigarette smoking.

Morgado and co-workers (Morgado et al. 1994) reported retinal vascular reactivity to 60% O_2 was significantly reduced immediately after smoking a cigarette compared to before smoking. Nevertheless their study did not compare the results with a non-smoking group. Robinson and co-workers (Robinson et al. 1985) reported increase in macular leukocyte velocity (12 $\pm$ 5%) after smoking using blue field simulation technique. In both the studies

mentioned above, neither COHb level in blood nor breath carbon monoxide level was measured in smokers. A small pilot data from present study showed a reducing trend in retinal vascular reactivity in response to normoxic hypercapnia 30 minutes after smoking compared to before smoking, but the results were not conclusive due to a small sample size. The carbon monoxide level measured before and after smoking was significantly different. Though the cut-off level to differentiate non-smoking and smoking status seem to vary between studies (Javors et al. 2005; Deveci et al. 2004), the present study has set a cut-off of 2ppm for non-smokers and 6ppm for smokers. Previous studies have reported that CO concentration in alveolar breath was found to be highly correlated with blood carboxyhaemoglobin levels (Wald et al. 1981).

Carbon monoxide and nicotine are two major constituents of cigarette smoke. CO has approximately 200-250 times greater affinity to haemoglobin than oxygen. The presence of carboxyhaemoglobin (CO-Hb) reduces the oxygen carrying capacity of the erythrocytes. The CO-Hb dissociates very slowly in the blood due to the tight bonding of CO to haemoglobin, thus having a half-life of approximately 3-4 hours (Ernst and Zibrak 1998). Nicotine on the other hand, initiates catecholamine release through the activation of the sympathetic nervous system resulting in increased heart rate, blood pressure, and vasoconstriction (Benowitz 1991).

Our study concludes that hypercapnia induced vasodilation is reduced in smokers. The enzyme nitric oxide synthase (eNOS) found in the vascular endothelium produces nitric oxide, which is thought to be a mediator for hypercapnia induced vasodilation. NO binds to

the iron atom of heme in guanylate cyclase and thereby increases intracellular cyclic guanosine monophosphate levels, in turn leading to a decrease in intracellular calcium levels and hence vasorelaxation. Inhibition of eNOS activity has been shown to result in impaired hypercapnia induced vasodilation (Schmetterer and Polak 2001). Studies report that cigarette smoking impairs eNOS activity, thereby reducing the bio availability of nitric oxide resulting in impaired endothelial-dependent relaxation (Powell 1998).

This study is the first to investigate retinal vascular reactivity in response to normoxic hypercapnia using CLBF and Doppler SDOCT in smokers. Previous studies have not simultaneously attained blood velocity and diameter measurements in smokers. Moreover, the hypercapnic gas provocation utilized in this study was also different from other studies.

The limitations of the current study in terms of blood flow measurement technique is that, the Doppler signal strength achieved for retinal vessels using Optovue RTvue, was not consistent during different breathing conditions (baseline, normoxic hypercapnia and recovery) resulting in inconsistency when assigning a confidence score based on Doppler signal strength. Another limitation in comparing retinal vascular reactivity before (Session 1) and after (Session 2) smoking is that a few subjects felt too fatigued to sit for session 2, for the same reason most of them exhibited difficulties in fixating during image acquisition. Therefore out of six CLBF measurements only three good quality measurements were considered for the analysis.

In conclusion, this study used a novel gas provocation technique to investigate the retinal vascular reactivity in smokers and non-smokers using CLBF and Doppler SD-OCT. Cigarrete smoking reduced retinal vascular reactivity in smokers, however most of the smokers in the present study were light smokers (approximately 15 cig/day), whether heavy smokers (>25 cig/day) would exhibit a different response to hypercapnia induced vasodilation needs further investigation.

5 Discussion

A growing body of evidence suggests that retinal blood flow measurement may play a role in the better understanding of major retinal diseases including glaucoma, diabetic retinopathy and age related macular degeneration (AMD) (Cuypers et al. 2000; Logan et al. 2004). Various blood flow techniques exist as explained in chapter 1. However, almost all of them have limitations. Laser Doppler velocimetry is limited to only blood velocity measurement (Riva and Feke 1981). Colour Doppler imaging enables only the measurement of blood velocity, thus retinal blood flow measurement is not possible (Baxter and Williamson 1995; Harris et al. 2003). Similarly, the blue field entoptic technique can only measure the density and velocity of moving leukocytes in the macular capillaries, providing information only on blood flow in macular area. In addition, there is lot of subjectivity involved in this technique, and the reproducibility remains poor (Yap and Brown 1994).

In contrast to the above mentioned techniques, the canon laser blood flowmeter (CLBF) simultaneously measures vessel diameter as well as blood velocity from major retinal arterioles and venules. The retinal blood flow measurement achieved using CLBF has proven to be repeatable and reproducible (Kida et al. 2002; Guan et al. 2003; Rose and Hudson 2007; Yoshida et al. 2003). The CLBF measures retinal blood flow from a single retinal vessel at a time. Achieving total retinal blood flow using CLBF is quite tedious, since each major retinal vessel needs to be measured individually, which is time consuming.

Recently, Doppler SD-OCT has evolved to be a promising tool in terms of achieving retinal blood flow measurement with minimum acquisition time and optimum consistency (Wang et al. 2009; Wang et al. 2007; Wang et al. 2008). Semi-automated software (DOCTORC) enables the calculation of TRBF measurement from the blood velocity and vessel cross-sectional area measurements. The cross-sectional areas and position of the vessels within the B-scan OCT images are refined by a human grader. The present study found optimum reproducibility among trained graders for TRBF and venous area measurements. However, a novice grader showed a learning effect in venous area measurements which might possibly influence TRBF measurements.

Wang and co-workers (Wang et al. 2008) reported variability of 10.5% in a sample of ten subjects using Doppler SD-OCT. In the current study, the overall variability of TRBF and venous area measurements between sessions within a trained grader were 20.90% and 17.64% respectively. The COV reported in our study was higher compared to those values reported by Wang and co-workers (Wang et al. 2008). It needs to be emphasized here that, in the present study, same subject datasets were graded twice by a trained grader, so the variability might be more appropriately attributed to the grading technique itself. In order to improve the image grading protocol, efforts are being taken to obtain automatic retinal blood vessel parameter calculations by modifying the scan protocol (Wehbe et al. 2007).

In chapter 4, retinal vascular reactivity was investigated using CLBF and Doppler SD-OCT in a group of young healthy smokers and non-smokers. This study is the first to measure vascular reactivity using a standardized and stable hypercapnic gas provocation technique

in smokers. Studies which used flicker stimulation to assess vascular reactivity remain controversial. They reported smokers to show reduced flicker induced vasodilation (Garhöfer et al. 2011), whereas others have reported that retinal vasodilation to flicker stimuli is unaffected in smokers (Cubbidge et al. 2012). Garhofer and co-workers (Garhöfer et al. 2011) reported that retinal arterioles and venules showed varying response to flicker induced vasodilation in smokers. Retinal arterioles showed a reduced flicker response, whereas retinal veins only showed a tendency to reduce.

Studies which used gas provocation techniques coupled with blood flow measurement techniques to analyze vascular reactivity and blood flow changes in smokers are also equivocal. The retinal flow was reported to be reduced by 33% in response to 100% O_2 in healthy non-smokers, compared to only 10% decrease in smokers, which indicates impaired hyperoxia induced vasoconstriction (Langhans et al. 1997). Wimpissinger and co-workers (Wimpissinger et al. 2004) reported 10 minutes of breathing carbogen (95% O_2 & 5%CO_2) significantly increased choroidal blood flow in non-smokers by +8.0%, whereas smokers responded significantly less to carbogen (-5.7%). The study also reported that retinal vessel diameter decreased in response to carbogen to a similar degree in both group.

Only a few studies have reported the effect of cigarette smoking on CO_2 induced cerebrovascular reactivity in humans. Smoking decreased the cerebral blood flow velocity as well as regional cerebral blood flow (Silvestrini et al. 1996; Terborg et al. 2002). In

contrast, a few studies have reported increased basal cerebral flow along with a decreased cerebral vascular resistance in smokers (Wennmalm 1982; Skinhoj et al. 1973).

The possibility of contradictory results of smoking from different retinal and cerebral studies might be due to the difference in measurement technique, magnitude of gas provocation, different types of flicker stimuli, and different vascular bed studied. Though results from the present study could not be directly comparable to the above mentioned studies, we report reduced retinal vascular reactivity (especially diameter and flow response) to normoxic hypercapnia in young healthy smokers compared to non-smokers.

The acute effect of smoking (30 minute after smoking) on retinal blood flow and vascular reactivity in a small group of smokers was also analyzed. Tamaki and co-workers (Tamaki et al. 2000) reported that, smoking had little effect on optic nerve head blood velocity in light smokers, compared to a more pronounced effect in heavy smokers, using laser speckle method. In their study blood pressure and pulse rate were significantly elevated from baseline until 20 minutes post smoking, after which the values dropped down to baseline levels. Robinson and co-workers (Robinson and Riva 1986) reported an acute increase in macular blood flow by 12% when measured within 30 minutes of smoking. Morgado and co-workers (Morgado et al. 1994) reported retinal vascular reactivity response to 60% O_2 before and 10 minutes after smoking; before smoking velocity, vessel diameter and retinal blood flow reduced by -19%, -5.8% and -27.9% respectively. After smoking, velocity, diameter and flow changed by +1.4%, -5.3% and -9.6% respectively. Heart rate and blood pressure was significantly increased 10 minutes after smoking.

In contrast to these studies, our pilot data does not show significant differences before and after smoking for retinal vascular reactivity and blood flow. Pulse rate and respiration rate was significantly high in just one of the sessions compared to before smoking. No systemic or gas parameter showed significant differences before and after smoking. This could be due to the following reasons: The small sample size; that both chronic (session 1) and acute (session 2) sessions were scheduled on the same day which made the subjects fatigue during session 2; the acute effect of smoking was measured 30 minutes after smoking; and that there were different levels of nicotine absorption among smokers. The arterial concentration of nicotine was shown to reach its peak within 10 minutes after smoking, after which the level drops down gradually (Armitage et al. 1975). For this reason, any acute effect of smoking on retinal vascular reactivity should have been measured immediately after smoking. Future studies will address these potential limitations by modifying the study protocol.

In summary, results from this study indicate reduced retinal vascular reactivity to normoxic hypercapnia in young healthy smokers. A standardized and stable computer-controlled gas blender was used to provoke normoxic hypercapnia in all subjects. Total retinal blood flow and venous area measurements showed only a reducing trend in terms of retinal vascular reactivity; however retinal arteriolar diameter and flow response was significantly reduced to normoxic hypercapnia in smokers. The exact reason behind the impaired vasodilation to hypercapnic gas provocation remains unclear. Among other endothelial derived relaxing factors, nitric oxide is thought to play a key role in mediating hypercapnia induced vasodilation (Schmetterer and Polak 2001). Several human and animal studies report that

cigarette smoking is capable of inducing morphological alterations to the vascular endothelium (Pittilo et al. 1984), and also alters the production of endothelial derived constricting and dilating factors (Zhang et al. 2001; Powell 1998; Celermajer et al. 1996). Whether or not reduced retinal vascular reactivity reported in smokers reflects impaired endothelial function remains ambiguous.

5.1 Future directions

The novel gas provocation technique utilised in this study enabled a comprehensive assessment of retinal vascular reactivity changes in young healthy smokers. Smokers showed reduced response to normoxic hypercapnia compared to healthy non-smokers. Impaired endothelial function, decreased nitric oxide bioavailability and reduced eNOS activity are reported to be the reason for altered vascular reactivity and blood flow in smokers (Zhang et al. 2001; Powell 1998; Celermajer et al. 1996). The results from various retinal vascular reactivity studies on smokers remain equivocal. Therefore future work on smokers needs to quantitate systemic level of cyclic glucose monophosphate (cGMP), a biomarker for endothelial function to provide more information on vascular regulation in smokers.

A vast majority of studies have elucidated a causal relationship between cigarette smoking and ARMD (Thornton et al. 2005; Cheng et al. 2000; Klein et al. 1993; Vingerling et al. 1996; Smith et al. 1996). Therefore in future, it would be interesting to continue the present work in ARMD patients (smokers and non-smokers) compared to age-matched non-smoking controls. Retinal oximetry is an emerging tool to directly assess the oxygen

saturation and metabolic status of retina (Harris et al. 2003; Harris et al. 2008). Future study in ARMD patients would include retinal vascular reactivity and blood flow changes to normoxic hypercapnia, as well as assessment of retinal oxygen saturation using retinal oximetry to better understand the patho-physiology of this sight-threating disease in elderly population.

Copyright permissions

Fagerstrom tolerance questionnaire

Dear Dr. Fagerstrom,

I am a graduate student from university of waterloo working under supervision of Prof. Chris Hudson. My research study into retinal blood flow would involve a group of smokers and non-smokers. To quantitate the load of nicotine dependence and the daily cigarette consumption I prefer to use the Modified Fagerstrom Test for Nicotine Dependence (FTND), I would be very grateful if you permit me to use FTND questionnaire in my study. Please advise.

Thanking you,
Kalpana

From: karl.fagerstrom <karl.fagerstrom@swipnet.se>

To: kalpana rose <kalpanarose_2002@yahoo.co.in>

Sent: Sat, 25 June, 2011 3:34:40 AM

Subject: SV: Permission to use FTND

Dear Kalpana

Thank you for asking. I wish you good luck in your research and feel free to use the FTND as much as you like.

With my best regards
Karl Fagerstrom

Experimental eye research

ELSEVIER LICENSE
TERMS AND CONDITIONS

Jan 04, 2013

This is a License Agreement between kalpana rose ("You") and Elsevier ("Elsevier"). The license consists of your order details, the terms and conditions provided by Elsevier, and the payment terms and conditions.

License number	3062041436026
License date	Jan 04, 2013
Licensed content publisher	Elsevier
Licensed content publication	Experimental Eye Research
Licensed content title	Retinal arteriolar and capillary vascular reactivity in response to isoxic hypercapnia
Licensed content author	Subha T. Venkataraman, Chris Hudson, Joseph A. Fisher, Lisa Rodrigues, Alexandra Mardimae, John G. Flanagan
Licensed content date	10 December 2008
Licensed content volume number	87
Licensed content issue number	6
Number of pages	8
Start Page	535
End Page	542
Type of Use	Reuse in a thesis/dissertation
Portion	Figures/tables/illustrations
Number of figures/tables/illustrations	1
Format	Both print and electronic
Are you the author of this Elsevier article?	No

Will you be translating?	No
Title of your thesis/dissertation	Retinal blood flow and vascular reactivity in chronic smokers
Expected completion date	Feb 2013
Estimated size (number of pages)	145
Elsevier VAT number	GB 494 6272 12
Permissions price	0.00 USD
VAT/Local Sales Tax	0.0 USD / 0.0 GBP
Total	0.00 USD

Terms and Conditions

INTRODUCTION

1. The publisher for this copyrighted material is Elsevier. By clicking "accept" in connection with completing this licensing transaction, you agree that the following terms and conditions apply to this transaction (along with the Billing and Payment terms and conditions established by Copyright Clearance Center, Inc. ("CCC"), at the time that you opened your Rightslink account and that are available at any time at http://myaccount.copyright.com).

GENERAL TERMS

2. Elsevier hereby grants you permission to reproduce the aforementioned material subject to the terms and conditions indicated.

3. Acknowledgement: If any part of the material to be used (for example, figures) has appeared in our publication with credit or acknowledgement to another source, permission must also be sought from that source. If such permission is not obtained then that material may not be included in your publication/copies. Suitable acknowledgement to the source must be made, either as a footnote or in a reference list at the end of your publication, as follows:

"Reprinted from Publication title, Vol /edition number, Author(s), Title of article / title of chapter, Pages No., Copyright (Year), with permission from Elsevier [OR APPLICABLE SOCIETY COPYRIGHT OWNER]." Also Lancet special credit - "Reprinted from The Lancet, Vol. number, Author(s), Title of article, Pages No., Copyright (Year), with permission from Elsevier."

4. Reproduction of this material is confined to the purpose and/or media for which permission is hereby given.

5. Altering/Modifying Material: Not Permitted. However figures and illustrations may be altered/adapted minimally to serve your work. Any other abbreviations, additions, deletions and/or any other alterations shall be made only with prior written authorization of Elsevier Ltd. (Please contact Elsevier at permissions@elsevier.com)

6. If the permission fee for the requested use of our material is waived in this instance, please be advised that your future requests for Elsevier materials may attract a fee.

7. Reservation of Rights: Publisher reserves all rights not specifically granted in the combination of (i) the license details provided by you and accepted in the course of this licensing transaction, (ii) these terms and conditions and (iii) CCC's Billing and Payment terms and conditions.

8. License Contingent Upon Payment: While you may exercise the rights licensed immediately upon issuance of the license at the end of the licensing process for the transaction, provided that you have disclosed complete and accurate details of your proposed use, no license is finally effective unless and until full payment is received from you (either by publisher or by CCC) as provided in CCC's Billing and Payment terms and conditions. If full payment is not received on a timely basis, then any license preliminarily granted shall be deemed automatically revoked and shall be void as if never granted. Further, in the event that you breach any of these terms and conditions or any of CCC's Billing and Payment terms and conditions, the license is automatically revoked and shall be void as if never granted. Use of materials as described in a revoked license, as well as any use of the materials beyond the scope of an unrevoked license, may constitute copyright infringement and publisher reserves the right to take any and all action to protect its copyright in the materials.

9. Warranties: Publisher makes no representations or warranties with respect to the licensed material.

10. Indemnity: You hereby indemnify and agree to hold harmless publisher and CCC, and their respective officers, directors, employees and agents, from and against any and all claims arising out of your use of the licensed material other than as specifically authorized pursuant to this license.

11. No Transfer of License: This license is personal to you and may not be sublicensed, assigned, or transferred by you to any other person without publisher's written permission.

12. No Amendment Except in Writing: This license may not be amended except in a writing signed by both parties (or, in the case of publisher, by CCC on publisher's behalf).

13. Objection to Contrary Terms: Publisher hereby objects to any terms contained in any purchase order, acknowledgment, check endorsement or other writing prepared by you, which terms are inconsistent with these terms and conditions or CCC's Billing and Payment terms and conditions. These terms and conditions, together with CCC's Billing and Payment terms and conditions (which are incorporated herein), comprise the entire agreement between you and publisher (and CCC) concerning this licensing transaction. In the event of any conflict between your obligations established by these terms and conditions and those established by CCC's Billing and Payment terms and conditions, these terms and conditions shall control.

14. Revocation: Elsevier or Copyright Clearance Center may deny the permissions described in this License at their sole discretion, for any reason or no reason, with a full refund payable to you. Notice of such denial will be made using the contact information provided by you. Failure to receive such notice will not alter or invalidate the denial. In no event will Elsevier or Copyright Clearance Center be responsible or liable for any costs, expenses or damage incurred by you as a result of a denial of your permission request, other than a refund of the amount(s) paid by you to Elsevier and/or Copyright Clearance Center for denied permissions.

LIMITED LICENSE

The following terms and conditions apply only to specific license types:

15. **Translation**: This permission is granted for non-exclusive world **English** rights only unless your license was granted for translation rights. If you licensed translation rights you may only translate this content into the languages you requested. A professional translator must perform all translations and reproduce the

content word for word preserving the integrity of the article. If this license is to re-use 1 or 2 figures then permission is granted for non-exclusive world rights in all languages.

16. **Website**: The following terms and conditions apply to electronic reserve and author websites:
Electronic reserve: If licensed material is to be posted to website, the web site is to be password-protected and made available only to bona fide students registered on a relevant course if:
This license was made in connection with a course,
This permission is granted for 1 year only. You may obtain a license for future website posting,
All content posted to the web site must maintain the copyright information line on the bottom of each image,
A hyper-text must be included to the Homepage of the journal from which you are licensing athttp://www.sciencedirect.com/science/journal/xxxxx or the Elsevier homepage for books athttp://www.elsevier.com , and Central Storage: This license does not include permission for a scanned version of the material to be stored in a central repository such as that provided by Heron / XanEdu.

17. **Author website** for journals with the following additional clauses:

All content posted to the web site must maintain the copyright information line on the bottom of each image, and the permission granted is limited to the personal version of your paper. You are not allowed to download and post the published electronic version of your article (whether PDF or HTML, proof or final version), nor may you scan the printed edition to create an electronic version. A hyper-text must be included to the Homepage of the journal from which you are licensing athttp://www.sciencedirect.com/science/journal/xxxxx . As part of our normal production process, you will receive an e-mail notice when your article appears on Elsevier's online service Science Direct (www.sciencedirect.com). That e-mail will include the article's Digital Object Identifier (DOI). This number provides the electronic link to the published article and should be included in the posting of your personal version. We ask that you wait until you receive this e-mail and have the DOI to do any posting.

Central Storage: This license does not include permission for a scanned version of the material to be stored in a central repository such as that provided by Heron/XanEdu.

18. **Author website** for books with the following additional clauses:
Authors are permitted to place a brief summary of their work online only.
A hyper-text must be included to the Elsevier homepage at http://www.elsevier.com . All content posted to the web site must maintain the copyright information line on the bottom of each image. You are not allowed to download and post the published electronic version of your chapter, nor may you scan the printed edition to create an electronic version.

Central Storage: This license does not include permission for a scanned version of the material to be stored in a central repository such as that provided by Heron/XanEdu.

19. **Website** (regular and for author): A hyper-text must be included to the Homepage of the journal from which you are licensing at http://www.sciencedirect.com/science/journal/xxxxx. or for books to the Elsevier homepage at http://www.elsevier.com

20. **Thesis/Dissertation**: If your license is for use in a thesis/dissertation your thesis may be submitted to your institution in either print or electronic form. Should your thesis be published commercially, please reapply for permission. These requirements include permission for the Library and Archives of Canada to supply single copies, on demand, of the complete thesis and include permission for UMI to supply single copies, on demand, of the complete thesis. Should your thesis be published commercially, please reapply for permission.

21. Other Conditions:

v1.6

If you would like to pay for this license now, please remit this license along with your payment made payable to "COPYRIGHT CLEARANCE CENTER" otherwise you will be invoiced within 48 hours of the license date. Payment should be in the form of a check or money order referencing your account number and this invoice number RLNK500927542.
Once you receive your invoice for this order, you may pay your invoice by credit card. Please follow instructions provided at that time.

Make Payment To:
Copyright Clearance Center
Dept 001
P.O. Box 843006
Boston, MA 02284-3006

For suggestions or comments regarding this order, contact RightsLink Customer Support:customercare@copyright.com or +1-877-622-5543 (toll free in the US) or +1-978-646-2777.

Gratis licenses (referencing $0 in the Total field) are free. Please retain this printable license for your reference. No payment is required.

Ophthalmology Management

Dear Dr. Rose:

Dr. David Huang has granted his permission for you to use the figure.

Warmest regards,

Rich

Richard Mark Kirkner
Executive Editor
Ophthalmology Management
Retinal Physician
Springer Science + Business Media
323 Norristown Road, Suite 200
Ambler, PA 19002
o: 215-628-7748
m: 267-300-8620

Dear publisher,

I would like to have permission to use one of the figure published in your article in my master's thesis. The specifications are:

Title of the article: OCT Terminology ? Demystified! A pioneer of the technology provides a translation of the latest jargon.

Author: Dr. David Huang

Article Date: 4/1/2009

Figure: "Schematics of a spectrometer-based Fourier-domain OCT system"

Thank you,

Kalpana Rose

References

Armitage A, Dollery C, George C, Houseman T, Lewis P, Turner D. Absorption and metabolism of nicotine from cigarettes. *Br Med J*. 1975; 4(5992):313-316.

Azizi B, Buehler H, Venkataraman ST, Hudson C. Impact of simulated light scatter on the quantitative, non-invasive assessment of retinal arteriolar hemodynamics. *J Biomed Opt*. 2007; 12(3):034021-1.

Barua, R.S, JA Ambrose, LJ Eales-Reynolds, MC. DeVoe, JG. Zervas, Dhanonjoy C. Saha. Dysfunctional endothelial nitric oxide biosynthesis in healthy smokers with impaired endothelium-dependent vasodilatation. *Circulation*. 2001; 104:1905-1910.

Baxter GM WT. Color Doppler imaging of the eye: Normal ranges, reproducibility, and observer variation. *J Ultrasound Med*. 1995; 14(2):91-96.

Benowitz NL. Nicotine and coronary heart disease. *Trends Cardiovasc Med.* 1991; 1(8):315-321.

Bertram KM, Baglole CJ, Phipps RP, Libby RT. Molecular regulation of cigarette smoke induced-oxidative stress in human retinal pigment epithelial cells: Implications for age-related macular degeneration. *Am J Physiol Cell Physiol*. 2009; 297(5):1200-1210.

Blum M, Bachmann K, Wintzer D, Riemer T, Vilser W, Strobel J. Noninvasive measurement of the Bayliss effect in retinal autoregulation. *Graefes Arch Clin Exp Ophthalmol*. 1999; 237(4):296-300.

Burke A, FitzGerald GA. Oxidative stress and smoking-induced vascular injury. *Prog Cardiovasc Dis*. 2003; 46(1):79-90.

Bursell SE, Clermont AC, Kinsley BT, Simonson DC, Aiello LM, Wolpert HA. Retinal blood flow changes in patients with insulin-dependent diabetes mellitus and no diabetic retinopathy. *Invest Ophthalmol Vis Sci*. 1996; 37(5):886-897.

Celermajer DS, Adams MR, Clarkson P, et al. Passive smoking and impaired endothelium-dependent arterial dilatation in healthy young adults. *N Engl J Med*. 1996; 334(3):150-155.

Cheng A, Pang C, Leung A, Chua J, Fan D, Lam D. The association between cigarette smoking and ocular diseases. *Hong Kong M J*. 2000; 6(2):195-202.

Chittari MV, McTernan P, Bawazeer N, Constantinides K, Ciotola M, O'Hare JP, Kumar S, Ceriello A. Impact of acute hyperglycaemia on endothelial function and retinal vascular reactivity in patients with type 2 diabetes. *Diabet Med*. 2011; 28(4):450-454.

Chung H, Harrisa A, Ciulla T, Kagemann L. Progress in measurement of ocular blood flow and relevance to our understanding of glaucoma and age-related macular degeneration. *Prog Retin Eye Res*. 1999; 18(5):669-687.

Cong R, Zhou B, Sun Q, Gu H, Tang N, Wang B. Smoking and the risk of age-related macular degeneration: A meta-analysis. *Ann Epidemiol*. 2008; 18(8):647-56.

Cubbidge R, Summers R, Heitmar R. Retinal vessel reactivity after cigarette smoking. *Acta Ophthalmol*. 2012; 90(249):0.

Cuypers MHM, Kasanardjo JS, Polak BCP. Retinal blood flow changes in diabetic retinopathy measured with the heidelberg scanning laser Doppler flowmeter. *Graefes Arch Clin Exp.* 2000; 238(12):935-941.

Dallinger S, Dorner GT, Wenzel R, et al. Endothelin-1 contributes to hyperoxia-induced vasoconstriction in the human retina. *Invest Ophthalmol Vis Sci*. 2000; 41(3):864-869.

Davignon J, Ganz P. Role of endothelial dysfunction in atherosclerosis. *Circulation*. 2004; 109 (23 suppl 1): III-27-32.

Deveci SE, Deveci F, Açik Y, Ozan AT. The measurement of exhaled carbon monoxide in healthy smokers and non-smokers. *Respir Med*. 2004; 98(6):551-556.

Dorner GT, Garhofer G, Kiss B, Polska E, Polak K, Riva CE, Schmetterer L. Nitric oxide regulates retinal vascular tone in humans. *Am J Physiol Heart Circ Physiol 2003 285(2):*631-636.

Dorner G, Garhoefer G, Zawinka C, Kiss B, Schmetterer L. Response of retinal blood flow to CO_2-breathing in humans. *Eur J Ophthalmol*. 2002; 12(6):459-466.

Drexler W FJ. State-of-the-art retinal optical coherence tomography. *Prog Retin Eye Res*. 2008; 27(1):45-88.

Ernst A, Zibrak JD. Carbon monoxide poisoning. *N Engl J Med*. 1998; 339(22):1603-1608.

Fagerstrom KO, Schneider NG. Measuring nicotine dependence: A review of the fagerstrom tolerance questionnaire. *J Behav Med*. 1989; 12(2):159-82.

Fagerström KO. Effects of a nicotine-enriched cigarette on nicotine titration, daily cigarette consumption, and levels of carbon monoxide, cotinine, and nicotine. *Psychopharmacology (Berl)*. 1982; 77(2):164-167.

Feke GT, Goger DG, Tagawa H, Delori FC. Laser doppler technique for absolute measurement of blood speed in retinal vessels. *IEEE Trans Biomed Eng.*1987; 9:673-800.

Feke GT. Laser Doppler instrumentation for the measurement of retinal blood flow: Theory and practice. *Bull Soc Belge Ophtalmol*. 2006; 302:171-84.

Feke G, Tagawa H, Deupree D, Goger D, Sebag J, Weiter J. Blood flow in the normal human retina. *Invest Ophthalmol Vis Sci*. 1989; 30(1):58-65.

Frayser R and Hickam J B. Retinal vascular response to breathing increased carbon dioxide and oxygen concentrations. *Invest Ophthalmol Vis Sci*. 1964; 3(4):427-431.

Friedman DS, O'Colmain BJ, Muñoz B, Tomany SC, McCarty C, de Jong PT, Nemesure B, Mitchell P, Kempen J. Prevalence of age-related macular degeneration in the united states. *Arch Ophthalmol*. 2004; 122(4):564-572.

Furchgott R F and Vanhoutte P M. Endothelim-derived relaxing and contracting factors. *The FASEB J* 1989; 3(9):2007-2018.

Furchgott RF CP. Endothelial cells as mediators of vasodilation of arteries. *J cardiovascpharmacol* 1984; 6(2):S336-43.

Garcia Jr JPS, Garcia PT, Rosen RB. Retinal blood flow in the normal human eye using the canon laser blood flowmeter. *Ophthalmic Res*. 2002; 34(5):295-299.

Garhöfer G, Resch H, Sacu S, et al. Effect of regular smoking on flicker induced retinal vasodilatation in healthy subjects. *Microvasc Res*. 2011; 82(3):351-355.

Garhofer G, Werkmeister R, Dragostinoff N, Schmetterer L. Retinal blood flow in healthy young subjects. *Invest Ophthalmol Vis Sci*. 2012; 53(2):698-703.

Geitzenauer W, Hitzenberger CK, Schmidt-Erfurth UM. Retinal optical coherence tomography: Past, present and future perspectives. *Br J Ophthalmol*. 2011; 95(2):171-177.

Gilmore ED, Hudson C, Preiss D, Fisher J. Retinal arteriolar diameter, blood velocity, and blood flow response to an isocapnic hyperoxic provocation. *Am J Physiol Heart Circ Physiol 2005; 288(6)2912*-2917.

Gilmore ED, Hudson C, Venkataraman ST, Preiss D, Fisher J. Comparison of different hyperoxic paradigms to induce vasoconstriction: Implications for the investigation of retinal vascular reactivity. *Invest Ophthalmol Vis Sci*. 2004; 45(9):3207-3212.

Gilmore ED, Hudson C, Nrusimhadevara RK, et al. Retinal arteriolar diameter, blood velocity, and blood flow response to an isocapnic hyperoxic provocation in early sight-threatening diabetic retinopathy. *Invest Ophthalmol Vis Sci*. 2007; 48(4):1744-1750.

Goldstein IM, Ostwald P, Roth S. Nitric oxide: A review of its role in retinal function and disease. *Vision Res*. 1996; 36(18):2979-2994.

Goodall MC, Kirshner N. Biosynthesis of epinephrine and norepinephrine by sympathetic nerves and ganglia. *Circulation*. 1958; 17(3):366-371.

Gornik HL. Arginine metabolism enzymology nutrition clinical significance. 2004; 134(10):2880S-2887S. *J Nutrition*. 2004; 134(10):S2880- 2887.

Granstam E, Wang L, Bill A. Ocular effects of endothelin-1 in the cat. *Curr Eye Res*. 1992; 11(4):325-32.

Grieshaber MC Flammer J. Blood flow in glaucoma. *Curr Opin Ophthalmol*. 2005; 16(2):79-83.

Grunwald, JE, Sinclair SH, Riva CE. Autoregulation of the retinal circulation in response to decrease of intraocular pressure below normal. *Invest Ophthalmol Vis Sci*. 1982; 23(1):124-127.

Guan K, Hudson C, Flanagan JG. Variability and repeatability of retinal blood flow measurements using the canon laser blood flowmeter. *Microvasc Res*. 2003; 65(3):145-51.

Guyton AC, Hall J Text book of medical physiology. 10th edition ed. Philadelphia, Penncylvania: W.B. Saunders Company, 2000: 144-150.

Guyton AC. Evidence for tissue oxygen demand as the major factor causing autoregulation. *Circ Res.* 1964; 15:60-69.

Haefliger I O, Flammer J. Endothelium dependent vasoactive modulation in the ophthalmic circulation. *Prog retin eye res*. 2001; 20(2):209-225.

Harino S, Grunwald JE, Petrig BJ, Riva CE. Rebreathing into a bag increases human retinal macular blood velocity. *Br J Ophthalmol*. 1995; 79(4):380-383.

Harris A, Dinn RB, Kagemann L, Rechtman E. A review of methods for human retinal oximetry. *Ophthalmic Surg Lasers Imaging*. 2003; 34(2):152-64.

Harris A, Kagemann L, Ehrlich R, Rospigliosi C, Moore D, Siesky B. Measuring and interpreting ocular blood flow and metabolism in glaucoma. *Can J Ophthalmol.* 2008*;* 43(3):328-36.

Harris A, Jonescu-Cuypers C, Kagemann L, Ciulla T, Krieglstein G. *Atlas of Ocular Blood Flow: Vascular anatomy, pathophysiology, and metabolism*. Philadelphia: Butterworth Heinemann; 2003.

Harris A, Kagemann L, Cioffi GA. Assessment of human ocular hemodynamics. *Surv Ophthalmol*. 1998; 42(6):509-533.

Hart WM, Adler FH. *Adler's Physiology of the Eye: Clinical Application.* 9th Edition ed. St. Louis; Toronto: Mosby Inc; 1992.

Hayreh S. The ophthalmic artery: iii. branches. *Br. J ophthalmol*. 1962; 46:212 - 247.

Heitmar R, Blann AD, Cubbidge RP, Lip GYH, Gherghel D. Continuous retinal vessel diameter measurements: The future in retinal vessel assessment?. *Invest Ophthalmol Vis Sci*. 2010; 51(11):5833-5839.

Heitmar R, Blann AD, Cubbidge RP, Lip GYH, Gherghel D. Continuous retinal vessel diameter measurements: The future in retinal vessel assessment?. *Invest Ophthalmol Vis Sci*. 2010; 51(11):5833-5839.

Hsueh W A, Anderson P W. Hypertension, the endothelial cell, and the vascular complications of diabetes mellitus. *Hypertension*. 1992; 20:253-263.

Hurley BR, Regillo CD. In Arevalo JF eds.Fluorescein angiography: General principles and interpretation. *Retinal angiography and optical coherence tomography*.New York, Springer; 2009:27-42.

Lester M, Torre PG, Bricola G, Bagnis A, Calabria G. Retinal blood flow autoregulation after dynamic exercise in healthy young subjects. *Ophthalmologica*. 2007; 221(3):180-185.

Jakobiec FA. *Ocular Anatomy, Embryology, and Teratology*. Harper and Row Publishers, Inc. Philadelphia, 1982.

Javors MA, Hatch JP, Lamb RJ. Cut-off levels for breath carbon monoxide as a marker for cigarette smoking. *Addiction*. 2005; 100(2):159-167.

Johnson P C. Autoregulation of blood flow. *Circ Res*. 1986; 59(5):483-495.

Kagemann L, Harris A, Chung HS, Evans D, Buck S, Martin B. Heidelberg retinal flowmetry: Factors affecting blood flow measurement. . *Br J Ophthalmol*. 1998; 82(2):131-136.

Kaufman P, Alm A. *Adler's physiology of the eye: Clinical application*, 10th ed, Mosby, St. Louis, 2003.

Kida T, Harino S, Sugiyama T, Kitanishi K, Iwahashi Y, Ikeda T. Change in retinal arterial blood flow in the contralateral eye of retinal vein occlusion during glucose tolerance test. *Graefes Arch Clin Exp Ophthalmol*. 2002; 240(5):342-347.

Kisilevsky M, Mardimae A, Slessarev M, Han J, Fisher J, Hudson C. Retinal arteriolar and middle cerebral artery responses to combined hypercarbic/hyperoxic stimuli. *Invest Ophthalmol Vis Sci*. 2008; 49(12):5503-5509.

Klein R, Klein BEK, Linton KLP, DeMets DL. The Beaver dam eye study: The relation of age-related maculopathy to smoking. *Am J Epidemiol*. 1993; 137(2):190-200.

Konduru RK, Tan O, Nittala MG, Huang D, Sadda SR. Reproducibility of retinal blood flow measurements derived from semi-automated Doppler OCT analysis. *Ophthalmic Surg Lasers Imaging*. 2012; 43(1):25-31.

Langhans M, Michelson G, Groh MJM. Effect of breathing 100% oxygen on retinal and optic nerve head capillary blood flow in smokers and non-smokers. *Br J Ophthalmol*. 1997; 81(5):365-369.

Leske MC. Ocular perfusion pressure and glaucoma: Clinical trial and epidemiologic findings. *Curr Opin Ophthalmol*. 2009; 20(2):73-78.

Linsenmeier R.A, Lissa Padnick–Silver. Metabolic dependence of photoreceptors on the choroid in the normal and detached retina. *Invest Ophthalmol Vis Sci*. 2000; 41(10):3117-3123.

Logan J, Rankin S, Jackson A. Retinal blood flow measurements and neuroretinal rim damage in glaucoma. . *Br J Ophthalmol 2004; 88(8):1049-1054*. 2004; 88(8):1049-1054.

Lotfi K and Grunwald JE. The effect of caffeine on the human macular circulation. *Invest Ophthalmol Vis Sci*. 1991; 32:3028-3032.

Luksch A, Garhöfer G, Imhof A, et al. Effect of inhalation of different mixtures of O_2 and CO_2 on retinal blood flow. *Br J Ophthalmol*. 2002; 86(10):1143-1147.

Lüscher TF and Balton M. Biology of the endothelium. *Clin Cardol*1997; 20(11):3-10.

Knudtson MD, Klein BEK, Klein R,Wong TY, Hubbard LD, Lee KE, Meuer SM, and Bulla CP. Variation associated with measurement of retinal vessel diameters at different points in the pulse cycle. *Br J Ophthalmol*. 2004; 88(1):57-61.

Martin Bland J, Altman DG. Statistical methods for assessing agreement between two methods of clinical measurement. *The Lancet* 1986; 327(8476):307-310.

Mathew RJ & Wilson WH. Caffeine-induced changes in cerebral circulation. *Stroke*. 1985; 16:814-817.

McVeigh GE, Lemay L, Morgan D, Cohn JN. Effects of long-term cigarette smoking on endothelium-dependent responses in humans. *Am J Cardiol*. 1996; 78(6):668-672.

Michelson G, Schmauss B, Langhans M, Harazny J, Groh M. Principle, validity, and reliability of scanning laser Doppler flowmetry. *J Glaucoma*. 1996; 5(2):99-105.

Morgado PB, Chen HC, Patel V, Herbert L, Kohner EM. The acute effect of smoking on retinal blood flow in subjects with and without diabetes. *Ophthalmol*. 1994; 101(7):1220-1226.

Nakahashi K, Asai T, Okubo K, Yamamoto M, Masumi K. Analysis of the retinal blood flow by means of the blue field entoptic phenomenon and simulation of entoptic leucocytes with a personal-computer system. *Nihon Ganka Gakkai Zasshi*. 1989; 93(5):533-539.

Novotny HR, Alvis DL. A method of photographing fluorescence in circulating blood in the human retina. *Circulation*. 1961; 24(1):82-86.

Okuno T, Sugiyama T, Tominaga M et al. Effects of caffeine on microcirculation of the humanocular fundus. *Jpn J Ophthalmol 46*. 2002; 46:170-176.

O'Shea JG. Age-related macular degeneration: A leading cause of blindness. *Med J Aust*. 1996; 165(10):561-564.

Ozaki K, Hori T, Ishibashi T, Nishio M, Aizawa Y. Effects of chronic cigarette smoking on endothelial function in young men. *J Cardiol*. 2010; 56(3):307-313.

Petrig BL, Riva CE, Hayreh SS. Laser doppler flowmetry and optic nerve head blood flow. *Am J Ophthalmol*. 1999; 127(4):413-422.

Pittilo, R.M., Clarke, J.M.F., Harris, D. Cigarette smoking and platelet adhesion. *Br J Haematol* 1984; 58(4):627-632.

Polak K, Dorner G, Kiss B, et al. Evaluation of the zeiss retinal vessel analyser. *Br J Ophthalmol*. 2000; 84(11):1285-1290.

Pomerleau CS, Carton SM, Lutzke ML, Flessland KA, Pomerleau OF. Reliability of the fagerstrom tolerance questionnaire and the fagerstrom test for nicotine dependence. *Addict Behav*. 1994; 19(1):33-39.

Pournaras CJ. Regulation of retinal blood flow in health and disease. *Prog Retin **Eye** Res*. 2008; 27(3):284-330.

Powell JT. Vascular damage from smoking: Disease mechanisms at the arterial wall. *Vasc Med*. 1998; 3(1):21-28.

Prokhorov AV, Pallonen UE, Fava JL, Ding L, Niaura R. Measuring nicotine dependence among high-risk adolescent smokers. *Addict Behav*. 1996; 21(1):117-27.

Prokhorov, A.V, Koehly, L.M, Pallonen, U.E, Hudmon, K.S. Adolescent nicotine dependence measured by the modified fagerström tolerance questionnaire at two time points. *J Child Adolesc Subst Abus*. 1998; 7(4):35-47.

Rensen S S M, Doevendans P.A.F.M. Regulation and characteristic of smooth muscle cell phenotypic diversity. *Neth Heart J*. 2007; 15(3):100–108.

Riva CE and Feke GT: Laser Doppler Velocimetry in the measurement of retinal blood flow. In The Biomedical Laser: Technology and Clinical Applications, Goldman L, eds; New York, Springer-Verlag, 1981, 135-161.

Riva CE, Grunwald JE, Sinclair SH, Petrig BL. Blood velocity and volumetric flow rate in human retinal vessels. *Invest Ophthalmol Vis Sci*. 1985; 26(8):1124-32.

Riva CE, Hero M, Titze P, Petrig B. Autoregulation of human optic nerve head blood flow in response to acute changes in ocular perfusion pressure. *Graefes Arch Clin Exp Ophthalmol*1997; 235(10):618-626.

Riva C, Grunwald J, Petrig B. Autoregulation of human retinal blood flow. An investigation with laser Doppler velocimetry. *Invest Ophthalmol Vis Sci*. 1986; 27(12):1706-1712.

Robinson F, Riva C E. Retinal autoregulation in response to an acute increase in blood pressure. *Invest Ophthalmol Vis Sci*. 1986; 27:722-726.

Robinson F, Petrig B, Riva CE. The acute effect of cigarette smoking on macular capillary blood flow in humans. *Invest Ophthalmol Vis Sci*. 1985; 26(5):609.

Rodgman, A. and Perfetti, T.A. The Chemical Components of Tobacco and Tobacco Smoke. Boca Raton, FL: CRC Press; 2009.

Roff EJ, Harris A, Chung HS, et al. Comprehensive assessment of retinal, choroidal and retrobulbar haemodynamics during blood gas perturbation. *Graefes Arch Clin Exp Ophthalmol*. 1999; 237(12):984-990.

Rogers RL, Meyer JS, Shaw TG, Mortel KF, Thornby J. The effects of chronic cigarette smoking on cerebrovascular responsiveness to 5 per cent CO2 and 100 per cent O2 inhalation. *J Am Geriatr Soc*. 1984; 32(6):415-420.

Sparks HV, Rooke TW: *Essentials of Cardiovascular Physiology*. Minneapolis, University of Minnesota Press, 1987.

Rose PA, Hudson C. Comparison of retinal arteriolar and venular variability in healthy subjects. *Microvasc Res*. 2007; 73(1):35-38.

Saint-Geniez M, D'Amore PA. Development and pathology of the hyaloid, choroidal and retinal vasculature. *Int J Dev Biol*. 2004; 48(8-9):1045-1058.

Schiffrin EL, Touyz RM. Vascular biology of endothelium. *JCardiovascPharmacol* 1998; 32(3):S2-13.

Schmetterer L, Garhofer G. How can blood flow be measured? *Surv Ophthalmol*. 2007; 52(6):S134-S138.

Schmetterer L, Polak K. Role of nitric oxide in the control of ocular blood flow. *Prog Retin Eye Res*. 2001; 20(6):823-847.

Schmetterer L, Findl O, Strenn K, et al. Role of NO in the O_2 and CO_2 responsiveness of cerebral and ocular circulation in humans. *Am J Physiol Regul Integr Comp Physiol*. 1997; 273(6):R2005-R2012.

Schulte K, Wolf S. Retinal hemodynamics during increased intraocular pressure. *Ger J Ophthalmol*. 1996; 5(1):1-5.

Seddon JM, George S, Rosner B. Cigarette smoking, fish consumption, omega-3 fatty acid intake, and associations with age-related macular degeneration: The US twin study of age-related macular degeneration. *Arch Ophthalmol*. 2006; 124(7):995.

Silverthorn DU. *Human physiology: An integrated approach.* 3rd edition. San Francisco, USA, Pearson/Benjamin Cummings. 2004.

Silvestrini M, Troisi E, Matteis M, Cupini LM, Bernardi G. Effect of smoking on cerebrovascular reactivity.
J Cereb Blood Flow Metab. 1996; 16(4):746-749.

Skinhoj E, Olesen J, Paulson OB. Influence of smoking and nicotine on cerebral blood flow and metabolic rate of oxygen in man. *J Appl Physiol*. 1973; 35(6):820-822.

Slessarev M, Han J, Mardimae A, et al. Prospective targeting and control of end-tidal CO_2 and O_2 concentrations. *J Physiol (Lond)*. 2007; 581(3):1207-1219.

Slessarev M, Somogyi R, Preiss D, Vesely A, Sasano H, Fisher JA. Efficiency of oxygen administration: Sequential gas delivery versus" flow into a cone" methods. *Crit Care Med*. 2006; 34(3):829-834.

Smith W, Mitchell P, Leeder SR. Smoking and age-related maculopathy: The Blue mountains eye study. *Arch Ophthalmol*. 1996; 114(12):1518-1523.

Smith CJ, Fischer TH. Particulate and vapor phase constituents of cigarette mainstream smoke and risk of myocardial infarction. *Atherosclerosis*. 2001; 158(2):257-267.

Sponsel WE, DePaul KL, Zetlan S. Retinal hemodynamic effects of carbon dioxide, hyperoxia, and mild hypoxia. *Invest Ophthalmol Vis Sci*. 1992; 33(6):1864.

Steigerwalt Jr RD, Laurora G, Incandela L, Cesarone MR, Belcaro GV, De Sanctis MT. Ocular and orbital blood flow in cigarette smokers. *Retina*. 2000; 20(4):394.

Tamaki Y, Araie M, Nagahara M, Tomita K, Matsubara M. The acute effects of cigarette smoking on human optic nerve head and posterior fundus circulation in light smokers. *Eye*. 2000; (14):67-72.

Terai N, Spoerl E, Pillunat LE, Stodtmeister R. The effect of caffeine on retinal vessel diameter in young healthy subjects. *Acta Ophthalmol*. 2012; 90(7): 524-528.

Terborg C, Bramer S, Weiller C, Röther J. Short-term effect of cigarette smoking on CO_2-induced vasomotor reactivity in man: A study with near-infrared spectroscopy and tanscranial doppler sonography. *J Neurol Sci*. 2002; 205(1):15-20.

Thornton J, Edwards R, Mitchell P, Harrison R, Buchan I, Kelly S. Smoking and age-related macular degeneration: A review of association. *Eye*. 2005; 19(9):935-944.

Tønnesen P, Fryd V, Hansen M, Helsted J, Gunnersen AB, Forchammer H, Stockner M. Two and four mg nicotine chewing gum and group counselling in smoking cessation: An open, randomized, controlled trial with a 22 month follow-up. *Addict Behav*. 1988; 13(1):17-27.

Toussaint D. Retinal vascular patterns part II. Human retinal vessels studied in three dimensions. *Arch Ophthalmol*. 1961; 65:575-581.

Vane JR, Botting RM. Pharmacodynamic profile of prostacyclin. *Am J Cardiol*. 1995; 75(3):3-10.

Vaz JC, Fonseca JR, Jose RF de Abreu, Lima JJP. Studies on retinal blood flow II Diabetic retinopathy. *Arch Ophthalmol.* 1978; 96(5):809-811.

Venkataraman ST, Hudson C, Fisher JA, Flanagan JG. Novel methodology to comprehensively assess retinal arteriolar vascular reactivity to hypercapnia. *Microvasc Res*. 2006; 72(3):101-107.

Venkataraman ST, Hudson C, Fisher JA, Flanagan JG. The impact of hypercapnia on retinal capillary blood flow assessed by scanning laser Doppler flowmetry. *Microvasc Res*. 2005; 69(3):149-155.

Venkataraman ST, Hudson C, Fisher JA, Rodrigues L, Mardimae A, Flanagan JG. Retinal arteriolar and capillary vascular reactivity in response to isoxic hypercapnia. *Exp Eye Res*. 2008; 87(6):535-542.

Venkataraman, S.T., Hudson, C., Rachmiel, R., Buys, Y.M., Markowitz, S.N., Fisher, J.A.,Trope, G.E., Flanagan, J.G. Retinal arteriolar vascular reactivity in untreated and progressive primary open-angle glaucoma. *Invest. Ophthalmol.Vis. Sci*. 2010; 51, 2043-2050.

Vingerling JR, Hofman A, Grobbee DE, de Jong PTVM. Age-related macular degeneration and smoking: The Rotterdam study. *Arch Ophthalmol*. 1996; 114(10):1193-1196.

Wald NJ, Idle M, Boreham J, Bailey A. Carbon monoxide in breath in relation to smoking and carboxyhaemoglobin levels. *Thorax*. 1981; 36(5):366-369.

Wang Y, Fawzi AA, Varma R, et al. Pilot study of optical coherence tomography measurement of retinal blood flow in retinal and optic nerve diseases. . *Invest Ophthalmol Vis Sci*. 2011; 52(2):840-845.

Wang Y, Bower BA, Izatt JA, Tan O, Huang D. *In vivo* total retinal blood flow measurement by Fourier domain Doppler optical coherence tomography. *J Biomed Opt*. 2007; 12:041215.

Wang Y, Fawzi A, Tan O, Gil-Flamer J, Huang D. Retinal blood flow detection in diabetic patients by Doppler fourier domain optical coherence tomography. *Opt express*. 2009; 17(5):4061-4073.

Wang Y, Lu A, Gil-Flamer J, Tan O, Izatt JA, Huang D. Measurement of total blood flow in the normal human retina using Doppler fourier-domain optical coherence tomography. *Br J Ophthalmol*. 2008; 93(5):634.

Wehbe H, Ruggeri M, Jiao S, Gregori G, Puliafito C. Automatic retinal blood vessel parameter calculation in spectral domain optical coherence tomography. 2007; *Opt Express*. 2007; 15(23):15193-15206.

Wennmalm A. Effect of cigarette smoking on basal and carbon dioxide stimulated cerebral blood flow in man. *Clin Physiol*. 1982; 2(6):529-535.

Werkmeister RM, Palkovits S, Told R, et al. Response of retinal blood flow to systemic hyperoxia as measured with dual-beam bidirectional Doppler fourier-domain optical coherence tomography. *PLOS ONE*. 2012; 7(9):45876.

West SG. Effect of diet on vascular reactivity: An emerging marker for vascular risk. *Curr Atheroscler Rep*. 2001; 3(6):446-455.

White RP, Markus HS. Impaired dynamic cerebral autoregulation in carotid artery stenosis. *Stroke*. 1997; 28(7):1340-1344.

Wimpissinger B, Resch H, Berisha F, Weigert G, Schmetterer L, Polak K. Response of retinal blood flow to systemic hyperoxia in smokers and nonsmokers. *Graefes Arch Clin Exp Ophthalmol*. 2005; 243(7):646-652.

Wimpissinger B, Resch H, Berisha F, Weigert G, Schmetterer L, Polak K. Response of choroidal blood flow to carbogen breathing in smokers and non-smokers. *Br J Ophthalmol*. 2004; 88(6):776.

Yap MK BB. The repeatability of the non-invasive blue field entoptic phenomenon method for measuring macular capillary blood flow. *Optom Vis Sci* 1994; 71(5):346-349.

Yoshida A, Feke GT, Mori F, Nagaoka T, Fujio N, Ogasawara H, Konno S, Mcmeel JW. Reproducibility and clinical application of a newly developed stabilized retinal laser Doppler instrument. *Am J Ophthalmol*. 2003; 135(3):356-61.

Zeiher AM, Schächinger V, Minners J. Long-term cigarette smoking impairs endothelium-dependent coronary arterial vasodilator function. *Circulation*. 1995; 92(5):1094-100.

Zhang S, Day l, Ye S. Nicotine induced changes in gene expression by human coronary artery endothelial cells. *Atherosclerosis*. 2001; (154):277-283.